

A. Appendix: PBPK Modeling of TCE and Metabolites – Detailed Methods and Results

CONTENTS

A. Appendix: PBPK Modeling of TCE and Metabolites – Detailed Methods and Results..... A-1

A.1. The hierarchical Bayesian approach to characterizing PBPK model uncertainty and variability A-2

A.2. Evaluation of the Hack et al. (2006) PBPK Model..... A-5

A.2.1. Convergence A-5

A.2.2. Evaluation of posterior distributions for population parameters A-7

A.2.3. Comparison of model predictions with data A-8

A.2.3.1. Mouse model..... A-10

A.2.3.1.1. Group-specific and population-based predictions..... A-10

A.2.3.1.1.1. Group-specific predictions and calibration data A-10

A.2.3.1.1.2. Population-based predictions and calibration and additional evaluation data A-10

A.2.3.1.2. Conclusions regarding mouse model A-14

A.2.3.2. Rat model..... A-16

A.2.3.2.1. Group-specific and population-based predictions..... A-16

A.2.3.2.1.1. Group-specific predictions and calibration data A-17

A.2.3.2.1.2. Population-based predictions and calibration and additional evaluation data A-17

A.2.3.2.2. Conclusions regarding rat model A-23

A.2.3.3. Human model..... A-25

A.2.3.3.1. Individual-specific and population-based predictions A-25

A.2.3.3.1.1. Individual-specific predictions and calibration data A-25

A.2.3.3.1.2. Population-based predictions and calibration and additional evaluation data A-26

A.2.3.3.2. Conclusions regarding human model..... A-34

A.3. Preliminary Analysis of Mouse Gas Uptake Data: Motivation for Modification of Respiratory Metabolism..... A-36

A.4. Details of the Updated PBPK Model for TCE and Its Metabolites A-43

A.4.1. Model Parameters and Baseline Values..... A-43

A.4.2. Statistical Distributions for Parameter Uncertainty and Variability A-51

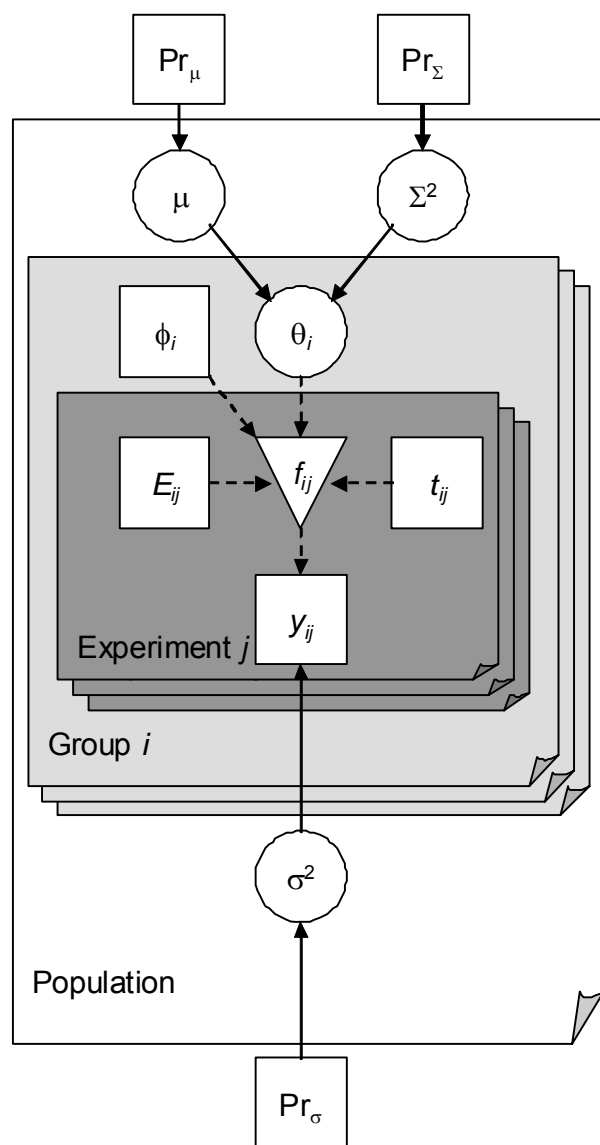
A.4.2.1. Initial Prior Uncertainty in Population Mean Parameters..... A-51

1 **A.4.2.2.** Inter-species scaling to update selected prior distributions in the rat and
2 human A-56
3 **A.4.2.3.** Population Variance: Prior Central Estimates and Uncertainty..... A-61
4 **A.4.2.4.** Prior distributions for residual error estimates..... A-65
5 A.5. Results of Updated PBPK Model A-67
6 A.5.1. Convergence and posterior distributions of sampled parameters A-68
7 A.5.2. Comparison of model predictions with data A-77
8 **A.5.2.1.** Mouse model..... A-77
9 **A.5.2.1.1.** Group-specific predictions and calibration data A-77
10 **A.5.2.1.2.** Population-based predictions and calibration data..... A-77
11 **A.5.2.2.** Rat model A-77
12 **A.5.2.2.1.** Group-specific predictions and calibration data A-77
13 **A.5.2.2.2.** Population-based predictions and calibration data..... A-77
14 **A.5.2.2.3.** Population-based predictions and additional evaluation data A-77
15 **A.5.2.3.** Human model..... A-77
16 **A.5.2.3.1.** Individual-specific predictions and calibration data A-77
17 **A.5.2.3.2.** Population-based predictions and calibration data..... A-77
18 **A.5.2.3.3.** Population-based predictions and additional evaluation data A-77
19 A.6. Updated PBPK Model Code A-77
20 **References**..... A-102
21

22 **A.1. The hierarchical Bayesian approach to characterizing PBPK model uncertainty and**
23 **variability**

24 The Bayesian approach for characterizing uncertainty and variability in PBPK model
25 parameters, used previously for TCE in Bois (2000a, b) and Hack et al. (2006), is briefly
26 described here as background. Once a PBPK model structure is specified, characterizing the
27 model reduces to calibrating and making inferences about model parameters. The use of least-
28 squares point estimators is limited by the large number of parameters and small amounts of data.
29 The use of least-squares estimation is reported after imposing constraints for several parameters
30 (Fisher, 2000; Clewell et al., 2000). This is reasonable for a first estimate, but it is important to
31 follow up with a more refined treatment. This is implemented by a Bayesian approach to
32 estimate posterior distributions on the unknown parameters, a natural choice, and almost a
33 compulsory consequence given the large number of parameters and relatively small amount of
34 data, and given the difficulties of frequentist estimation in this setting.

1 As described by Gelman et al. (1996), the Bayesian approach to population PBPK
2 modeling involves setting up the overall model in several stages. A nonlinear PBPK model, with
3 predictions denoted f , describes the absorption, distribution, metabolism, and excretion of a
4 compound and its metabolites in the body. This model depends on several, usually known,
5 parameters such as measurement times t , exposure E , and measured covariates φ . Additionally,
6 each subject i in a population has a set of unmeasured parameters θ_i . A random effects model
7 describes their population variability $P(\theta_i | \mu, \Sigma^2)$, and a prior distribution $P(\mu, \Sigma^2)$ on the
8 population mean μ and covariance Σ^2 (often assumed to be diagonal) incorporates existing
9 scientific knowledge about them. Finally, a “measurement error” model $P(y | f[\theta, \varphi, E, t], \sigma^2)$
10 describes deviations (with variance σ^2) between the data y and model predictions f (which of
11 course depends on the unmeasured parameters θ_i and the measured parameters t , E , and φ). This
12 “measurement error” level of the hierarchical model typically also encompasses intra-individual
13 variability as well as model misspecification, but for notational convenience we refer to it here as
14 “measurement error.” Because these other sources of variance are lumped into a single
15 “measurement error,” a prior distribution of its variance σ^2 must be specified even if the actual
16 analytic measurement error is known. All these components are illustrated graphically in
17 Figure A.1.
18



2 **Figure A.1 Hierarchical population statistical**
 3 **model for PBPK model parameter uncertainty**
 4 **and variability (see Gelman et al., 1996).**
 5 Square nodes denote fixed or observed quantities,
 6 circle nodes represent uncertain or unobserved
 7 quantities, and the non-linear model outputs are
 8 denoted by the inverted triangle. Solid arrows denote
 9 a stochastic relationship represented by a conditional
 10 distribution $[A \rightarrow B \text{ means } B \sim P(B|A)]$, while dashed
 11 arrows represent a function relationship $[B=f(A)]$.
 12 The population consists of groups (or subjects) i ,
 13 each of which undergoes one or more experiments j
 14 with exposure parameters E_{ij} with data y_{ij} collected at
 15 times t_{ij} . The PBPK model produces outputs f_{ij} for
 16 comparison with the data y_{ij} . The difference between
 17 them (“measurement error”) has variance σ^2 , with a
 18 fixed prior distribution Pr , which in this case is the
 19 same for the entire population. The PBPK model
 20 also depends on measured covariates ϕ_i (e.g., body
 21 weight) and unobserved model parameters θ_i (e.g.,
 22 V_{max}). The parameters θ_i are drawn from a
 23 population with mean μ and variance Σ^2 , each of
 24 which is uncertain and has a prior distribution
 25 assigned to it.
 26

1
 27

28 The posterior distribution for the unknown parameters is obtained in the usual manner by
 29 multiplying (i) the prior distribution for the population mean and variance and the
 30 “measurement” error $P(\mu, \Sigma^2) P(\sigma^2)$, (ii) the population distribution for the individual parameters
 31 $P(\theta | \mu, \Sigma^2)$, and (iii) the likelihood $P(y | \theta, \sigma^2)$, where for notational convenience, we drop the
 32 dependence on f, ϕ, E , and t (which are taken as fixed for a given dataset):

$$33 \quad P(\theta, \mu, \Sigma^2, \sigma^2 | y) \propto P(\mu, \Sigma^2) P(\sigma^2) P(\theta | \mu, \Sigma^2) P(y | \theta, \sigma^2)$$

34 Here, each subject’s parameters θ_i have the same sampling distribution (i.e., they are
 35 independently and identically distributed), so their joint prior distribution is

$$36 \quad P(\theta | \mu, \Sigma^2) = \prod_{i=1 \dots n} P(\theta_i | \mu, \Sigma^2)$$

37 Different experiments $j = 1 \dots n_j$ may have different exposure and different data collected and
 38 different time points. In addition, different types of measurements $k = 1 \dots n_k$ (e.g., TCE blood,

1 TCE breath, TCA blood, etc.) may have different errors, but errors are otherwise assumed to be
 2 iid. Since the individuals are treated as independent given $\theta_{1...n}$, the total likelihood function is
 3 simply

$$4 \quad P(y | \theta, \sigma^2) = \prod_{i=1...n} \prod_{j=1...n_{ij}} \prod_{k=1...m} \prod_{l=1...N_{ijk}} P(y_{ijkl} | \theta_i, \sigma_k^2, t_{ijkl})$$

5 where n is the number of subjects, n_{ij} is the number of experiments in that subject, m is the
 6 number of different types of measurements, N_{ijk} is the number (possibly 0) of measurements
 7 (e.g., time points) for subject i of type k in experiment j , and t_{ijkl} are the times at which
 8 measurements for individual i of type k were made in experiment j .

9 Given the large number of parameters, complex likelihood functions, and nonlinear
 10 PBPK model, Markov chain Monte Carlo (MCMC) simulation was used to generate samples
 11 from the posterior distribution. An important practical advantage of MCMC sampling is the
 12 ability to implement inference in nearly any probability model and the possibility to report
 13 inference on any event of interest. MCMC simulation was introduced by Gelfand and Smith
 14 (1990) as a generic tool for posterior inference. See Gilks et al. (1996) for a review. In the
 15 context of PBPK models, the MCMC simulation can be carried out as described by Hack et al.
 16 (2006). The simulation program MCSim (version 5.0.0) was used to implement MCMC
 17 posterior simulation, with analysis of the results performed using the R statistical package.
 18 Simulation-based parameter estimation with MCMC posterior simulation gives rise to an
 19 additional source of uncertainty. For instance, averages computed from the MCMC simulation
 20 output represent the desired posterior means only asymptotically, in the limit as the number of
 21 iterations goes to infinity. Any implementation needs to include a convergence diagnostic to
 22 judge practical convergence. The potential scale-reduction-factor convergence diagnostic R of
 23 Gelman et al. (1996) was used here, as it was in Hack et al. (2006).

24 **A.2. Evaluation of the Hack et al. (2006) PBPK Model**

25 EPA obtained the original model code for the version of the TCE PBPK model published
 26 in Hack et al. (2006) and conducted a detailed evaluation of the model, focusing on the following
 27 areas: convergence, posterior estimates for model parameters, and comparison of model
 28 predictions with *in vivo* data.

29 **A.2.1. Convergence**

30 As noted in Hack et al. (2006), the diagnostics for the MCMC simulations (3 chains of
 31 length 20,000–25,000 for each species) indicated that additional samples might further improve
 32 convergence. A recent analysis of tetrachloroethylene pharmacokinetics indicated the need to be
 33 especially careful in ensuring convergence (Chiu and Bois, 2006). Therefore, the number of

1 MCMC samples per chain was increased to 75,000 for rats (first 25,000 discarded) and 175,000
2 for mice and humans (first 75,000 discarded). Using these chain lengths, the vast majority of the
3 parameters had potential scale reduction factors $R \leq 1.01$, and all population parameters had
4 $R \leq 1.05$, indicating that longer chains would be expected to reduce the standard deviation (or
5 other measure of scale, such as a confidence interval) of the posterior distribution by less than
6 this factor (Gelman et al., 2004).

7 In addition, analysis of autocorrelation within chains using the R-CODA package
8 (Plumber et al., 2008) indicated that there was significant serial correlation, so additional
9 “thinning” of the chains was performed in order to reduce serial correlations. In particular, for
10 rats, for each of 3 chains, every 100th sample from the last 50,000 samples was used; and for
11 mice and humans, for each of 3 chains, every 200th sample from the last 100,000 samples was
12 used. This thinning resulted in a total of 1,500 samples for each species available for use for
13 posterior inference.

14 Finally, an evaluation was made of the “convergence” of dose metric predictions—that is,
15 the extent to which the standard deviation or confidence intervals for these predictions would be
16 reduced with additional samples. This is analogous to a “sensitivity analysis” performed so that
17 most effort is spent on parameters that are most influential in the result. In this case, the purpose
18 is to evaluate whether one can sample chains only long enough to ensure convergence of
19 predictions of interest, even if certain more poorly identified parameters take longer chains to
20 converge. The motivation for this analysis is that for a more complex model, running chains
21 until all parameters have $R \leq 1.01$ or 1.05 may be infeasible given the available time and
22 resource. In addition, as some of the model parameters had prior distributions derived from
23 “visual fitting” to the same data, replacing those distributions with less informative distributions
24 (in order to reduce bias from “using the same data twice”) may require even longer chains for
25 convergence.

26 Indeed, it was found that R-values for dose metric predictions approached 1 more quickly
27 than PBPK model input parameters. The most informative simulations were for mice, which
28 converged the slowest and thus had the most potential for convergence-related error. Results for
29 rats could not be assessed because the model converged so rapidly, and results for humans were
30 similar to those in mice, though the deviations were all less because of the more rapid
31 convergence. In the mouse model, after 25,000 iterations, many PBPK model parameters had R-
32 values > 2 , with more than 25% greater than 1.2. However, all dose metric predictions had
33 $R < 1.4$, with the more than 96% of them < 1.2 and the majority of them < 1.01 . In addition,
34 when compared to the results of the last 100,000 iterations (after the total of 175,000 iterations),
35 more than 90% of the medians estimates shifted by less than 20%, with the largest shifts less
36 than 40% (for GSH metabolism dose metrics, which had no relevant calibration data). Tail

1 quantiles had somewhat larger shifts, which was expected given the limited number of samples
2 in the tail, but still more than 90% of the 2.5th and 97.5th quantiles had shifts of less than
3 40%. Again, the largest shifts, on order of 2-fold, were for GSH-related dose metrics that had
4 high uncertainty, so the relative impact of limited sample size is small.

5 Therefore, the additional simulations performed in this evaluation, with 3- to 7-fold
6 longer chains, did not result in much change in risk assessment predictions from the original
7 Hack et al. (2006) results. Thus, assessing prediction convergence appears sufficient for
8 assessing convergence of the TCE PBPK model for the purposes of risk assessment prediction.

9 **A.2.2. Evaluation of posterior distributions for population parameters**

10 Posterior distributions for the population parameters were first checked for whether they
11 appeared reasonable given the prior distributions. Inconsistency between the prior and posterior
12 distributions may indicate an insufficiently broad prior distribution (i.e., overconfidence in their
13 specification), a misspecification of the model structure, or an error in the data. Parameters that
14 were flagged for further investigation were those for which the interquartile ranges (intervals
15 bounded by the 25th and 75th percentiles) of the prior and posterior distributions did not overlap.
16 In addition, lumped metabolism and clearance parameters for TCA, TCOH, and TCOG were
17 checked to make sure that they remained physiological – e.g., metabolic clearance was not more
18 than hepatic blood flow and urinary clearance not more than kidney blood flow (constraints that
19 were not present in the Hack et al., 2006 priors).

20 In mice, population mean parameters that had lack of overlap between priors and
21 posteriors included the affinity of oxidative metabolism ($\ln K_M$), the TCA plasma-blood
22 concentration ratio ($\ln TCAP_{\text{plasma}}$), the TCE stomach to duodenum transfer coefficient ($\ln KTSD$),
23 and the urinary excretion rates of TCA and TCOG ($\ln k_{\text{UrnTCA}}$ $\ln k_{\text{UrnTCOG}}$). For K_M , this
24 is not unexpected, as previous investigators have noted inconsistency in the K_M values between
25 *in vitro* values (upon which the prior distribution was based) and *in vivo* values derived from oral
26 and inhalation exposures in mice (Abbas and Fisher, 1997; Greenberg et al., 1999). For the other
27 mean parameters, the central estimates were based on visual fits, without any other a priori data,
28 so it is reasonable to assume that the inconsistency is due to insufficiently broad prior
29 distributions. In addition, the population variance for the TCE absorption coefficient from the
30 duodenum (k_{AD}) was rather large compared to the prior distribution, likely due to the fact that
31 oral studies included TCE in both oil and aqueous solutions, which are known to have very
32 different absorption properties. Thus, the larger population variance was required to
33 accommodate both of them. Finally, the estimated clearance rate for glucuronidation of TCOH
34 was substantially greater than hepatic blood flow. This is an artifact of the one-compartment

1 model used for TCOH and TCOG, and suggests that first pass effects are important for TCOH
2 glucuronidation. Therefore, the model would benefit from the additional of a separate liver
3 compartment so that first pass effects can be accounted for, particularly when comparing across
4 dose-routes.

5 In rats, the only population mean or variance parameter for which the posterior
6 distribution was somewhat inconsistent with the prior distribution was the population mean for
7 the affinity for oxidative metabolism ($\ln K_M$). While the inter-quartile regions did not overlap,
8 the 95%-ile regions did, so the discordance was relatively minor. However, as with mice, the
9 estimated clearance rate for glucuronidation of TCOH was substantially greater than hepatic
10 blood flow.

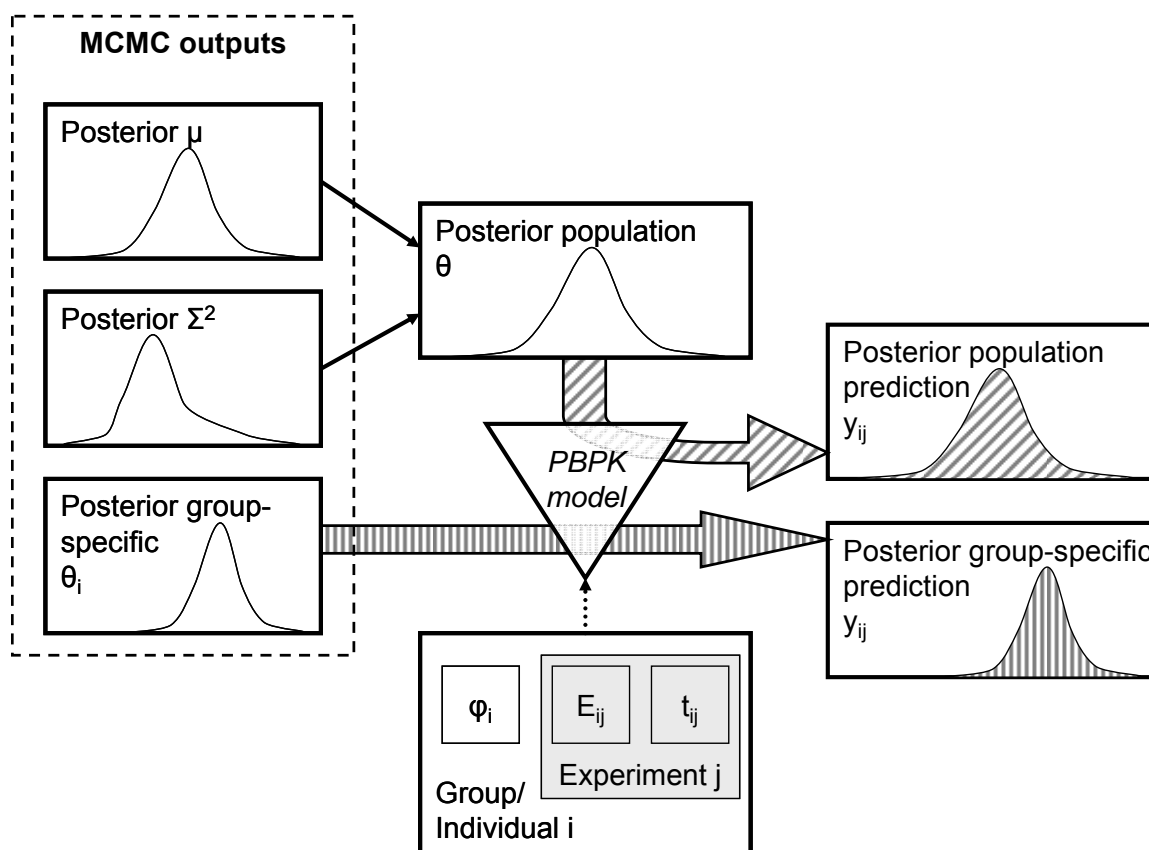
11 In humans, some of the chemical-specific parameters for which priors were established
12 using visual fits had posterior distributions that were somewhat inconsistent, including the
13 oxidative split between TCA and TCOH ($\ln \text{FracTCE}$), biliary excretion of TCOG ($\ln k_{\text{BileC}}$),
14 and the TCOH distribution volume (V_{BodC}). More concerning was the fact that the posterior
15 distributions for several physiological volumes and flows were rather strongly discordant with
16 the priors and/or near their truncation limits, including gut, liver, and slowly perfused blood
17 flow, the volumes of the liver and rapidly perfused compartments. In addition, a number of
18 tissue partition coefficients were somewhat inconsistent with their priors, including those for
19 TCE in the gut, rapidly perfused, and slowly perfused tissues, and TCA in the body and liver.
20 Finally, a number of population variances (for TCOH clearance [C_{ITCOHC}], urinary excretion
21 of TCOG [k_{UrnTCOGC}], ventilation-perfusion ratio [V_{PR}], cardiac output [Q_{CC}], fat blood
22 flow and volume [Q_{FatC} and V_{FatC}], and TCE blood-air partition coefficient [P_{B}]) were
23 somewhat high compared to their prior distributions, indicating much greater population
24 variability than expected.

25 **A.2.3. Comparison of model predictions with data**

26 A schematic of the comparisons between model predictions and data is shown in
27 Figure A.2. In the hierarchical population model, group-specific parameters were estimated for
28 each dataset used in calibrating the model (posterior group-specific θ_i in Figure A.2). Because
29 these parameters are in a sense “optimized” to the experimental data themselves, the group-
30 specific predictions (posterior group-specific y_{ij} in Figure A.2) using these parameters should be
31 accurate by design. Poor fits to the data using these group-parameters may indicate a
32 misspecification of the model structure, prior parameter distributions, or an error in the data. In
33 addition, it is useful to generate “population-based” parameters (posterior population θ) using
34 only the posterior distributions for the population means (μ) and variances (Σ^2), instead of the

1 estimated group-specific parameters. These population predictions provide a sense as to whether
 2 the model and the predicted degree of population uncertainty and variability adequately account
 3 for the range of heterogeneity in the experimental data. Furthermore, assuming the group-
 4 specific predictions are accurate, the population-based predictions are useful to identify whether
 5 one or more of the datasets are “outliers” with respect to the predicted population. In addition, a
 6 substantial number of *in vivo* datasets was available in all three species that were not previously
 7 used for calibration. Thus, it is informative to compare the population-based model predictions,
 8 discussed above, to these additional “validation” data in order to assess the predictive power of
 9 the PBPK model.

10
 11
 12



13
 14 Figure A.2. Schematic of how posterior predictions were generated for comparison with
 15 experimental data. Two sets of posterior predictions were generated: population predictions
 16 (diagonal hashing) and group-specific predictions (vertical hashing).

1
2
3
4
5
6
7
8
9
10
11
12
13
14
15
16
17
18
19
20
21
22
23
24

A.2.3.1. *Mouse model*

A.2.3.1.1. *Group-specific and population-based predictions*

Initially, the sampled group-specific parameters were used to generate predictions for comparison to the calibration data. Because these parameters were “optimized” for each group, these “group-specific” predictions should be accurate by design. However, unlike for the rat (see below), this was not the case for some experiments (this is partially responsible for the slower convergence). In particular, the predictions for TCE and TCOH concentrations for the Abbas and Fisher (1997) data were poor. In addition, TCE blood concentrations for the Greenberg et al. (1999) data were consistently overpredicted. These data are discussed further in Table A.1.

Next, only samples of the population parameters (means and variances) were used, and “new groups” were sampled from appropriate distributions using these population means and variances. These “new groups” then represent the predicted population distribution, incorporating both variability in the population as well as uncertainty in the population means and variances. These “population-based” predictions were then compared to both the data used in calibration, as well as the additional data identified that was not used in calibration. The PBPK model was modified to accommodate some of the different outputs (e.g., tissue concentrations) and exposure routes (TCE, TCA, and TCOH iv) used in the “non-calibration” data, but otherwise it is unchanged.

A.2.3.1.1.1. *Group-specific predictions and calibration data*

[See [Appendix.linked.files\AppA.2.3.1.1.1.Hack.mouse.group.calib.TCE.DRAFT.pdf](#)]

A.2.3.1.1.2. *Population-based predictions and calibration and additional evaluation data*

[See [Appendix.linked.files\AppA.2.3.1.1.2.Hack.mouse.pop.calib.eval.TCE.DRAFT.pdf](#)]

1 **Table A.1.** Evaluation of Hack et al. (2006) PBPK model predictions for *in vivo* data in mice.

Reference	Simulation #	Calibration data	Discussion
Abbas and Fisher, 1996	41–42		These data are only published as an abstract. They consist of TCA and TCOH blood and urine data from TCA and TCOH iv dosing. Blood levels of TCA and TCOH are fairly accurately predicted. From TCOH dosing, urinary TCOG excretion is substantially overpredicted, and from TCA dosing, urinary TCA excretion is substantially overpredicted.
Abbas and Fisher, 1997	3–6	√	<p>Results for these data were mixed. TCA levels were the best fit. The calibration data included TCA blood and liver data, which were well predicted except at the earliest time-point. In addition, TCA concentrations in the kidney were fairly consistent with the surrogate TCA body concentrations predicted by the model. Urinary TCA was well predicted at the lower two and highest doses, but somewhat underpredicted (though still in the 95% confidence region) at 1,200 mg/kg.</p> <p>TCE levels were in general not well fit. Calibration data included blood, fat, and liver concentrations, which were predicted poorly particularly at early and late times. One reason for this is probably the representation of oral uptake. Although both the current model and the original Abbas and Fisher (1997) model had two-compartments representing oral absorption, in the current model uptake can only occur from the second compartment. By contrast, the Abbas and Fisher (1997) model had uptake from both compartments, with the majority occurring from the first compartment. Thus, the explanation for the poor fit, particularly of blood and liver concentrations, at early times is probably simply due to differences in modeling oral uptake. This is also supported by the fact that the oral uptake parameters tended to be among those that took the longest to converge.</p> <p>Group-specific blood TCOH predictions were poor, with under-prediction at early times and overprediction at late times. Population-based blood TCOH predictions tended to be underpredicted, though generally within the 95% confidence region. Group-specific urinary TCOG predictions were fairly accurate except at the highest dose. These predictions are also probably affected by the apparent misrepresentation of oral uptake. In addition, a problem as found in the calibration data in that data on free TCOH was calibrated against predictions of total TCOH (TCOH+TCOG).</p> <p>A number of TCOH and TCOG measurements were not included in the calibration—among them tissue concentrations of TCOH and tissue and blood concentrations of TCOG. Blood concentrations (the only available surrogate) were poor predictors of tissue concentrations of TCOH and TCOG (model generally under-predicted). For TCOG, this may be due in part to the model assumption that the distribution volume of TCOG is equal to that of TCOH.</p>

INTER-AGENCY REVIEW DRAFT–DO NOT CITE OR QUOTE

Reference	Simulation #	Calibration data	Discussion
Fisher et al., 1991	1–2 (open chamber)	√	Venous blood TCE concentrations were somewhat underpredicted (a common issue with inhalation exposures in mice – see discussion of Greenberg et al., 1999 below), but within the 95% confidence region of both group-specific and population-based predictions. Plasma TCA levels were well predicted, with most of the data near the inter-quartile region of both group-specific and population-based predictions (but with substantial scatter in the male mice). However, it should be noted that only a single exposure concentration for each sex was used in calibration, with 6 additional exposures (3 for each sex) not included (see simulations 21–26, below).
	7–16 (closed chamber)	√	Good posterior fits were obtained for these data – closed chamber data with initial concentrations from 300 ppm to 10,000 ppm. Some variability in V_{max} , however, was noted in the posterior distributions for that parameter. Using group-specific V_{max} values resulted in better fits to these data. However, there appears to be a systematic trend of lower estimated apparent V_{max} at higher exposures. Similarly, posterior estimates of cardiac output and the ventilation-perfusion ratio declined (slightly) with higher exposures. These could be related to documented physiological changes (e.g., reduced ventilation rate and body temperature) in mice when exposed to some volatile organics.
	21–26 (open chamber, additional exposures)		Data from three additional exposures for each sex were available for comparison to model predictions. Plasma TCA levels were generally well predicted, though the predictions for female mice data showed some systematic over-prediction, particularly at late times (i.e., data showed shorter apparent half-life). Blood TCE concentrations were consistently overpredicted, sometimes by almost an order of magnitude, except in the case of female mice at 236 ppm, for which predictions were fairly accurate.
Fisher and Allen, 1993	31–36		Predictions for these gavage data were generally fairly accurate. There was a slight tendency to overpredict TCA plasma concentrations, with predictions tending to be worse in the female mice. Blood levels of TCE were adequately predicted, though there was some systematic underprediction at 2–6 hr after dosing.
Green and Prout, 1985	40		This datum consists of a single measurement of urinary excretion of TCA at 24 hr as a fraction of dose, from TCA iv dosing. The model substantially over-predicts the amount excreted. Whereas Green and Prout (1985) measured 35% excreted at 24 hr, the model predicts virtually complete excretion at 24 hr.

INTER-AGENCY REVIEW DRAFT–DO NOT CITE OR QUOTE

Reference	Simulation #	Calibration data	Discussion
Greenberg et al., 1999	17–18	√	The calibration data included blood TCE, TCOH, and TCA data. Fits to blood TCA and TCOH were adequate, but as with the Fisher et al. (1991) inhalation data, TCE levels were overpredicted (outside the 95% confidence region during and shortly after exposure). As with Abbas and Fisher (1997), there were additional data in the study that was not used in calibration, including blood levels of TCOG and tissue levels of TCE, TCA, TCOH, and TCOG. Tissue levels of TCE were somewhat overpredicted, but generally within the 95% confidence region. TCA levels were adequately predicted, and mostly in or near the inter-quartile region. TCOH levels were somewhat underpredicted, though within the 95% confidence region. TCOG levels, for which blood served as a surrogate for all tissues, were well predicted in blood and the lung, generally within the inter-quartile region. However, blood TCOG predictions underpredicted liver and kidney concentrations.
Larson and Bull, 1992b	37–39		Blood TCA predictions were fairly accurate for these data. However, TCE and TCOH blood concentrations were underpredicted by up to an order of magnitude (outside the 95% confidence region). Part of this may be due to uncertain oral dosing parameters. Urinary TCA and TCOG were also generally underpredicted, in some cases outside of the 95% confidence region.
Prout et al., 1985	19	√	Fits to these data were generally adequate – within or near the inter-quartile region.
	27–30 (urinary excretion at different doses)		These data consisted of mass balance studies of the amount excreted in urine and exhaled unchanged at doses from 10 to 2,000 mg/kg. TCA excretion was consistently overpredicted, except at the highest dose. TCOG excretion was generally well predicted – within the inter-quartile range. The amount exhaled was somewhat overpredicted, with a 4-fold difference (but still within 95% confidence) at the highest dose.
Templin et al., 1993	20	√	Blood TCA levels from these data were well predicted by the model. Blood TCE and TCOH levels were well predicted using group-specific parameters, but did not appear representative using population-derived parameters. However, this is probably a result of the group-specific oral absorption parameter, which was substantially different than the population mean.

1

2 **A.2.3.1.2. *Conclusions regarding mouse model***3 **TCE concentrations in blood and tissues not well-predicted**

4 The PBPK model for the parent compound does not appear to be robust. Even group-
5 specific fits to datasets used for calibration were not always accurate. For oral dosing data, there
6 is clearly high variability in oral uptake parameters, and the addition of uptake through the first
7 (stomach) compartment should improve the fit. Unfortunately, inaccurate TCE uptake
8 parameters may lead to inaccurately estimated kinetic parameters for metabolites TCA and
9 TCOH, even if current fits are adequate.

10 The TCE data from inhalation experiments also are not well estimated, particularly blood
11 levels of TCE. While fractional uptake has been hypothesized, direct evidence for this is
12 lacking. In addition, physiologic responses to TCE vapors (reduced ventilation rates, lowered
13 body temperature) are a possibility. These are weakly supported by the closed chamber data, but
14 the amount of the changes is not sufficient to account for the low blood levels of TCE observed
15 in the open chamber experiments. It is also not clear what role pre-systemic elimination due to
16 local metabolism in the lung may play. It is known that the mouse lung has a high capacity to
17 metabolize TCE (Green et al., 1997). However, in the Hack et al. (2006) model, lung
18 metabolism is limited by flow to the tracheobronchial region. An alternative formulation for
19 lung metabolism in which TCE is available for metabolism directly from inhaled air (similar to
20 that used for styrene, Sarangapani et al., 2003), may allow for greater pre-systemic elimination of
21 TCE, as well as for evaluating the possibility of wash-in/wash-out effects. Furthermore, the
22 potential impact of other extra-hepatic metabolism has not been evaluated. Curiously,
23 predictions for the tissue concentrations of TCE observed by Greenberg et al. (1999) were not as
24 discrepant as those for blood. A number of these hypotheses could be tested; however, the
25 existing data may not be sufficient to distinguish them. The Merdink et al. (1998) study, in
26 which TCE was given by iv (thereby avoiding both first pass in the liver and any fractional
27 uptake issue in the lung), may be somewhat helpful, but unfortunately only oxidative metabolite
28 concentrations were reported, not TCE concentrations.

29 **TCA blood concentrations well predicted following TCE exposures, but TCA flux and**
30 **disposition may not be accurate**

31 TCA blood and plasma concentrations following TCE exposure are consistently well
32 predicted. However, the total flux of TCA may not be correct, as evidenced by the varying
33 degrees of consistency with urinary excretion data. Of particular importance are TCA dosing
34 studies, none of which were included in the calibration. In these studies, total recovery of
35 urinary TCA was found to be substantially less than the administered dose. However, the current
36 model assumes that urinary excretion is the only source of clearance of TCA, leading to

1 overestimation of urinary excretion. This fact, combined with the observation that under TCE
2 dosing, the model appears to give accurate predictions of TCA urinary excretion for several
3 datasets, strongly suggests a discrepancy in the amount of TCA formed from TCE. That is, since
4 the model appears to overpredict the fraction of TCA that appears in urine, it may be reducing
5 TCA production to compensate. Inclusion of the TCA dosing studies (including some oral
6 dosing studies), along with inclusion of a non-renal clearance pathway, would probably be
7 helpful in reducing these discrepancies. Finally, improvements in the TCOH-TCOG sub-model,
8 below, should also help to ensure accurate estimates of TCA kinetics.

9 **TCOH-TCOG sub-model requires revision and recalibration**

10 Blood levels of TCOH and TCOG were inconsistently predicted. Part of this is due to the
11 problems with oral uptake, as discussed above. In addition, the problems identified with the use
12 of the Abbas and Fisher (1997) data (i.e., free TCOH vs. total TCOH), mean that this sub-model
13 is not likely to be robust.

14 An additional concern is the over-prediction of urinary TCOG from the Abbas and Fisher
15 (1996) TCOH i.v. data. Like the case of TCA, this indicates that some other source of TCOH
16 clearance (not to TCA or urine—e.g., to DCA or some other untracked metabolite) is possible.
17 This pathway can be considered for inclusion, and limits can be placed on it using the available
18 data.

19 Also, like for TCA, the fact that blood and urine are relatively well predicted from TCE
20 dosing strongly suggests a discrepancy in the amount of TCOH formed from TCE. That is, since
21 the model appears to overpredict the fraction of TCOH that appears in urine, it may be reducing
22 TCOH production to compensate. Including the TCOH dosing data would likely be helpful in
23 reducing these discrepancies (however, the fact that Abbas and Fisher was only published as an
24 abstract may be a problem).

25 Finally, as with the rat, the model needs to ensure that any first pass effect is accounted
26 for appropriately. Importantly, the estimated clearance rate for glucuronidation of TCOH is
27 substantially greater than hepatic blood flow. As was shown in Okino et al. (2005), in such a
28 situation, the use of a single compartment model across dose routes will be misleading because it
29 implies a substantial first-pass effect in the liver that cannot be modeled in a single compartment
30 model. That is, since TCOH is formed in the liver from TCE, and TCOH is also glucuronidated
31 in the liver to TCOG, a substantial portion of the TCOH may be glucuronidated before reaching
32 systemic circulation. This suggests that a liver compartment for TCOH is necessary.
33 Furthermore, because substantial TCOG can be excreted in bile from the liver prior to systemic
34 circulation, a liver compartment for TCOG may also be necessary to address that first pass
35 effect.

1 The addition of the liver compartment will necessitate several changes to model
2 parameters. The distribution volume for TCOH will be replaced by two parameters: the
3 liver: blood and body: blood partition coefficients. Similarly for TCOG, liver: blood and
4 body: blood partition coefficients will need to be added. Clearance of TCOH to TCA and TCOG
5 can be redefined as occurring in the liver, and urinary clearance can be redefined as coming from
6 the rest of the body. Fortunately, there are substantial data on circulating TCOG that has not
7 been included in the calibration. These data should be extremely informative in better estimating
8 the TCOH-TCOG sub-model parameters.

9 **Uncertainty in estimates of total metabolism**

10 Closed chamber data are generally thought to provide a good indicator of total
11 metabolism. Both group-specific and population-based predictions of the only available closed
12 chamber data (Fisher et al., 1991) were fairly accurate. Unfortunately, no additional closed
13 chamber data were available. In addition, the discrepancies in observed and predicted TCE
14 blood concentrations following inhalation exposures remain unresolved. Hypothesized
15 explanations such as fractional uptake or pre-systemic elimination could have a substantial
16 impact on estimates of total metabolism.

17 In addition, no data are directly informative as to the fraction of total metabolism in the
18 lung, the amount of “untracked” hepatic oxidative metabolism (parameterized as “FracDCA”), or
19 any other extra-hepatic metabolism. The lung metabolism as currently modeled could just as
20 well be located in other extra-hepatic tissues, with little change in calibration. In addition, it is
21 difficult to distinguish between untracked hepatic oxidative metabolism and GSH conjugation,
22 particularly at low doses.

23 **A.2.3.2. *Rat model***

24 **A.2.3.2.1. *Group-specific and population-based predictions***

25 As with the mouse model, initially, the sampled group-specific parameters were used to
26 generate predictions for comparison to the calibration data. Because these parameters were
27 “optimized” for each group, these “group-specific” predictions should be accurate by design, and
28 indeed they were, as discussed in more detail in Table A.2.

29 Next, as with the mouse, only samples of the population parameters (means and
30 variances) were used, and “new groups” were sampled from appropriate distribution using these
31 population means and variances. These “new groups” then represent the predicted population
32 distribution, incorporating both variability in the population as well as uncertainty in the
33 population means and variances. These “population-based” predictions were then compared to
34 both the data used in calibration, as well as the additional data identified that was not used in
35 calibration. The Hack et al. (2006) PBPK model used for prediction was modified to

1 accommodate some of the different outputs (e.g., tissue concentrations) and exposure routes (iv,
2 ia, pv) used in the “non-calibration” data, but otherwise unchanged.

3

4 **A.2.3.2.1.1. *Group-specific predictions and calibration data***

5 [See [Appendix.linked.files\AppA.2.3.2.1.1.Hack.rat.group.calib.TCE.DRAFT.pdf](#)]

6 **A.2.3.2.1.2. *Population-based predictions and calibration and additional evaluation data***

7 [See [Appendix.linked.files\AppA.2.3.2.1.2.Hack.rat.pop.calib.eval.TCE.DRAFT.pdf](#)]

8

1 **Table A.2.** Evaluation of Hack et al. (2006) PBPK model predictions for *in vivo* data in rats.

Reference	Simulation #	Calibration data	Discussion
Andersen et al., 1987	7–11	√	Good posterior fits were obtained for these data – closed chamber data with initial concentrations from 100 ppm to 4,640 ppm.
Barton et al., 1995	17–20		It was assumed that the closed chamber volume was the same as for Andersen et al. (1987). However, the initial chamber concentrations are not clear in the paper. The values that were used in the simulations do not appear to be correct, since in many cases the time-course is inaccurately predicted even at the earliest time-points. Conclusions as to these data need to await definitive values for the initial chamber concentrations, which were not available.
Bernauer et al., 1996	1–3	√	<p>Urinary time-course data (Fig 6-7) for TCA, TCOG, and NAcDCVC was given in concentration units (mg/mg creat-hr), whereas total excretion at 48 hr (Table 2) was given in molar units (mmol excreted). In the original calibration files, the conversion from concentration to cumulative excretion was not consistent-i.e., the amount excreted at 48 hr was different. The data were revised using a conversion that forced consistency. One concern, however, is that this conversion amounts to 6.2 mg creatinine over 48 hr, or 1.14 micromol/hr. This seems very low for rats; Trevisan et al. (2001), in samples from 195 male control rats, found a median value of 4.95 micromol/hr, a mean of 5.39 micromol/hr, and a 1–99 percentile range of 2.56–10.46 micromol/hr.</p> <p>In addition, the NAcDCVC data were revised to include both 1,2- and 2,2- isomers, since the goal of the GSH pathway is primarily to constrain the total flux. Furthermore, because of the extensive inter-organ processing of GSH conjugates, and the fact that excretion was still ongoing at the end of the study (48 hr), the amount of NAcDCVC recovered can only be a lower bound on the amount ultimately excreted in urine. However, the model does not attempt to represent the excretion time-course of GSH conjugates – it merely models the total flux. This is evinced by the fact that the model predicts complete excretion by the first time point of 12 hr, whereas in the data, there is still substantial excretion occurring at 48 hr.</p> <p>Posterior fits to these data were poor in all cases except urinary TCA at the highest dose. In all other cases, TCOH/TCOG and TCA excretion was substantially overpredicted, though this is due to the revision of the data (i.e., the different assumptions about creatinine excretion). Unfortunately, of the original calibration data, this is the only one with TCA and TCOH/TCOG urinary excretion. Therefore, that part of the model is poorly calibrated. On the other hand, NAcDCVC was underpredicted for a number of reasons, as noted above.</p> <p>Because of the incomplete capture of NAcDCVC in urine, unless the model can accurately portray the time-course of NAcDCVC in urine, it should probably not be used for calibration of the GSH pathway, except perhaps as a lower bound.</p>

INTER-AGENCY REVIEW DRAFT–DO NOT CITE OR QUOTE

Reference	Simulation #	Calibration data	Discussion
Birner et al., 1993	21–22		These data only showed urine concentrations, so a conversion was made to cumulative excretion based on an assumed urine flow rate of 22.5 mL/day. Based on this, urinary NAcDCVC was underestimated by 100- to 1,000-fold. Urinary TCA was underestimated by about 2-fold in females (barely within the 95% confidence interval), and was accurately estimated in males. Note that data on urinary flow rate from Trevisan et al. (2001) in samples from 195 male control rats showed high variability, with a geometric standard deviation of 1.75, so this may explain the discrepancy in urinary TCA. However, the underestimation of urinary NAcDCVC cannot be explained this way.
Dallas et al., 1991	23–24		At the lower (50 ppm) exposure, arterial blood concentrations were consistently overpredicted by about 2.5-fold, while at the higher (500 ppm) exposure, arterial blood was overpredicted by 1.5- to 2-fold, but within the range of variability. Exhaled breath concentrations were in the middle of the predicted range of variability at both exposure levels. The ratio of exhaled breath and arterial blood should depend largely on the blood-air partition coefficient, with minor dependence on the assumed dead space. This suggests the possibility of some unaccounted-for variability in the partition coefficient (e.g., posterior mean estimated to be 15.7; <i>in vitro</i> measured values from the literature: 25.82 [Sato et al., 1977], 21.9 [Gargas et al., 1989], 25.8 [Koizumi, 1989], 13.2 [Fisher et al., 1989], posterior). Alternatively, there may be a systematic error in these data, since, as discussed below, the fit of the model to the arterial blood data of Keys et al. (2003) was highly accurate.
Fisher et al., 1989	25–28		Good posterior fits were obtained for these data (in females) – closed chamber data with initial concentrations from 300 to 5,100 ppm. There was some slight overprediction of chamber concentrations (i.e., data showed more uptake/metabolism) at the lower doses, but still within the 95% confidence interval.
Fisher et al., 1991	4–6	√	Good posterior fits were obtained from these data – plasma levels of TCA and venous blood levels of TCE.
Green and Prout, 1985	29–30		In naive rats at 500 mg/kg, urinary excretion of TCOH/TCOG and TCA at 24 hr was underpredicted (2-fold), although within the 95% confidence interval. With bile-cannulated rats at the same dose, the amount of TCOG in bile was well within the 95% confidence interval. Urinary TCOH/TCOG was still underpredicted by about 2-fold, but again still within the 95% confidence interval.
Jakobson et al., 1986	31		The only data from the experiment (500 ppm in female rats) were venous blood concentrations during exposure. There were somewhat overpredicted at early times (outside of 95% confidence interval for first 30 minutes) but was well predicted at the termination of exposure. This suggests some discrepancies in uptake to tissues that reach equilibrium quickly—the model approaches the peak concentration at a faster rate than the data suggest.

INTER-AGENCY REVIEW DRAFT–DO NOT CITE OR QUOTE

Reference	Simulation #	Calibration data	Discussion
Kaneko et al., 1994	32–35		<p>In these inhalation experiments (50–1,000 ppm), urinary excretion of TCOH/TCOG and TCA are consistently overpredicted, particularly at lower doses. The discrepancy decreases systematically as dose increases, with TCA excretion accurately predicted at 1,000 ppm (TCOH/TCOG excretion slightly below near the lower 95% confidence interval at this dose). This suggests a discrepancy in the dose-dependence of TCOH, TCOG, and TCA formation and excretion.</p> <p>On the other hand, venous blood TCE concentrations post-exposure are well predicted. TCE blood concentrations right at the end of the exposure are overpredicted; however, concentrations are rapidly declining at this point, so even a few minutes delay in obtaining the blood sample could explain the discrepancy.</p>
Keys et al., 2003	36–39		<p>These experiments collected extensive data on TCE in blood and tissues following intra-arterial (ia), oral, and inhalation exposures. For the ia exposure, blood and tissue concentrations were very well predicted by the model, even with the use of the rapidly perfused tissue concentration as a surrogate for brain, heart, kidney, liver, lung, and spleen concentrations. Similarly accurate predictions were found with the higher (500 ppm) inhalation exposure. At the lower inhalation exposure (50 ppm), there was some minor overprediction of concentrations (2-fold), particularly in fat, but values were still within the 95% confidence intervals.</p> <p>For oral exposure, the GI absorption parameters needed to be revised substantially to obtain a good fit. When the values reported by Keys et al. (2003) were used, the model generally had accurate predictions. Two exceptions were the values in the gut and fat in the first 30 minutes after exposure. In addition, the liver concentration was over-predicted in the first 30 minutes, and under-predicted at 2–4 hr, but still within the 95% confidence interval during the entire period.</p>
Kimmerle and Eben, 1973a	40–44		<p>In these inhalation experiments (49 ppm to 3,160 ppm), urinary excretion of TCOH/TCOG was systematically overpredicted (> 2-fold; outside 95% confidence interval), while excretion of TCA was accurately predicted. In addition, elimination by exhaled breath was substantially overpredicted at the lowest exposure. Blood TCOH levels were accurately predicted, but blood TCE levels were overpredicted at the 55 ppm. Part of the discrepancies may be due to limited analytic sensitivities at the lower exposures.</p>
Larson and Bull, 1992b	12–14	√	<p>The digitization in the calibration file did not appear to be accurate, as there was a 10-fold discrepancy with the original paper in the TCOH data. The data were replaced with those used by Clewell et al. (2000) and Bois (2000b). Except for the TCOH data, differences between the digitizations were 20% or less.</p> <p>Adequate posterior predictions were obtained for these data (oral dosing from 200 mg/kg to 3,000 mg/kg). All predictions were within the 95% confidence interval of posterior predictions. Better fits were obtained using group-specific posterior parameters, for which gut absorption and TCA urinary excretion parameters were more highly identified.</p>

INTER-AGENCY REVIEW DRAFT–DO NOT CITE OR QUOTE

Reference	Simulation #	Calibration data	Discussion
Lash et al., 2006	45–46		In these corn-oil gavage experiments, almost all of the measurements appeared to be systematically low, sometimes by many orders of magnitude. For example, at the lowest dose (263 mg/kg), urinary excretion of TCOH/TCOG and TCA, and blood concentrations of TCOH were overpredicted by the model by around $>10^5$ -fold. TCE concentrations in blood and tissues at 2, 4, and 8 hr were underpredicted by 10^3 - to 10^4 -fold. Many studies, including those using the corn oil gavage (Green and Prout, 1985; Hissink et al., 2002 [TBD]), with similar ranges of oral doses show good agreement with the model, it seems likely that these data are aberrant.
Lee et al., 1996	47–61		This extensive set of experiments involved multi-route administration of TCE (oral, iv, ia, portal vein), with serial measurements of arterial blood concentrations. For the oral route (8 mg/kg–64 mg/kg), the GI absorption parameters had to be modified. The values from Keys et al. (2003) were used, and the resulting predictions were quite accurate, albeit a more prominent peak was predicted. Predictions > 30 minutes after dosing were highly accurate. For the iv route (0.71 mg/kg–64 mg/kg), predictions were also highly accurate in almost all cases. At the lower doses (0.71 mg/kg and 2 mg/kg), there was slight overprediction in the first 30 minutes after dosing. At highest dose (64 mg/kg), there was slight underprediction between 1 and 2 hr after dosing. In all cases, the values were within the 95% confidence interval. For the ia route (0.71 mg/kg–16 mg/kg), all predictions were very accurate. For the pv route (0.71 mg/kg–64 mg/kg), predictions still remained in the 95% confidence interval, although there was more variation. At the lowest dose, there was overprediction in the first 30 minutes after dosing. At the highest two doses (16 mg/kg and 64 mg/kg), there was slight underprediction between 1 and 5 hr after dosing. This may in part be because a pharmacodynamic change in metabolism (e.g., via direct solvent injury proposed by Lee et al., 2000).
Lee et al., 2000	62–69		In the pv and iv exposures, blood and liver concentrations were accurately predicted. For oral exposures, the GI absorption parameters needed to be changed. While the values from Keys et al. (2003) led to accurate predictions for lower doses (2 mg/kg–16 mg/kg), at the higher doses (48 mg/kg–432 mg/kg), much slower absorption was evident. Comparisons at these higher dose are not meaningful without calibration of absorption parameters.
Prout et al., 1985	15	√	Adequate posterior fits were obtained for these data —rat dosing at 1,000 mg/kg in corn oil. All predictions were within the 95% confidence interval of posterior predictions. Better fits were obtained using group-specific posterior parameters, for which gut absorption and TCA urinary excretion parameters were more highly identified.

INTER-AGENCY REVIEW DRAFT–DO NOT CITE OR QUOTE

Reference	Simulation #	Calibration data	Discussion
Stenner et al., 1997	70		As with other oral exposures, different GI absorption parameters were necessary. Again, the values from Keys et al. (2003) were used, with some success. Blood TCA levels were accurately predicted, while TCOH blood levels were systematically under-predicted (up to 10-fold). Additional data with TCOH and TCA dosing, including naive and bile-cannulated rats, can be added when those exposure routes are added to the model. These could be useful in better calibrating the enterohepatic recirculation parameters.
Templin et al., 1995	16	√	Adequate posterior fits were obtained for blood TCA from these data—oral dosing at 100 mg/kg in Tween. Blood levels of TCOH were underpredicted, while the time-course of TCE in blood exhibited an earlier peak. Better fits were obtained using group-specific posterior parameters, for which gut absorption and TCA urinary excretion parameters (and to a lesser extent glucuronidation of TCOH and biliary excretion of TCOG) were more highly identified.

1
2

1

2 A.2.3.2.2. Conclusions regarding rat model**3 TCE concentrations in blood and tissues generally well-predicted**

4 The PBPK model for the parent compound appears to be robust. Multiple datasets not
5 used for calibration with TCE measurements in blood and tissues were simulated, and overall the
6 model gave very accurate predictions. A few datasets seemed somewhat anomalous—Dallas et
7 al. (1991), Kimmerle and Eben (1973a), Lash et al. (2006). However, data from Kaneko et al.
8 (1994), Keys et al. (2003), and Lee et al. (1996, 2000) were all well simulated, and corroborated
9 the data used for calibration (Fisher et al., 1991; Larson and Bull, 1992b; Prout et al., 1985;
10 Templin et al., 1995). Particularly important is the fact that tissue concentrations from Keys et
11 al. (2003) were well simulated.

12 Total metabolism probably well simulated, but ultimate disposition is less certain

13 Closed chamber data are generally thought to provide a good indicator of total
14 metabolism. Two closed chamber studies not used for calibration were available—Barton et al.
15 (1995) and Fisher et al. (1989). Additional experimental information is required to analyze the
16 Barton et al. (1995) data, but the predictions for the Fisher et al. (1989) data were quite accurate.

17 However, the ultimate disposition of metabolized TCE is much less certain. Clearly, the
18 flux through the GSH pathway is not well constrained, with apparent discrepancies between the
19 NAcDCVC data of Bernauer et al. (1996) and Birner et al. (1993). Moreover, each of these data
20 has limitations – in particular the Bernauer et al. (1996) data show that excretion is still
21 substantial at the end of the reporting period, so that the total flux of mercapturates has not been
22 collected. Moreover, there is some question as to the consistency of the Bernauer et al. (1996)
23 data (Table 2 versus Figures 6 7), since a direct comparison seems to imply a very low creatinine
24 excretion rate. The Birner et al. (1993) data only report concentrations—not total excretion—so
25 a urinary flow rate needs to be assumed.

26 In addition, no data are directly informative as to the fraction of total metabolism in the
27 lung or the amount of “untracked” hepatic oxidative metabolism (parameterized as “FracDCA”).
28 The lung metabolism could just as well be located in other extra-hepatic tissues, with little
29 change in calibration. In addition, there is a degeneracy between untracked hepatic oxidative
30 metabolism and GSH conjugation, particularly at low doses.

31 The ultimate disposition of TCE as excreted TCOH/TCOG or TCA is also poorly
32 estimated in some cases, as discussed in more detail below.

33 TCOH-TCOG sub-model requires revision and recalibration

34 TCOH blood levels of TCOH were inconsistently predicted in non-calibration datasets
35 (well predicted for Larson and Bull [1992b]; Kimmerle and Eben [1973a]; but not Stenner et al.
36 [1997] or Lash et al. [2006]), and the amount of TCE ultimately excreted as TCOG/TCOH also

1 appeared to be poorly predicted. The model generally underpredicted TCOG/TCOH urinary
2 excretion (underpredicted Green and Prout [1985], overpredicted Kaneko et al. [1994],
3 Kimmerle and Eben [1973a], and Lash et al. [2006]). This may in part be due to discrepancies in
4 the Bernauer et al. (1996) data as to the conversion of excretion relative to creatinine.

5 Moreover, there are relatively sparse data on TCOH in combination with a relatively
6 complex model, so the identifiability of various pathways – conversion to TCA, enterohepatic
7 recirculation, and excretion in urine – is questionable.

8 This could be improved by the ability to incorporate TCOH dosing data from Merdink et
9 al. (1999) and Stenner et al. (1997), the latter of which included bile duct cannulation to better
10 estimate enterohepatic recirculation parameters. However, the TCOH dosing in these studies is
11 by the intravenous route, whereas with TCE dosing, TCOH first appears in the liver. Thus, the
12 model needs to ensure that any first pass effect is accounted for appropriately. Importantly, the
13 estimated clearance rate for glucuronidation of TCOH is substantially greater than hepatic blood
14 flow. That is, since TCOH is formed in the liver from TCE, and TCOH is also glucuronidated in
15 the liver to TCOG, a substantial portion of the TCOH may be glucuronidated before reaching
16 systemic circulation. This suggests that a liver compartment for TCOH is necessary.
17 Furthermore, because substantial TCOG can be excreted in bile from the liver prior to systemic
18 circulation, a liver compartment for TCOG may also be necessary to address that first pass
19 effect.

20 The addition of the liver compartment will necessitate several changes to model
21 parameters. The distribution volume for TCOH will be replaced by two parameters: the
22 liver:blood and body:blood partition coefficients. Similarly for TCOG, liver:blood and
23 body:blood partition coefficients will need to be added. Clearance of TCOH to TCA and TCOG
24 can be redefined as occurring in the liver, and urinary clearance can be redefined as coming from
25 the rest of the body.

26 Finally, additional clearance of TCOH (not to TCA or urine – e.g., to DCA or some other
27 untracked metabolite) is possible. This may in part explain the discrepancy between the accurate
28 predictions to blood data along with poor predictions to urinary excretion (i.e., there is a missing
29 pathway). This pathway can be considered for inclusion, and limits can be placed on it using the
30 available data.

31 **TCA submodel would benefit from revised TCOH/TCOG sub-model and incorporating** 32 **TCA dosing studies**

33 While blood levels of TCA were well predicted in the one non-calibration dataset
34 (Stenner et al., 1997), the urinary excretion of TCA was inconsistently predicted (underpredicted
35 in Green and Prout [1985]; overpredicted in Kaneko et al. [1994] and Lash et al. [2006];

1 accurately predicted in Kimmerle and Eben [1973a]). Because TCA is in part derived from
2 TCOH, a more accurate TCOH/TCOG sub-model would probably improve the TCA sub-model.

3 In addition, there are a number of TCA dosing studies that could be used to isolate the
4 TCA kinetics from the complexities of TCE and TCOH. These could be readily incorporated
5 into the TCA sub-model.

6 Finally, as with TCOH, additional clearance of TCA (not to urine – e.g., to DCA or some
7 other untracked metabolite) is possible. This may in part explain the discrepancy between the
8 accurate predictions to blood data along with poor predictions to urinary excretion (i.e., there is a
9 missing pathway). As with TCOH, this pathway can be considered for inclusion, and limits can
10 be placed on it using the available data.

11 **A.2.3.3. *Human model***

12 **A.2.3.3.1. *Individual-specific and population-based predictions***

13 As with the mouse and rat models, initially, the sampled individual-specific parameters
14 (the term “individual” instead of “group” is used since human variability was at the individual
15 level) were used to generate predictions for comparison to the calibration data. Because these
16 parameters were “optimized” for each individual, these “individual-specific” predictions should
17 be accurate by design. However, unlike for the rat, this was not the case for some experiments
18 (this is partially responsible for the slower convergence), although the inaccuracies were
19 generally less than those in the mouse. For example, alveolar air concentrations were
20 systematically overpredicted for several datasets. There was also variability in the ability to
21 predict the precise time-course of TCA and TCOH blood levels, with a few datasets more
22 difficult for the model to accommodate. These data are discussed further in Table A.3.

23 Next, only samples of the population parameters (means and variances) were used, and
24 “new individuals” were sampled from appropriate distribution using these population means and
25 variances. These “new individuals” then represent the predicted population distribution,
26 incorporating both variability as well as uncertainty in the population means and variances.
27 These “population-based” predictions were then compared to both the data used in calibration, as
28 well as the additional data identified that was not used in calibration. The Hack et al. (2006)
29 PBPK model was modified to accommodate some of the different outputs (e.g., arterial blood,
30 intermittently collected urine, retained dose) and exposure routes (TCA iv, oral TCA and TCOH)
31 used in the “non-calibration” data, but otherwise unchanged.

32 **A.2.3.3.1.1. *Individual-specific predictions and calibration data***

33 [See [Appendix linked files\AppA.2.3.3.1.1.Hack.human.indiv.calib.TCE.DRAFT.pdf](#)]

- 1 **A.2.3.3.1.2. *Population-based predictions and calibration and additional evaluation data***
- 2 [See [Appendix.linked.files\AppA.2.3.3.1.2.Hack.human.pop.calib.eval.TCE.DRAFT.pdf](#)]
- 3

1 **Table A.3.** Evaluation of Hack et al. (2006) PBPK model predictions for *in vivo* data in humans.

Reference	Simulation #	Calibration data	Discussion
Bartonicek, 1962	38–45		<p>The measured minute-volume was multiplied by a factor of 0.7 to obtain an estimate for alveolar ventilation rate, which was fixed for each individual. These data are difficult to interpret because they consist of many single data points. It is easiest to go through the measurements one at a time:</p> <p><i>Alveolar retention</i> (1 – exhaled dose/inhaled dose during exposure) and <i>Retained dose</i> (inhaled dose – exhaled dose during exposure): Curiously, retention was generally under-predicted, which in many cases retained dose was accurately predicted. However, alveolar retention was an adjustment of the observed total retention:</p> $\text{TotRet} = (\text{CInh} - \text{CExh})/\text{CInh} = \text{QAlv} \times (\text{CInh} - \text{CAIv})/(\text{MV} \times \text{CInh}), \text{ so that}$ $\text{AlvRet} = \text{TotRet} \times (\text{QAlv}/\text{MV}), \text{ with QAlv/MV assumed to be 0.7}$ <p>Because retained dose is the more relevant quantity, and is less sensitive to assumptions about QAlv/MV, then this is the better quantity to use for calibration.</p> <p><i>Urinary TCOG</i>: This was generally underpredicted, although generally within the 95% confidence interval. Thus, these data will be informative as to inter-individual variability.</p> <p><i>Urinary TCA</i>: Total collection (at 528 hr) was accurately predicted, although the amount collected at 72 hr was generally under-predicted, sometimes substantially so.</p> <p><i>Plasma TCA</i>: Generally well predicted.</p>

INTER-AGENCY REVIEW DRAFT–DO NOT CITE OR QUOTE

Reference	Simulation #	Calibration data	Discussion
Bernauer et al., 1996	1–3	√	<p>Individual-specific predictions were good for the time-courses of urinary TCOG and TCA, but poor for total urinary TCOG+TCA and for urinary NAcDCVC. One reason for the discrepancy in urinary excretion of TCA and TCOG is that the urinary time-course data (Fig 4-5) for TCA, TCOG, and NAcDCVC was given in concentration units (mg/mg creat-hr), whereas total excretion at 48 hr (Tab 2) was given in molar units (mmol excreted). In the original calibration files, the conversion from concentration to cumulative excretion was not consistent – i.e., the amount excreted at 48 hr was different. For population-based predictions, the data were revised using a conversion that forced consistency. One concern, however, is that this conversion amounts to 400–500 mg creatinine over 48 hr, or 200–250 mg/day, which seems rather low. For instance, Araki (1978) reported creatinine excretion of 11.5+/-1.8 mmol/24 hr (mean +/- SD) in 9 individuals, corresponding to 1,300 +/- 200 mg/day.</p> <p>In addition, for population-based predictions, the NAcDCVC data were revised include both 1,2- and 2,2-isomers, since the goal of the GSH pathway is primarily to constrain the total flux. Furthermore, because of the extensive inter-organ processing of GSH conjugates, and the fact that excretion was still ongoing at the end of the study (48 hr), the amount of NAcDCVC recovered can only be a lower bound on the amount ultimately excreted in urine. However, the model does not attempt to represent the excretion time-course of GSH conjugates – it merely models the total flux. This is evinced by the fact that the model predicts complete excretion by the first time point of 12 hr, whereas in the data, there is still substantial excretion occurring at 48 hr.</p> <p>Population-based posterior fits to these data were quite good for urinary TCA and TCOH, but not for NAcDCVC in urine. Because of the incomplete capture of NAcDCVC in urine, unless the model can accurately portray the time-course of NAcDCVC in urine, it should probably not be used for calibration of the GSH pathway, except perhaps as a lower bound.</p>
Bloemen et al., 2001	72–75		<p>Like Bartonicek (1962), these data are more difficult to interpret due to their being single data points for each individual and exposure. However, in general, posterior population-based estimates of retained dose, urinary TCOG, and urinary TCA were fairly accurate, staying within the 95% confidence interval, and mostly inside the inter-quartile range. The data on GSH mercapturates are limited – first they are all non-detects. In addition, because of the 48–56 hr collection period, excretion of GSH mercapturates is probably incomplete, as noted above in the discussion of Bernauer et al. (1996).</p>

INTER-AGENCY REVIEW DRAFT–DO NOT CITE OR QUOTE

Reference	Simulation #	Calibration data	Discussion
Chiu et al., 2007	66–71		<p>The measured minute-volume was multiplied by a factor of 0.7 to obtain an estimate for alveolar ventilation rate, which was fixed for each individual. Alveolar air concentrations of TCE were generally well predicted, especially during the exposure period. Post-exposure, the initial drop in TCE concentration was generally further than predicted, but the slope of the terminal phase was similar. Blood concentrations of TCE were consistently overpredicted for all subjects and occasions.</p> <p>Blood concentrations of TCA were consistently over-predicted, though mostly staying in the lower 95% confidence region. Blood TCOH (free) levels were generally over-predicted, in many cases falling below the 95% confidence region, though in some cases the predictions were accurate. On the other hand, total TCOH (free+glucuronidated) was well predicted (or even under-predicted) in most cases – in the cases where free TCOH was accurately predicted, total TCOH was underpredicted. The free and total TCOH data reflect the higher fraction of TCOH as TCOG than previously reported (e.g., Fisher et al. [1998] reported no detectable TCOG in blood).</p> <p>Data on urinary TCA and TCOG were complicated by some measurements being saturated, as well as the intermittent nature of urine collection after day 3. Thus, only the non-saturated measurements for which the time since the last voiding was known were included for direct comparison to the model predictions. Saturated measurements were kept track of separately for comparison, but were considered only rough lower bounds.</p> <p>TCA excretion was generally over-predicted, whether looking at unsaturated or saturated measurements (the latter, would of course, be expected). Urinary excretion of TCOG generally stayed within the 95% confidence range.</p>
Fernandez et al., 1977			Alveolar air concentrations are somewhat over-estimated. Other measurements are fairly well predicted.
Fisher et al., 1998	13–33	√	<p>The majority of the data used in the calibration (both in terms of experiments and data points) came from this study. In general, the individual-specific fits to these data were good, with the exception of alveolar air concentrations, which were consistently over-predicted. In addition, for some individuals, the shape of the TCOH time-course deviated from the predictions (#14, #24, #29, and #30) – the predicted peak was too “sharp,” with underprediction at early times. Simulation #23 showed the most deviation from predictions, with substantial inaccuracies in blood TCA, TCOH, and urinary TCA.</p> <p>Interestingly, in the population-based predictions, in some cases the predictions were not very accurate – indicating that the full range of population variability is not accounted for in the posterior simulations. This is particularly the case with venous blood TCE concentrations, which are generally under-predicted in population estimates (although in some cases the predictions are accurate).</p> <p>One issue with the way in which these data were utilized in the calibration is that in some cases, the same individual was exposed to two different concentrations, but in the calibration, they were treated as separate “individuals.” Thus, parameters were allowed to vary between exposures, mixing inter-individual and inter-occasion variability. It is recommended that in subsequent calibrations, the different occasions with the same individual be modeled together. This will also allow identification of any dose-related changes in parameters (e.g., saturation).</p>

INTER-AGENCY REVIEW DRAFT–DO NOT CITE OR QUOTE

Reference	Simulation #	Calibration data	Discussion
Kimmerle and Eben, 1973b	46–57		<p>Blood TCE levels are generally over-predicted for both single and multi-exposure experiments. However, levels at the end of exposure are rapidly changing, so some of those values may be better predicted if the “exact” time after cessation of exposure were known.</p> <p>Blood TCOH levels are fairly accurately predicted, although in some individuals in single exposure experiments, there is a tendency to overpredict at early times and underpredict at late times. In multi-exposure experiments, the decline after the last exposure was somewhat steeper than predicted. Urinary excretion of TCA and TCOH was well predicted.</p> <p>Only grouped data on alveolar air concentrations were available, so they were not used.</p>
Laparé et al., 1995	34	√	<p>Predictions for these data were not accurate. However, there was an error in some of the exposure concentrations used in the original calibration. In addition, the last exposure “occasion” in these experiments involved exercise/workload, and so should be excluded. Finally, individual data are available for these experiments.</p>
	62–65 (individual data)		<p>Taking into account these changes, population-based predictions were somewhat more accurate. However, alveolar air concentrations and venous blood TCE concentrations were still over-predicted.</p>
Monster et al., 1976	5–6 (summary data)	√	<p>Individual-specific predictions were quite good, except that for blood TCA concentrations exhibited a higher peak than predicted. However, TCOH values were entered as free TCOH, whereas the TCOH data were actually total (free+glucuronidated) TCOH. Therefore, for population-based predictions, this change was made. In addition, as with the Monster et al. (1979) data, minute-volume and exhaled air concentrations were measured and incorporated for population-based predictions. Finally, individual-specific data are available, so in those data should replace the grouped data in any revised calibration. These individual data also included estimates of retained dose based on complete inhaled and exhaled air samples during exposure.</p> <p>For population-based predictions, as with the Monster et al. (1979) data, grouped urinary and blood TCOH/TCOG was somewhat under-predicted in the population-based predictions, and grouped alveolar and blood TCE concentrations were somewhat over-predicted.</p>
	58–61 (individual data)		<p>The results for the individual data were similar, but exhibited substantially greater variability than predicted. For instance, in subject A, blood TCOH levels were generally greater than the 95% confidence interval at both 70 ppm and 140 ppm, whereas predictions for blood TCOH in subject D were quite good. In another example, for blood TCE levels, predictions for subject B were quite good, but those for subject D were poor (substantially overpredicted). Thus, it is anticipated that adding these individual data will be substantially informative as to inter-individual variability, especially since all 4 individuals were exposed at 2 different doses.</p>

INTER-AGENCY REVIEW DRAFT–DO NOT CITE OR QUOTE

Reference	Simulation #	Calibration data	Discussion
Monster et al., 1979	4	√	<p>Individual-specific predictions for these data were quite good. However, TCA values were entered as plasma, whereas the TCA data were actually in whole blood. Therefore, for population-based predictions, this change was made. In addition, two additional time-courses were available that were not used in calibration: exhaled air concentrations and total TCOH blood concentrations. These were added for population-based predictions. In addition, the original article had data on ventilation rate, which as incorporated into the model. The minute volume needed to be converted to alveolar ventilation rate for the model, but this required adjusted for an extra dead-space volume of 0.15 L due to use of a mask, as suggested in the article. The measured mean minute volume was 11 L/min, and with a breathing rate of 14 breaths/min (assumed in the article), this corresponding to a total volume of 0.79 L. Subtracting the 0.15 L of mask dead space and 0.15 L of physiological dead space (suggested in the article) gives 0.49 L of total physiological dead space. Thus, the minute volume of 11 L/m was adjusted by the factor 0.49/0.79 to give an alveolar ventilation rate of 6.8 L/min, which is a reasonably typical value at rest.</p> <p>Due to extra non-physiological dead-space issue, some adjustment to the exhaled air predictions also needed to be made. The alveolar air concentration CA_{lv} was therefore estimated based on the formula:</p> $CA_{lv} = (C_{Exh} \times V_{Tot} - C_{Inh} \times V_{Ds}) / V_{Alv}$ <p>where C_{Exh} is the measured exhaled air concentration, V_{Tot} is the total volume (alveolar space V_{Alv} of 0.49 L, physiological dead space of 0.15 L, and mask dead space of 0.15 L), V_{Ds} is the total dead-space of 0.3 L, and C_{Inh} is the inhaled concentration.</p> <p>Population-based predictions for these data lead to slight under-estimation urinary TCOG and blood TCOH levels, as well as some over-prediction of alveolar air and venous blood concentrations by factors of 3~10-fold.</p>

INTER-AGENCY REVIEW DRAFT–DO NOT CITE OR QUOTE

Reference	Simulation #	Calibration data	Discussion
Muller et al., 1972, 1974, 1975	7–10	√	<p>Individual-specific predictions for these data were good, except for alveolar air concentrations. However, several problems were found with these data as utilized in the original calibration:</p> <ul style="list-style-type: none"> • Digitization problems, particular with the time axis in the multi-day exposure study (Simulation 9) that led to measurements taken prior to an exposure modeled as occurring during the exposure. The original digitization from Bois (2000b) and Clewell et al. (2000) was used for population-based estimates. • Original article showed TCA as measured in plasma, not blood as was assumed in the calibration. • Blood was taken from the earlobe, which is thought to be indicative of arterial blood concentrations, rather than venous blood concentrations. • TCOH in blood was free, not total, as Ertle et al. (1972 [cited in Methods]) had no use of beta-glucuronidase in analyzing blood samples. Separate free and total measurements were done in plasma (not whole blood), but these data were not included. • Simulation 9, contiguous data on urinary excretion were only available out to 6 days, so only that data should be included. • Simulation 10, is actually the same as the first day of simulation 9, from Muller et al. (1972, 1975) (the data were reported in both papers), and thus should be deleted. <p>These were corrected in the population-based estimates. Alveolar air concentration measurements remained over-predicted, while the change to arterial blood led to over-prediction of those measurements during exposure (but post-exposure predictions were accurate).</p>
Muller et al., 1974	81–82 (TCA and TCOH dosing)		<p>The experiment with TCA showed somewhat more rapid decline in plasma levels than predicted, but still well within the 95% confidence range. Urinary excretion was well predicted, but only accounted for 60% of the administered dose – this is not consistent with the rapid decline in TCA plasma levels (10-fold lower than peak at the end of exposure), which would seem to suggest the majority of TCA has been eliminated. With TCOH dosing, blood levels of TCOH were over-predicted in the first 5 hours, perhaps due to slower oral absorption (the augmented model used instantaneous and complete absorption). TCA plasma and urinary excretion levels were fairly well predicted. However, urinary excretion of TCOG was near the bottom of the 95% confidence interval; while, in the same individuals with TCE dosing (Simulation 7), urinary excretion of TCOG was substantially greater (near slightly above the inter-quartile region). Furthermore, total TCA and TCOG urinary excretion accounted for <40% of the administered dose.</p>
Paycok and Powell, 1945	35–37		<p>Population-based fits were good, within the inner quartile region.</p>
Sato et al., 1977	76		<p>Both alveolar air and blood concentrations are over-predicted in this model. Urinary TCA and TCOG, on the other hand, are well predicted.</p>

INTER-AGENCY REVIEW DRAFT–DO NOT CITE OR QUOTE

Reference	Simulation #	Calibration data	Discussion
Stewart et al., 1970	11	√	<p>Individual-specific predictions for these data were good, except for some alveolar air concentrations. However, a couple of problems were found with these data as utilized in the original calibration:</p> <ul style="list-style-type: none"> • The original article noted that individual took a lunch break during which there was no exposure. This was not accounted for in the calibration runs, which assumed a continuous 7-hr exposure. The exposures were therefore revised with a 3-hr morning exposure (9–12), a 1 hour lunch break (12–1), and 4-hr afternoon exposure (1–5), to mimic a typical workday. The times of the measurements had to be revised as well, since the article gave “relative” rather than “absolute” times (e.g., x hours post-exposure). • Contiguous data on urinary excretion were only available out to 11 days, so only that data should be included (Table 2). <p>With these changes, population-based predictions of urinary TCA and TCOG were still accurate, but alveolar air concentrations were over-predicted.</p>
Triebig et al., 1976	12	√	<p>Only two data points are available for alveolar air, and blood TCA and TCOH. Only one data point is available on blood TCE. Alveolar air was underpredicted at 24 hr. Blood TCA and TCOH were within the 95% confidence ranges. Blood TCE was over-predicted substantially (outside 95% confidence range).</p>

1
2
3

1 **A.2.3.3.2. *Conclusions regarding human model***

2 **TCE concentrations in blood and air are often not well-predicted**

3 Except for the Chiu et al. (2007) during exposure, TCE alveolar air levels were
4 consistently overpredicted. Even in Chiu et al. (2007), TCE levels post-exposure were over-
5 predicted, as the drop-off after the end of exposure was further than predicted. Because
6 predictions for retained dose appear to be fairly accurate, this implies that less clearance is
7 occurring via exhalation than predicted by the model. This could be the result of additional
8 metabolism or storage not accounted for by the model.

9 Except for the Fisher et al. (1998) data, TCE blood levels were consistently
10 overpredicted. Because the majority of the data used for calibration was from Fisher et al.
11 (1998), this implies that the Fisher et al. (1998) data had blood concentrations that were
12 consistently higher than the other studies. This could be due to differences in metabolism and/or
13 distribution among studies.

14 Interestingly, the mouse inhalation data also exhibited inaccurate prediction of blood
15 TCE levels. Hypotheses such as fractional uptake or pre-systemic elimination due to local
16 metabolism in the lung have not been tested experimentally, nor is it clear that they can explain
17 the discrepancies.

18 Due to the difficulty in accurately predicted blood and air concentrations, there may be
19 substantial uncertainty in tissue concentrations of TCE. However, such potential model errors
20 can be characterized estimated and estimated as part of a revised calibration.

21 **TCA blood concentrations well predicted following TCE exposures, but some uncertainty**
22 **in TCA flux and disposition**

23 TCA blood and plasma concentrations and urinary excretion, following TCE exposure,
24 are generally well predicted. Even though the model's central estimates over-predicted the Chiu
25 et al. (2007) TCA data, the confidence intervals were still wide enough to encompass those data.

26 However, the total flux of TCA may not be correct, as evidenced by TCA dosing studies,
27 none of which were included in the calibration. In these studies, total recovery of urinary TCA
28 was found to be substantially less than the administered dose. However, the current model
29 assumes that urinary excretion is the only source of clearance of TCA. This leads to
30 overestimation of urinary excretion. This fact, combined with the observation that under TCE
31 dosing, the model appears to give accurate predictions of TCA urinary excretion for several
32 datasets, strongly suggests a discrepancy in the amount of TCA formed from TCE. That is, since
33 the model appears to overpredict the fraction of TCA that appears in urine, it may be reducing
34 TCA production to compensate. Inclusion of the TCA dosing studies, along with inclusion of a
35 non-renal clearance pathway, would probably be helpful in reducing these discrepancies.

1 Finally, improvements in the TCOH-TCOG sub-model, below, should also help to insure
2 accurate estimates of TCA kinetics.

3 **TCOH-TCOG sub-model requires revision and recalibration**

4 Blood levels of TCOH and urinary excretion of TCOG were generally well predicted.
5 Additional individual data show substantial inter-individual variability than can be incorporated
6 into the calibration. Several errors as to the measurement of free or total TCOH in blood need to
7 be corrected.

8 A few inconsistencies with non-calibration datasets stand out. The presence of
9 substantial TCOG in blood in the Chiu et al. (2007) data is not predicted by the model.
10 Interestingly, only two studies that included measurements of TCOG in blood (rather than just
11 total TCOH or just free TCOH) – Muller et al. (1975), which found about 17% of total TCOH to
12 be TCOG, and Fisher et al. (1998), who could not detect TCOG. Both of these studies had
13 exposures at 100 ppm. Interestingly Muller et al. (1975) reported increased TCOG (as fraction
14 of total TCOH) with ethanol consumption, hypothesizing the inhibition of a glucuronyl
15 transferase that slowed glucuronidation. This also would result in a greater half-life for TCOH in
16 blood with ethanol consumptions, which was observed.

17 An additional concern is the over-prediction of urinary TCOG following TCOH
18 administration from the Muller et al. (1974) data. Like the case of TCA, this indicates that some
19 other source of TCOH clearance (not to TCA or urine – e.g., to DCA or some other untracked
20 metabolite) is possible. This pathway can be considered for inclusion, and limits can be placed
21 on it using the available data.

22 Also, as for TCA, the fact that blood and urine are relatively well predicted from TCE
23 dosing strongly suggests a discrepancy in the amount of TCOH formed from TCE. That is, since
24 the model appears to overpredict the fraction of TCOH that appears in urine, it may be reducing
25 TCOH production to compensate.

26 Finally, as with the rat and mice, the model needs to ensure that any first pass effect is
27 accounted for appropriately. Particularly for the Chiu et al. (2007) data, in which substantial
28 TCOG appears in blood, since TCOH is formed in the liver from TCE, and TCOH is also
29 glucuronidated in the liver to TCOG, a substantial portion of the TCOH may be glucuronidated
30 before reaching systemic circulation. Thus suggests that a liver compartment for TCOH is
31 necessary. Furthermore, because substantial TCOG can be excreted in bile from the liver prior
32 to systemic circulation, a liver compartment for TCOG may also be necessary to address that
33 first pass effect. In addition, in light of the Chiu et al. (2007) data, it may be useful to expand the
34 prior range for the K_m of TCOH glucuronidation.

35 The addition of the liver compartment will necessitate several changes to model
36 parameters. The distribution volume for TCOH will be replaced by two parameters: the

1 liver:blood and body:blood partition coefficients. Similarly for TCOG, liver:blood and
2 body:blood partition coefficients will need to be added. Clearance of TCOH to TCA and TCOG
3 can be redefined as occurring in the liver, and urinary clearance can be redefined as coming from
4 the rest of the body. Fortunately, there are *in vitro* partition coefficients for TCOH. It may be
5 important to incorporate the fact that Fisher et al. (1998) found no TCOG in blood. This can be
6 included by having the TCOH data be used for both free and total TCOH (particularly since that
7 is how the estimation of TCOG was made – by taking the difference between total and free).

8 **Uncertainty in estimates of total metabolism**

9 Estimates of total recovery after TCE exposure (TCE in exhaled air, TCA and TCOG in
10 urine) have been found to be only 60–70% (Monster et al., 1976, 1979; Chiu et al., 2007). Even
11 estimates of total recovery after TCA and TCOH dosing have found 25–50% unaccounted for in
12 urinary excretion (Paycok and Powell, 1945; Muller et al., 1974). Bartonicek found some TCOH
13 and TCA in feces, but this was about 10-fold less than that found in urine, so this cannot account
14 for the discrepancy. Therefore, it is likely that additional metabolism of TCE, TCOH, and/or
15 TCA are occurring. Additional metabolism of TCE could account for the consistent over-
16 estimation of TCE in blood and exhaled breath found in many studies. However, no data are
17 *directly* informative as to the fraction of total metabolism in the lung, the amount of “untracked”
18 hepatic oxidative metabolism (parameterized as “FracDCA”), or any other extra-hepatic
19 metabolism. The lung (TB) metabolism as currently modeled could just as well be located in
20 other extra-hepatic tissues, with little change in calibration. In addition, it is difficult to
21 distinguish between untracked hepatic oxidative metabolism and GSH conjugation, particularly
22 at low doses.

23 **A.3. Preliminary Analysis of Mouse Gas Uptake Data: Motivation for Modification of** 24 **Respiratory Metabolism**

25 Potential different model structures can be investigated using the core PBPK model
26 containing averaged input parameters, since this approach saves computational time and is more
27 efficient when testing different structural hypotheses. This approach is particularly helpful for
28 quick comparisons of data with model predictions. During the calibration process, this approach
29 was used for different routes of exposure and across all three species. For both mice and rats, the
30 closed chamber inhalation data resulted in fits that were considered not optimal when visually
31 examined. Although closed chamber inhalation usually combines multiple animals per
32 experiment, and may not be as useful in differentiating between individual and experimental
33 uncertainty (Hack et al., 2006), closed chamber data do describe *in vivo* metabolism and have
34 been historically used to quantify averaged *in vivo* Michaelis-Menten kinetics in rodents.

1 There are several assumptions used when combining PBPK modeling and closed
 2 chamber data to estimate metabolism via regression. The key experimental principles require a
 3 tight, sealed, or air-closed system where all chamber variables are controlled to known set points
 4 or monitored, that is all except for metabolism. For example, the inhalation chamber is
 5 calibrated without an animal, to determine normal absorption to the empty system. This empty
 6 chamber calibration is then followed with a dead animal experiment, identical in every way to
 7 the *in vivo* exposure, and is meant to account for every factor other than metabolism, which is
 8 zero in the dead animal. When the live animal(s) are placed in the chamber, oxygen is provided
 9 for, and carbon dioxide accumulated during breathing is removed by absorption with a chemical
 10 scrubber. A bolus injection of the parent chemical, TCE, is given and this injection time starts
 11 the inhalation exposure. The chemical inside the chamber will decrease with time, as it is
 12 absorbed by the system and the metabolic process inside the rodent. Since all known processes
 13 contributing to the decline are quantified, except for metabolism, the metabolic parameters can
 14 be extracted from the total chamber concentration decline using regression techniques.

15 The basic structure for the PBPK model that is linked to closed chamber inhalation data
 16 has the same basic structure as described before. The one major difference is the inclusion of
 17 one additional equation that accounts for mass balance changes inside the inhalation chamber or
 18 system, and connects the chamber with the inhaled and exhaled concentrations breathed in and
 19 out by the animal:
 20

$$\frac{dA_{Ch}}{dt} = RATS(Q_P)(C_X - \frac{A_{Ch}}{V_{Ch}}) - K_{LOSS}A_X$$

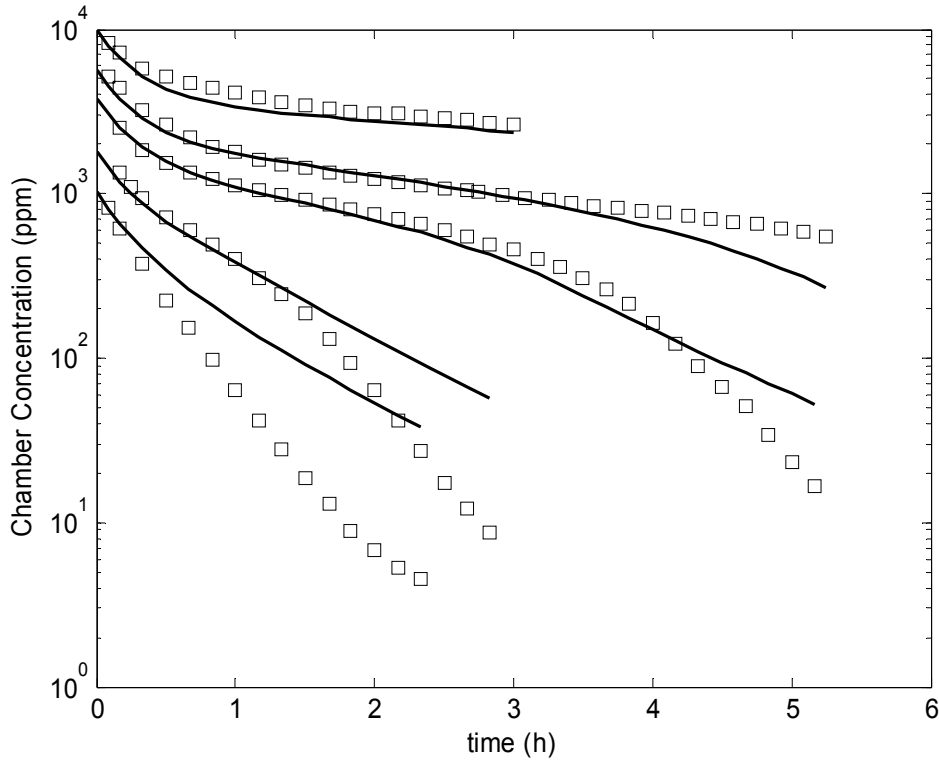
21
 22 where,
 23 RATS = number of animals in the chamber,
 24 Q_P = alveolar ventilation rate
 25 C_X = exhaled concentration
 26 C_{inh} = net chemical concentration inside chamber = net chemical amount/volume of chamber
 27 K_{LOSS} = loss rate constant to glassware
 28 A_X = amount of chemical exhaled

29 An updated model was developed that included updated physiological and chemical-
 30 specific parameters as well as GSH metabolism in the liver and kidney, as discussed in
 31 Chapter 3. The PBPK model code was translated from MCSim to use in Matlab© (version
 32 7.2.0.232, R2006a, Natick, MA) using their m language. This PBPK model made use of fixed or
 33 constant, averaged values for physiological, chemical and other input parameters; there were no
 34 statistical distributions attached to each average value. As an additional step in QC, mass

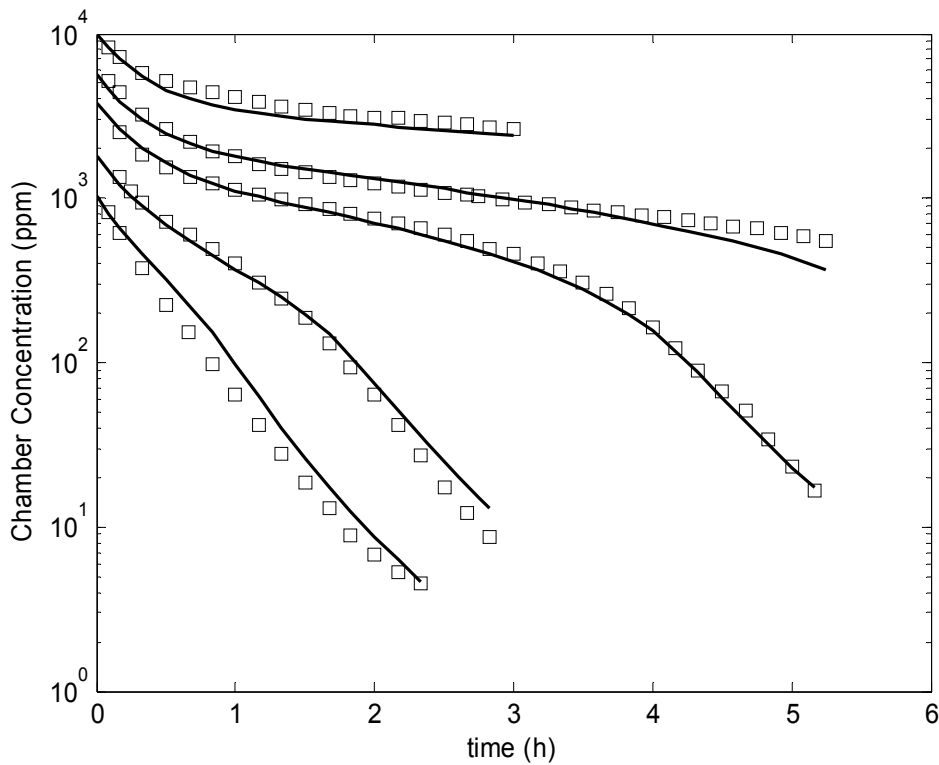
1 balance was checked for the MCSim code, and comparisons across both sets of code were made
2 to ensure that both sets of predictions were the same.

3 The resulting simulations were compared to mice gas uptake data (Fisher et al., 1991)
4 after some adjustments of the fat compartment volumes and flows based on visual fits, and
5 limited least-squares optimization of just V_{\max} (different for males and females) and K_M (same
6 for males and females). The results are shown in the top panels of Figures A.3–A.4, which
7 showed poor fits particularly at lower chamber concentrations. In particular, metabolism is
8 observed to be faster than predicted by simulation. This is directly related to metabolism of TCE
9 being limited by hepatic blood flow at these exposures. Indeed, Fisher et al. (1991) was able to
10 obtain adequate fits to these data by using cardiac output and ventilation rates that were about 2-
11 fold higher than is typical for mice. Although their later publication reporting inhalation
12 experiments (Greenberg et al., 1999) used the lower values from Brown et al. (1997) for these
13 parameters, they did not revisit the Fisher et al. (1991) data with the updated model. In addition,
14 the Hack et al. (2006) model estimated the cardiac output and ventilation rate and for these
15 experiments to be about 2-fold higher than typical. However, it seems unlikely that cardiac
16 output and ventilation rate were really as high as used in these models, since TCE and other
17 solvents typically have CNS-depressing effects. Therefore, we hypothesized that a more refined
18 treatment of respiratory metabolism may be necessary to account for the additional metabolism.

- 1 **Figure A.3. Limited optimization results for male closed chamber data from Fisher et al.**
- 2 **(1991) without (top) and with (bottom) respiratory metabolism.**

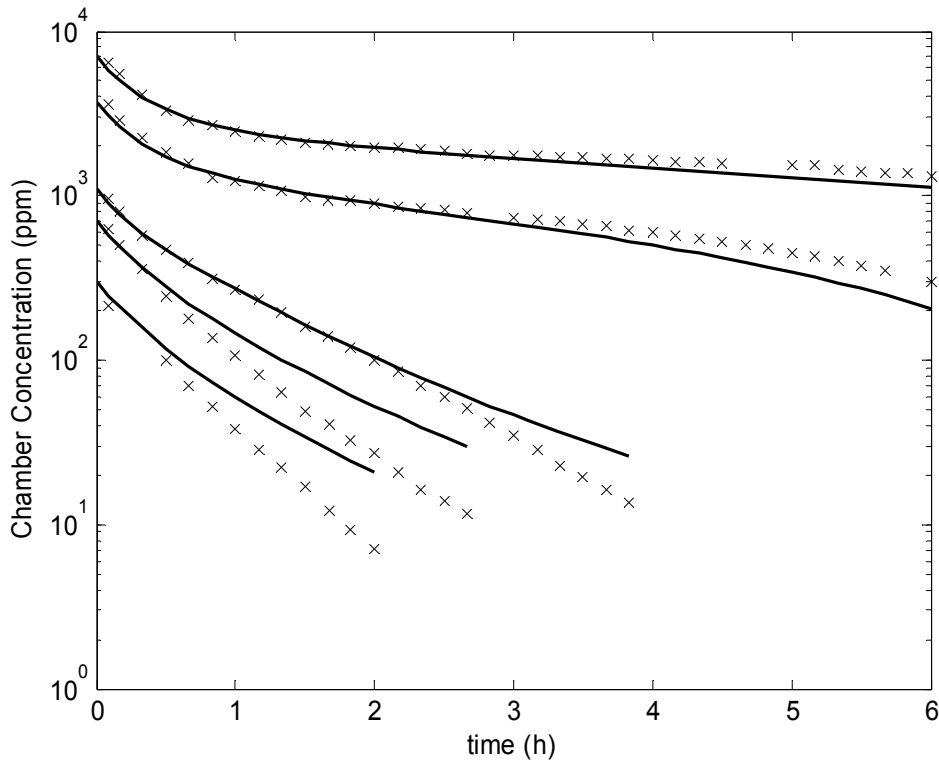


3

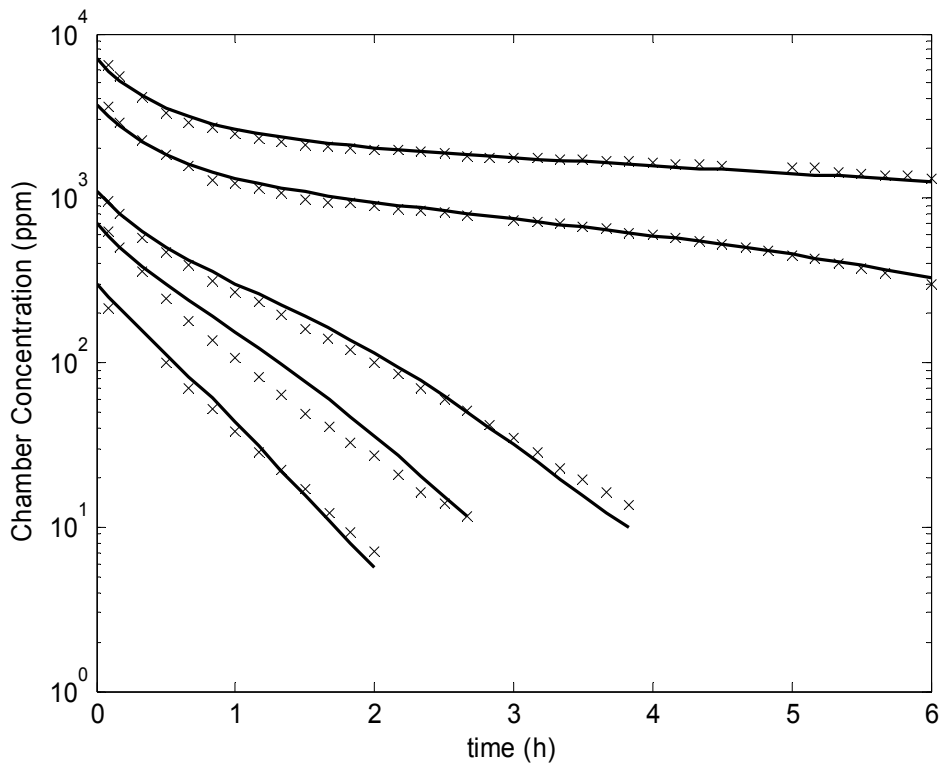


4

1 **Figure A.4. Limited optimization results for female closed chamber data from Fisher et al.**
2 **(1991) without (top) and with (bottom) respiratory metabolism.**



3

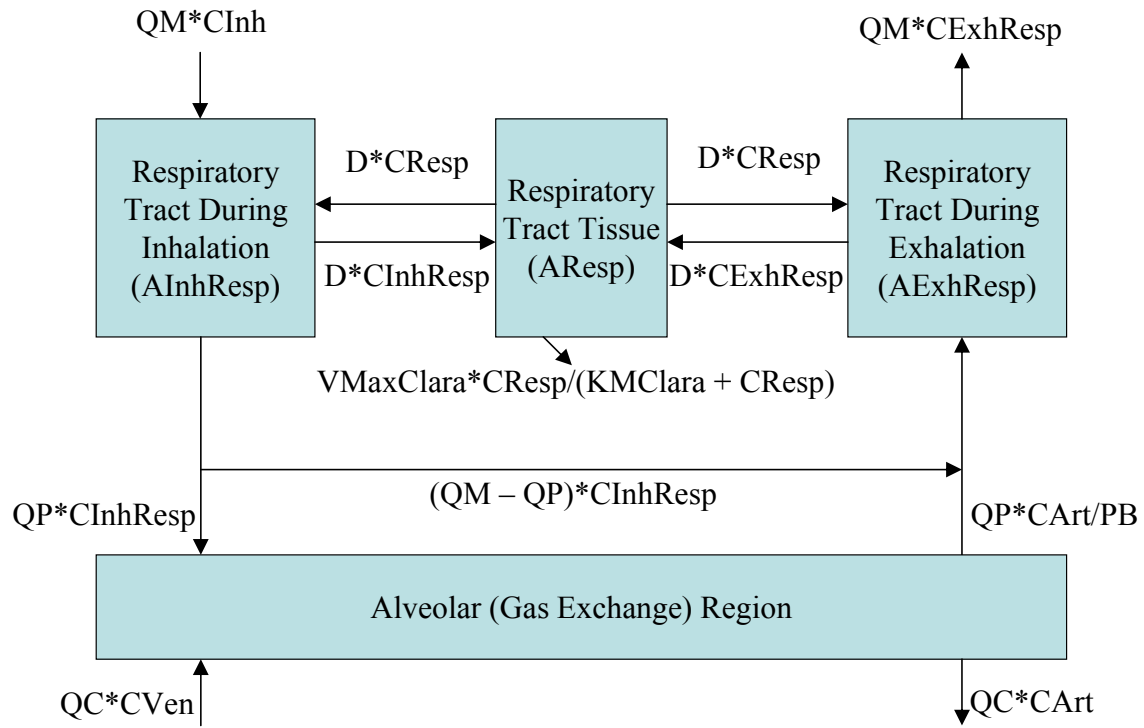


4

1 The structure of the updated respiratory metabolism model is shown in Figure A.5, with
2 the mathematical formulation shown in the model code in section A.6, where the “D” is the
3 diffusion rate, “concentrations” and “amounts” are related by the compartment volume, and the
4 other symbols have their standard meanings in the context of PBPK modeling. In brief, this is a
5 more highly “lumped” version of the Sarangapani et al. (2003) respiratory metabolism model for
6 styrene combined with a “continuous breathing” model to account for a possible wash-in/wash-
7 out effect. In brief, upon inhalation (at a rate equal to the full minute volume, not just the
8 alveolar ventilation), TCE can either (i) diffuse between the respiratory tract lumen and the
9 respiratory tract tissue; (ii) remain in the dead space, or (iii) enter the gas exchange region. In
10 the respiratory tract tissue, TCE can either be “stored” temporarily until exhalation, during which
11 it diffuses to the “exhalation” respiratory tract lumen, or be metabolized. In the dead space, TCE
12 is transferred directly to the “exhalation” respiratory tract lumen at a rate equal to the minute-
13 volume minus the alveolar ventilation rate, where it mixes with the other sources. In the gas
14 exchange region, it undergoes transfer to and from blood, as is standard for PBPK models of
15 volatile organics. Therefore, if respiratory metabolism is absent ($V_{\text{MaxClara}} = 0$), then the model
16 reduces to a wash-in/wash-out effect where TCE is temporarily adsorbed to the respiratory tract
17 tissue, the amount of which depends on the diffusion rate, the volume of the tissue, and the
18 partition coefficients.

19 The results of the same limited optimization, now with additional parameters V_{MaxClara} ,
20 K_{MClara} , and D being estimated simultaneously with the hepatic V_{Max} and K_{M} , are shown in the
21 bottom panels of Figures A.2 and A.3. The improvement in the model fits is obvious, and these
22 results served as a motivation to include this respiratory metabolism model for analysis by the
23 more formal Bayesian methods.

1 **Figure A.5. Respiratory Metabolism Model for Updated PBPK model**



1

2 **A.4. Details of the Updated PBPK Model for TCE and Its Metabolites**

3 The structure of the updated PBPK model and the statistical population model are shown
4 graphically in Chapter 3, with the model code shown below in section A.6. Details as to its
5 parameter values and their prior distributions are given below.

6 **A.4.1. Model Parameters and Baseline Values**

7 The multi-page Table A.4aA.4g below describes all the parameters of the updated PBPK
8 model, their baseline values (which are used as central estimates in the prior distributions for the
9 Bayesian analysis), and any scaling relationship used in their calculation. More detailed notes
10 are included in the comments of the model code (Section A.6).

1 **Explanatory note for all tables below:** Unless otherwise noted, the model parameter is obtained by multiplying (i) the “baseline value” (equals 1 if not
 2 specified) times (ii) the scaling parameter (or for those beginning with “ln,” which are natural-log transformed, $\exp(\ln XX)$) times (iii) any additional scaling as
 3 noted in the second to last column. Unless otherwise noted, all log-transformed scaling parameters have baseline value of 0 (i.e., $\exp(\ln XX)$ has baseline value
 4 of 1) and all other scaling parameters have baseline parameters of 1.

5 **Table A.4a. PBPK model parameters, baseline values, and scaling relationships.**

Model Parameter	Abbreviation	Baseline Value (if appl.)				Scaling (Sampled) Parameter	Additional scaling (if any)	Notes/ Source
		Mouse	Rat	Human				
				Female (or both)	Male			
Body Weight (kg)	BW	0.03	0.3	60	70			a
Flows								
Cardiac output (L/hr)	QC	11.6	13.3	16		InQCC	BW ^{3/4}	b
Alveolar ventilation (L/hr)	QP	2.5	1.9	0.96		InVPRC	QC	c
Respiratory lumen:tissue diffusion flow rate (L/hr)	DResp					InDRespC	QP	d
Physiological Blood Flows to Tissues								
Fat blood flow	QFat	0.07	0.07	0.085	0.05	QFatC	QC	e
Gut blood flow (portal vein)	QGut	0.141	0.153	0.21	0.19	QGutC	QC	
Liver blood flow (hepatic artery)	QLiv	0.02	0.021	0.065		QLivC	QC	
Slowly perfused blood flow	QSIw	0.217	0.336	0.17	0.22	QSIwC	QC	
Kidney blood flow	QKid	0.091	0.141	0.17	0.19	QKidC	QC	
Rapidly perfused blood flow	QRap							
Fraction of blood that is plasma	FracPlas	0.52	0.53	0.615	0.567	FracPlasC		f

6

^a Use measure value if available.

^b If QP is measured, then scale by QP using VPR. Baseline values are from Brown et al. (1997) (mouse and rat) and ICRP Publication 89 (2002) (human).

^c Use measured QP, if available; otherwise scale by QC using alveolar ventilation-perfusion ratio (VPR). Baseline values are from Brown et al. (1997) (mouse and rat) and ICRP Publication 89 (2002) (human).

^d Scaling parameter is relative to alveolar ventilation rate.

^e Fat represents adipose tissue only. Gut is the gastro-intestinal tract, pancrease, and spleen (all drain to the portal vein). Slowly perfused tissue is the muscle and skin. Rapidly perfused tissue is the rest of the organs, plus the bone marrow and lymph nodes, the blood flow for which is calculated as the difference between QC and the sum of the other blood flows. Baseline values are from Brown et al. (1997) (mouse and rat) and ICRP Publication 89 (2002) (human).

^f This is equal to 1 minus the hematocrit (measured value used if available). Baseline values from control animals in Hejtmancik et al. (2002) (mouse and rat) and ICRP Publication 89 (2002) (human).

1 Table A.4b. PBPK model parameters, baseline values, and scaling relationships (continued).

Model Parameter	Abbreviation	Baseline Value (if appl.)				Scaling (Sampled) Parameter	Additional scaling (if any)	Notes/ Source
		Mouse	Rat	Human				
				Female (or both)	Male			
Physiological Volumes								
Fat compartment volume (L)	VFat	0.07	0.07	0.317	0.199	VFatC	BW	^g
Gut compartment volume (L)	VGut	0.049	0.032	0.022	0.02	VGutC	BW	
Liver compartment volume (L)	VLiv	0.055	0.034	0.023	0.025	VLivC	BW	
Rapidly perfused compartment volume (L)	VRap	0.1	0.088	0.093	0.088	VRapC	BW	
Volume of respiratory lumen (L air)	VRespLum	0.004667	0.004667	0.002386		VRespLumC	BW	
Effective volume for respiratory tissue (L air)	VRespEff	0.0007	0.0005	0.00018	0.00018	VRespEffC	BW x PResp x PB	
Kidney compartment volume (L)	VKid	0.017	0.007	0.0046	0.0043	VKidC	BW	
Blood compartment volume (L)	VBld	0.049	0.074	0.068	0.077	VBldC	BW	
Total perfused volume (L)	VPerf	0.8897	0.8995	0.85778	0.8560		BW	
Slowly perfused compartment volume (L)	VSlw							
Plasma compartment volume (L)	VPlas							^h
TCA Body compartment volume (L)	VBod							ⁱ
TCOH/G Body compartment volume (L)	VBodTCOH							^j

^g Fat represents adipose tissue only, and the measured value is used, if available. Gut is the gastro-intestinal tract, pancreas, and spleen (all drain to the portal vein). Rapidly perfused tissue is the rest of the organs, plus the bone marrow and lymph nodes, minus the tracheobronchial region. The respiratory tissue volume is tracheobronchial region, with an effective air volume given by multiplying by its tissue:air partition coefficient (= tissue:blood times blood:air). The slowly perfused tissue is the muscle and skin. This leaves a small (10–15% of BW) unperfused volume that consists mostly of bone (minus marrow) and the gastro-intestinal tract contents. Baseline values are from Brown et al. (1997) (mouse and rat) and ICRP Publication 89 (2002) (human), except for volumes of the respiratory lumen, which are from Sarangapani et al. (2002).

^h Derived from blood volume using FracPlas.

ⁱ Sum of all compartments except the blood and liver.

^j Sum of all compartments except the liver.

1 Table A.4c. PBPK model parameters, baseline values, and scaling relationships (continued).

Model Parameter	Abbreviation	Baseline Value (if appl.)				Scaling (Sampled) Parameter	Additional scaling (if any)	Notes/ Source
		Mouse	Rat	Human				
				Female (or both)	Male			
TCE Distribution/Partitioning								
TCE Blood/air partition coefficient	PB	15	22	9.5	InPBC		k	
TCE Fat/Blood partition coefficient	PFat	36	27	67	InPFatC		l	
TCE Gut/Blood partition coefficient	PGut	1.9	1.4	2.6	InPGutC		m	
TCE Liver/Blood partition coefficient	PLiv	1.7	1.5	4.1	InPLivC		n	
TCE Rapidly perfused/Blood partition coefficient	PRap	1.9	1.3	2.6	InPRapC		o	
TCE Respiratory tissue:air partition coefficient	PResp	2.6	1	1.3	InPRespC		p	
TCE Kidney/Blood partition coefficient	PKid	2.1	1.3	1.6	InPKidC		q	
TCE Slowly perfused/Blood partition coefficient	PSlw	2.4	0.58	2.1	InPSlwC		r	

^k Mouse value is from pooling Abbas and Fisher (1997) and Fisher et al. (1991). Rat value is from pooling Sato et al. (1977), Gargas et al. (1989), Barton et al. (1995), Simmons et al. (2002), Koizumi (1989), and Fisher et al. (1989). Human value is from pooling Sato and Nakajima (1979), Sato et al. (1977), Gargas et al. (1989), Fiserova-Bergerova et al. (1984), Fisher et al. (1998), and Koizumi (1989).

^l Mouse value is from Abbas and Fisher (1997). Rat value is from pooling Barton et al. (1995), Sato et al. (1977), and Fisher et al. (1989). Human value is from pooling Fiserova-Bergerova et al. (1984), Fisher et al. (1998), and Sato et al. (1977).

^m Value is the geometric mean of liver and kidney (relatively high uncertainty) values.

ⁿ Mouse value is from Fisher et al. (1991). Rat value is from pooling Barton et al. (1995), Sato et al. (1977), and Fisher et al. (1989). Human value is from pooling Fiserova-Bergerova et al. (1984) and Fisher et al. (1998).

^o Mouse value is geometric mean of liver and kidney values. Rat value is the brain value from Sato et al. (1977). Human value is the brain value from Fiserova-Bergerova et al. (1984).

^p Mouse value is the lung value from Abbas and Fisher (1997). Rat value is the lung value from Sato et al. (1977). Human value is from pooling lung values from Fiserova-Bergerova et al. (1984) and Fisher et al. (1998).

^q Mouse value is from Abbas and Fisher (1997). Rat value is from pooling Barton et al. (1995) and Sato et al. (1977). Human value is from pooling Fiserova-Bergerova et al. (1984) and Fisher et al. (1998).

^r Mouse value is the muscle value from Abbas and Fisher (1997). Rat value is the muscle value from pooling Barton et al. (1995), Sato et al. (1977), and Fisher et al. (1989). Human value is the muscle value from pooling Fiserova-Bergerova et al. (1984) and Fisher et al. (1998).

1 Table A.4d. PBPK model parameters, baseline values, and scaling relationships (continued).

Model Parameter	Abbreviation	Baseline Value (if appl.)				Scaling (Sampled) Parameter	Additional scaling (if any)	Notes/ Source
		Mouse	Rat	Human				
				Female (or both)	Male			
TCA Distribution/Partitioning								
TCA blood/plasma concentration ratio	TCAPlas	0.5	0.5	0.5	InPRBCPlasTCAC	See note	^s	
Free TCA Body/blood plasma partition coefficient	PBodTCA	0.88	0.88	0.52	InPBodTCAC		^t	
Free TCA Liver/blood plasma partition coefficient	PLivTCA	1.18	1.18	0.66	InPLivTCAC			
TCA Plasma Binding								
Protein/TCA dissociation constant (umole/L)	kDissoc	107	275	182	InkDissocC		^u	
Protein concentration (umole/L)	BMax	0.88	1.22	4.62	InBMaxkDC			
TCOH and TCOG Distribution/Partitioning								
TCOH body/blood partition coefficient	PBodTCOH	1.11	1.11	0.91	InPBodTCOHC		^v	
TCOH liver/body partition coefficient	PLivTCOH	1.3	1.3	0.59	InPLivTCOHC			
TCOG body/blood partition coefficient	PBodTCOG	1.11	1.11	0.91	InPBodTCOGC		^w	
TCOG liver/body partition coefficient	PLivTCOG	1.3	1.3	0.59	InPLivTCOGC		^e	
DCVG Distribution/Partitioning								
DCVG effective volume of distribution	VDCVG				InPeffDCVG	See note	^x	

^s Scaling parameter is the effective partition coefficient between red blood cells and plasma. Thus, the TCA blood-plasma concentration ratio depends on the plasma fraction. Baseline value is based on the blood-plasma concentration ratio of 0.76 in rats (Schultz et al., 1999).

^t *In vitro* partition coefficients were determined at high concentration, when plasma binding is saturated, so should reflect the free blood:tissue partition coefficient. To get the plasma partition coefficient, the partition coefficient is multiplied by the blood:plasma concentration ratio (TCAPlas). *In vitro* values were from Abbas and Fisher (1997) in the mouse (used for both mouse and rat) and from Fisher et al. (1998). Body values based on measurements in muscle.

^u Values are based on the geometric mean of estimates based on data from Lumpkin et al. (2003), Schultz et al. (1999), Templin et al. (1993, 1995), and Yu et al. (2000). Scaling parameter for BMax is actually the ratio of BMax/kD, which determines the binding at low concentrations.

^v Data are from Abbas and Fisher (1997) in the mouse (used for the mouse and rat) and Fisher et al. (1998) (human).

^w Used *in vitro* measurements in TCOH as a proxy, but higher uncertainty is noted.

^x The scaling parameter (only used in the human model) is the effective partition coefficient for the “body” (non-blood) compartment, so that the distribution volume VDCVG is given by VBld + exp(lnPeffDCVG) × (VBod + VLiv).

1 Table A.4e. PBPK model parameters, baseline values, and scaling relationships (continued).

Model Parameter	Abbreviation	Baseline Value (if appl.)				Scaling (Sampled) Parameter	Additional scaling (if any)	Notes/ Source
		Mouse	Rat	Human				
				Female (or both)	Male			
TCE Metabolism								
V_{Max} for hepatic TCE oxidation (mg/hr)	V_{Max}	2,700	600	255		$\ln V_{Max}C$	VLiv	y
K_M for hepatic TCE oxidation (mg/L)	K_M	36	21	66		$\ln K_M C$		
Fraction of hepatic TCE oxidation not to TCA+TCOH	$FracOther$					$\ln C IC$	See note	
Fraction of hepatic TCE oxidation to TCA	$FracTCA$	0.32	0.32	0.32		$\ln FracOther C$	See note	z
V_{Max} for hepatic TCE GSH conjugation (mg/hr)	$V_{Max}DCVG$	300	66			$\ln FracTCA C$	See note	aa
K_M for hepatic TCE GSH conjugation (mg/L)	K_MDCVG	1.53	0.25	19		$\ln V_{Max}DCVGC$	VLiv	bb
V_{Max} for renal TCE GSH conjugation (mg/hr)	$V_{Max}KidDCVG$	60	6	2.9		$\ln CIDCVGC$		
K_M for renal TCE GSH conjugation (mg/L)	$K_MKidDCVG$	0.34	0.026	230		$\ln K_MDCVGC$		
				2.7		$\ln V_{Max}KidDCVGC$	VKid	
						$\ln CKidDCVGC$		
						$\ln K_MKidDCVGC$		

^y Baseline values have the following units: for V_{Max} , mg/hr/kg liver; for K_M , mg/L blood; and for clearance (Cl), L/hr/kg liver (in humans, K_M is calculated from $K_M = V_{Max}/(\exp(\ln C IC) \times V_{Liv})$. Values are based on *in vitro* (microsomal and hepatocellular preparations) from Elfarra et al. (1998), Lipscomb et al. (1997, 1998a, b). Scaling from *in vitro* data based on 32 mg microsomal protein/g liver and 99x106 hepatocytes/g liver (Barter et al., 2007). Scaling of K_M from microsomes were based on two methods: (i) assuming microsomal concentrations equal to liver tissue concentrations and (ii) using the measured microsome:air partition coefficient and a central estimate of the blood:air partition coefficient. For K_M from human hepatocyte preparations, the measured hepatocyte:air partition coefficient and a central estimate of the blood:air partition coefficient was used.

^z Scaling parameter is ratio of “DCA” to “non-DCA” oxidative pathway (where DCA is a proxy for oxidative metabolism not producing TCA or TCOH). Fraction of “other” oxidation is $\exp(\ln FracOther C)/(1 + \exp(\ln FracOther C))$.

^{aa} Scaling parameter is ratio of TCA to TCOH pathways. Baseline value based on geometric mean of Lipscomb et al. (1998) using fresh hepatocytes and Bronley-DeLancey et al. (2006) using cryogenically-preserved hepatocytes. Fraction of oxidation to TCA is $(1 - FracOther) \times \exp(\ln FracTCA C)/(1 + \exp(\ln FracTCA C))$.

^{bb} Baseline values are based on *in vitro* data. In the mouse and rat, the only *in vitro* data is at 1 or 2 mM (Lash et al., 1995, 1998). In most cases, rates at 2 mM were increased over the same sex/species at 1 mM, indicating V_{Max} has not yet been reached. These data therefore put lower bounds on both V_{Max} (in units of mg/hr/kg tissue) and clearance (in units of L/hr/kg tissue), so those are the scaling parameters used, with those bounds used as baseline values. For humans, data from Lash et al. (1999a) in the liver (hepatocytes) and the kidney (cytosol) and Green et al. (1997) (liver cytosol) was used to estimate the clearance in units of L/hr/kg tissue and K_M in units of mg/L in blood.

1 Table A.4f. PBPK model parameters, baseline values, and scaling relationships (continued).

Model Parameter	Abbreviation	Baseline Value (if appl.)				Scaling (Sampled) Parameter	Additional scaling (if any)	Notes/ Source
		Mouse	Rat	Human				
				Female (or both)	Male			
TCE Metabolism (respiratory tract)								
V_{Max} for Tracheo-bronchial TCE oxidation (mg/hr)	$V_{Max}Clara$	0.070102	0.014347	0.027273	0.025253	In$V_{Max}LungLivC$	V_{Max}	cc
K_M for Tracheo-bronchial TCE oxidation (mg/L air)	K_MClara					InK_MClara		
Fraction of respiratory oxidation entering systemic circulation	FracLungSys					InFracLungSysC	See note	dd
TCOH Metabolism								
V_{Max} for hepatic TCOH->TCA (mg/hr)	$V_{Max}TCOH$					In$V_{Max}TCOHC$	$BW^{3/4}$	
K_M for hepatic TCOH->TCA (mg/L)	K_MTCOH					InCITCOHC	$BW^{3/4}$	
V_{Max} for hepatic TCOH->TCOG (mg/hr)	$V_{Max}Gluc$					In$V_{Max}GlucC$	$BW^{3/4}$	
K_M for hepatic TCOH->TCOG (mg/L)	K_MGluc					InCIGlucC	$BW^{3/4}$	
Rate constant for hepatic TCOH->other (/hr)	$kMetTCOH$					In$kMetTCOHC$	$BW^{-1/4}$	
TCA metabolism/clearance								
Rate constant for TCA plasma->urine (/hr)	$kUrnTCA$	0.6	0.522	0.108		In$kUrnTCAC$	$VPlas^{-1}$	ee
Rate constant for hepatic TCA->other (/hr)	$kMetTCA$					In$kMetTCAC$	$BW^{-1/4}$	
TCOG metabolism/clearance								
Rate constant for TCOG liver->bile (/hr)	$kBile$					In$kBileC$	$BW^{-1/4}$	
Lumped rate constant for TCOG bile->TCOH liver (/hr)	$kEHR$					In$kEHRC$	$BW^{-1/4}$	
Rate constant for TCOG->urine (/hr)	$kUrnTCOG$	0.6	0.522	0.108		In$kUrnTCOGC$	$VBld^{-1}$	

cc Scaling parameter is the ratio of the lung to liver V_{Max} (each in units of mg/hr), with baseline values based on microsomal preparations (mg/hr/mg protein) assayed at ~ 1 mM (Green et al., 1997), further adjusted by the ratio of lung to liver tissue masses (Brown et al., 1997; ICRP Publication 89 [2002]).

dd Scaling parameter is the ratio of respiratory oxidation entering systemic circulation (translocated to the liver) to that locally cleared in the lung. Fraction of respiratory oxidation entering systemic circulation is $\exp(\ln \text{FracLungSysC}) / (1 + \exp(\ln \text{FracLungSysC}))$.

ee Baseline parameters for urinary clearance (L/hr) were based on glomerular filtration rate per unit body weight (L/hr/kg BW) from Lin (1995), multiplied by the body weights cited in the study. For TCA, these were scaled by plasma volume to obtain the rate constant (/hr), since the model clears TCA from plasma. For TCOG, these were scaled by the effective distribution volume of the body ($VBodTCOH \times PBodTCOG$) to obtain the rate constant (/hr), since the model clears TCOG from the body compartment.

INTER-AGENCY REVIEW DRAFT–DO NOT CITE OR QUOTE

1 Table A.4g. PBPK model parameters, baseline values, and scaling relationships (continued).

Model Parameter	Abbreviation	Baseline Value (if appl.)				Scaling (Sampled) Parameter	Additional scaling (if any)	Notes/ Source
		Mouse	Rat	Human				
				Female (or both)	Male			
DCVG metabolism Rate constant for hepatic DCVG->DCVC (/hr)	kDCVG					InkDCVGC	BW ^{-1/4}	ff
DCVC metabolism/clearance Lumped rate constant for DCVC->Urinary NAcDCVC (/hr)	kNAT					InkNATC	BW ^{-1/4}	gg
Rate constant for DCVC bioactivation (/hr)	kKidBioact					InkKidBioactC	BW ^{-1/4}	
Oral uptake/transfer coefficients TCE Stomach-duodenum transfer coefficient (/hr)	kTSD					InkTSD		hh
TCE Stomach absorption coefficient (/hr)	kAS					InkAS		
TCE Duodenum absorption coefficient (/hr)	kAD					InkAD		
TCA Stomach absorption coefficient (/hr)	kASTCA					InkASTCA		
TCOH Stomach absorption coefficient (/hr)	kASTCOH					InkASTCOH		

2
3

^{ff} Human model only.

^{gg} Rat and human models only.

^{hh} Baseline value for oral absorption scaling parameter are as follows: kTSD and kAS, 1.4/hr, based on human stomach half time of 0.5 hr; kAD, kASTCA, and kASTCOH, 0.75/hr, based on human small intestine transit time of 4 hr (ICRP Publication 89, 2002). These are noted to have very high uncertainty.

1
2
3
4
5
6
7
8
9

A.4.2. Statistical Distributions for Parameter Uncertainty and Variability

A.4.2.1. *Initial Prior Uncertainty in Population Mean Parameters*

The following multi-page Table A.5aA.5g describes the initial prior distributions for the population mean of the PBPK model parameters. For selected parameters, rat prior distributions were subsequently updated using the mouse posterior distributions, and human prior distributions were then updated using mouse and rat posterior distributions (see Section A.4.2.2).

1 **Explanatory note for all tables below:** All population mean parameters have either truncated normal (TruncNormal) or uniform distributions. For those with
 2 TruncNormal distributions, the mean for the population mean is 0 for natural-log transformed parameters (parameter name starting with “ln”) and 1 for
 3 untransformed parameters, with the truncation at the specified number of standard deviations (SD). All uniformly distributed parameters are natural-log
 4 transformed, so their untransformed minimum and maximum are exp(Min) and exp(Max), respectively.

5 **Table A.5a. Uncertainty distributions for the population mean of the PBPK model parameters.**

Scaling (Sampled) Parameter	Mouse			Rat			Human			Notes/ Source
	Distribution			Distribution			Distribution			
	For Trunc-Normal:	SD	Truncation (±nSD)	If Trunc-Normal:	SD	Truncation (±nSD)	For Trunc-Normal:	SD	Truncation (±nSD)	
	For Uniform:	Min	Max	If Uniform:	Min	Max	For Uniform:	Min	Max	
Flows										
InQCC	TruncNormal	0.2	4	TruncNormal	0.14	4	TruncNormal	0.2	4	ii
InVPRC	TruncNormal	0.2	4	TruncNormal	0.3	4	TruncNormal	0.2	4	
InDRespC	Uniform	-11.513	2.303	Uniform	-11.513	2.303	Uniform	-11.513	2.303	jj
Physiological Blood Flows to Tissues										
QFatC	TruncNormal	0.46	2	TruncNormal	0.46	2	TruncNormal	0.46	2	
QGutC	TruncNormal	0.17	2	TruncNormal	0.17	2	TruncNormal	0.18	2	
QLivC	TruncNormal	0.17	2	TruncNormal	0.17	2	TruncNormal	0.45	2	
QSIwC	TruncNormal	0.29	2	TruncNormal	0.3	2	TruncNormal	0.32	2	
QKidC	TruncNormal	0.32	2	TruncNormal	0.13	2	TruncNormal	0.12	2	
FracPlasC	TruncNormal	0.2	3	TruncNormal	0.2	3	TruncNormal	0.05	3	kk
Physiological Volumes										
VFatC	TruncNormal	0.45	2	TruncNormal	0.45	2	TruncNormal	0.45	2	
VGutC	TruncNormal	0.13	2	TruncNormal	0.13	2	TruncNormal	0.08	2	
VLivC	TruncNormal	0.24	2	TruncNormal	0.18	2	TruncNormal	0.23	2	
VRapC	TruncNormal	0.1	2	TruncNormal	0.12	2	TruncNormal	0.08	2	
VRespLumC	TruncNormal	0.11	2	TruncNormal	0.18	2	TruncNormal	0.2	2	
VRespEffC	TruncNormal	0.11	2	TruncNormal	0.18	2	TruncNormal	0.2	2	
VKidC	TruncNormal	0.1	2	TruncNormal	0.15	2	TruncNormal	0.17	2	
VBldC	TruncNormal	0.12	2	TruncNormal	0.12	2	TruncNormal	0.12	2	

ii Uncertainty based on CV or range of values in Brown et al. (1997) (mouse and rat) and a comparison of values from ICRP Publication 89 (2002), Brown et al. (1997), and Price et al. (2003) (human).

jj Non-informative prior distribution. These priors for the rat and human were subsequently updated (see A.4.2.2)

kk Because of potential strain differences, uncertainty in mice and rat assumed to be 20%. In humans, Price et al. (2003) reported variability of about 5%, and this is also used for the uncertainty in the mean.

1 **Table A.5b. Uncertainty distributions for the population mean of the PBPK model parameters (continued).**

Scaling (Sampled) Parameter	Mouse			Rat			Human			Notes/ Source
	Distribution			Distribution			Distribution			
	For Trunc-Normal:	SD	Truncation (±nxSD)	If Trunc-Normal:	SD	Truncation (±nxSD)	For Trunc-Normal:	SD	Truncation (±nxSD)	
	For Uniform:	Min	Max	If Uniform:	Min	Max	For Uniform:	Min	Max	
TCE Distribution/ Partitioning										
InPBC	TruncNormal	0.25	3	TruncNormal	0.25	3	TruncNormal	0.2	3	ii
InPFatC	TruncNormal	0.3	3	TruncNormal	0.3	3	TruncNormal	0.2	3	
InPGutC	TruncNormal	0.4	3	TruncNormal	0.4	3	TruncNormal	0.4	3	
InPLivC	TruncNormal	0.4	3	TruncNormal	0.15	3	TruncNormal	0.4	3	
InPRapC	TruncNormal	0.4	3	TruncNormal	0.4	3	TruncNormal	0.4	3	
InPRespC	TruncNormal	0.4	3	TruncNormal	0.4	3	TruncNormal	0.4	3	
InPKidC	TruncNormal	0.4	3	TruncNormal	0.3	3	TruncNormal	0.2	3	
InPSlwC	TruncNormal	0.4	3	TruncNormal	0.3	3	TruncNormal	0.3	3	
TCA Distribution/ Partitioning										
InPRBCPlasTCAC	Uniform	-4.605	4.605	TruncNormal	0.336	3	Uniform	-4.605	4.605	mm
InPBodTCAC	TruncNormal	0.336	3	TruncNormal	0.693	3	TruncNormal	0.336	3	nn
InPLivTCAC	TruncNormal	0.336	3	TruncNormal	0.693	3	TruncNormal	0.336	3	
TCA Plasma Binding										
InkDissocC	TruncNormal	1.191	3	TruncNormal	0.61	3	TruncNormal	0.06	3	oo
InBMaxkDC	TruncNormal	0.495	3	TruncNormal	0.47	3	TruncNormal	0.182	3	
TCOH and TCOG Distribution/ Partitioning										
InPBodTCOHC	TruncNormal	0.336	3	TruncNormal	0.693	3	TruncNormal	0.336	3	
InPLivTCOHC	TruncNormal	0.336	3	TruncNormal	0.693	3	TruncNormal	0.336	3	
InPBodTCOGC	Uniform	-4.605	4.605	Uniform	-4.605	4.605	Uniform	-4.605	4.605	
InPLivTCOGC	Uniform	-4.605	4.605	Uniform	-4.605	4.605	Uniform	-4.605	4.605	

ii For partition coefficients, it is not clear whether inter-study variability is due to inter-individual or assay variability, so uncertainty in the mean is based on inter-study variability among *in vitro* measurements. For single measurements, uncertainty SD of 0.3 was used for fat (mouse) and 0.4 for other tissues was used. In addition, where measurements were from a surrogate tissue (e.g., gut was based on liver and kidney), an uncertainty SD 0.4 was used.

mm Single *in vitro* data point available in rats, so a geometric standard deviation (GSD) of 1.4 was used. In mice and humans, where no *in vitro* data was available, a non-informative prior was used.

nn Single *in vitro* data points available in mice and humans, so a GSD of 1.4 was used. In rats, where the mouse data was used as a surrogate, a GSD of 2.0 was used, based on the difference between mice and rats *in vitro*.

oo GSD for uncertainty based on different estimates from different *in vitro* studies.

1 **Table A.5c. Uncertainty distributions for the population mean of the PBPK model parameters (continued).**

Scaling (Sampled) Parameter	Mouse			Rat			Human			Notes/Source
	Distribution			Distribution			Distribution			
	For Trunc-Normal:	SD	Truncation (±n×SD)	If Trunc-Normal:	SD	Truncation (±n×SD)	For Trunc-Normal:	SD	Truncation (±n×SD)	
	For Uniform:	Min	Max	If Uniform:	Min	Max	For Uniform:	Min	Max	
DCVG Distribution/Partitioning										
InPeffDCVG	Uniform	-6.908	6.908	Uniform	-6.908	6.908	Uniform	-6.908	6.908	pp
TCE Metabolism										
InV _{Max} C	TruncNormal	0.693	3	TruncNormal	0.693	3	TruncNormal	0.693	3	qq
InK _M C	TruncNormal	1.386	3	TruncNormal	1.386	3				b
InCIC							TruncNormal	1.386	3	b
InFracOtherC	Uniform	-6.908	6.908	Uniform	-6.908	6.908	Uniform	-6.908	6.908	a
InFracTCAC	TruncNormal	1.163	3	TruncNormal	1.163	3	TruncNormal	1.163	3	rr
InV _{Max} DCVGC	Uniform	-4.605	9.21	Uniform	-4.605	9.21				ss
InCIDCVGC	Uniform	-4.605	9.21	Uniform	-4.605	9.21	TruncNormal	4.605	3	d
InK _M DCVGC							TruncNormal	1.386	3	d
InV _{Max} KidDCVGC	Uniform	-4.605	9.21	Uniform	-4.605	9.21				d
InCIKidDCVGC	Uniform	-4.605	9.21	Uniform	-4.605	9.21	TruncNormal	4.605	3	d
InK _M KidDCVGC							TruncNormal	1.386	3	d
InV _{Max} LungLivC	TruncNormal	1.099	3	TruncNormal	1.099	3	TruncNormal	1.099	3	tt
InK _M Clara	Uniform	-6.908	6.908	Uniform	-6.908	6.908	Uniform	-6.908	6.908	a
InFracLungSysC	Uniform	-6.908	6.908	Uniform	-6.908	6.908	Uniform	-6.908	6.908	a

^{pp} Non-informative prior distribution.

^{qq} Assume 2-fold uncertainty GSD in V_{Max}, based on observed variability and uncertainties of *in vitro*-to-*in vivo* scaling. For K_M and CIC, the uncertainty is assumed to be 4-fold, due to the different methods for scaling of concentrations from TCE in the *in vitro* medium to TCE in blood.

^{rr} Uncertainty GSD of 3.2-fold reflects difference between *in vitro* measurements from Lipscomb et al. (1998) and Bronley-DeLancey et al. (2006).

^{ss} In mice and rats, the baseline values are notional lower-limits on V_{Max} and clearance, however, the lower bound of the prior distribution is set to 100-fold less because of uncertainty in *in vitro*-*in vivo* extrapolation, and because Green et al. (1997) reported values 100-fold smaller than Lash et al. (1995, 1998). In humans, the uncertainty GSD in clearance is assumed to be 100-fold, due to the difference between Lash et al. (1998) and Green et al. (1997). For K_M, the uncertainty GSD of 4-fold is based on differences between concentrations in cells and cytosol.

^{tt} Uncertainty GSD of 3-fold was assumed due to possible differences in microsomal protein content, the fact that measurements were at a single concentration, and the fact that the human baseline values was based on the limit of detection.

1 **Table A.5d. Uncertainty distributions for the population mean of the PBPK model parameters (continued).**

Scaling (Sampled) Parameter	Mouse			Rat			Human			Notes/Source
	Distribution			Distribution			Distribution			
	For Trunc-Normal:	SD	Truncation (±n×SD)	If Trunc-Normal:	SD	Truncation (±n×SD)	For Trunc-Normal:	SD	Truncation (±n×SD)	
	For Uniform:	Min	Max	If Uniform:	Min	Max	For Uniform:	Min	Max	
TCOH Metabolism										
InV _{Max} TCOHC	Uniform	-9.21	9.21	Uniform	-9.21	9.21	Uniform	-11.513	6.908	
InCITCOHC							Uniform	-9.21	9.21	
InK _M TCOH	Uniform	-9.21	9.21	Uniform	-9.21	9.21	Uniform	-9.21	9.21	
InV _{Max} GlucC	Uniform	-9.21	9.21	Uniform	-9.21	9.21				
InCIGlucC							Uniform	-9.21	4.605	
InK _M Gluc	Uniform	-6.908	6.908	Uniform	-6.908	6.908	Uniform	-6.908	6.908	
InkMetTCOHC	Uniform	-11.513	6.908	Uniform	-11.513	6.908	Uniform	-11.513	6.908	
TCA Metabolism/Clearance										
InkUrnTCAC	Uniform	-4.605	4.605	Uniform	-4.605	4.605	Uniform	-4.605	4.605	
InkMetTCAC	Uniform	-9.21	4.605	Uniform	-9.21	4.605	Uniform	-9.21	4.605	
TCOG Metabolism/Clearance										
InkBIleC	Uniform	-9.21	4.605	Uniform	-9.21	4.605	Uniform	-9.21	4.605	
InkEHRC	Uniform	-9.21	4.605	Uniform	-9.21	4.605	Uniform	-9.21	4.605	
InkUrnTCOGC	Uniform	-6.908	6.908	Uniform	-6.908	6.908	Uniform	-6.908	6.908	
DCVG Metabolism										
InFracKidDCVCC	Uniform	-6.908	6.908	Uniform	-6.908	6.908	Uniform	-6.908	6.908	
InkDCVGC	Uniform	-9.21	4.605	Uniform	-9.21	4.605	Uniform	-9.21	4.605	
DCVC Metabolism/Clearance										
InkNATC	Uniform	-9.21	4.605	Uniform	-9.21	4.605	Uniform	-9.21	4.605	
InkKidBioactC	Uniform	-9.21	4.605	Uniform	-9.21	4.605	Uniform	-9.21	4.605	
Oral uptake/Transfer Coefficients										
InkTSD	Uniform	-4.269	4.942	Uniform	-4.269	4.942	Uniform	-4.269	4.942	
InkAS	Uniform	-6.571	7.244	Uniform	-6.571	7.244	Uniform	-6.571	7.244	
InkTD	Uniform	-4.605	0	Uniform	-4.605	0	Uniform	-4.605	0	
InkAD	Uniform	-7.195	6.62	Uniform	-7.195	6.62	Uniform	-7.195	6.62	
InkASTCA	Uniform	-7.195	6.62	Uniform	-7.195	6.62	Uniform	-7.195	6.62	
InkASTCOH	Uniform	-7.195	6.62	Uniform	-7.195	6.62	Uniform	-7.195	6.62	

2 **Note:** No independent data are available on these remaining parameters, so they were given non-informative prior distributions intended to span a wide range of
 3 possibilities.

4
5

1

2 **A.4.2.2. *Inter-species scaling to update selected prior distributions in the rat and human***

3 As shown in Table A.5a–d. for several parameters, there is little or no *in vitro* or other
4 prior information available to develop informative prior distributions, so many parameters had
5 lognormal or log-uniform priors that spanned a wide range. Initially, the PBPK model for each
6 species was run with the initial prior distributions in Table A.5a–d, but, in the time available for
7 analysis (up to about 100,000 iterations), only for the mouse did all these parameters achieve
8 adequate convergence. Additional preliminary runs indicated replacing the log-uniform priors
9 with lognormal priors and/or requiring more consistency between species could lead to adequate
10 convergence. However, an objective method of “centering” the lognormal distributions that did
11 not rely on the *in vivo* data (e.g., via visual fitting or limited optimization) being calibrated
12 against was necessary in order to minimize potential bias.

13 Therefore, the approach taken was to consider three species sequentially, from mouse to
14 rat to human, and to use a model for inter-species scaling to update the prior distributions across
15 species (the original prior distributions define the prior bounds). This sequence was chosen
16 because the models are essentially “nested” in this order – the rat model adds to the mouse model
17 the “downstream” GSH conjugation pathways, and the human model adds to the rat model the
18 intermediary DCVG compartment. Therefore, for those parameters with little or no independent
19 data *only*, the mouse posteriors were used to update the rat priors, and both the mouse and rat
20 posteriors were used to update the human priors. A list of the parameters for which this scaling
21 was used to update prior distributions is contained in A.6, with the updated prior distributions.
22 The correspondence between the “scaling parameters” and the physical parameters generally
23 follows standard practice, and were explicitly described in Table A.4aA.4g. For instance, V_{Max}
24 and clearance rates are scaled by body weight to the $\frac{3}{4}$ power, whereas K_M values are assumed to
25 have no scaling, and rate constants (inverse time units) are scaled by body weight to the $-\frac{1}{4}$
26 power.

27 The scaling model is given explicitly as follows. If θ_i are the “scaling” parameters
28 (usually also natural-log-transformed) that are actually estimated, and A is the “universal”
29 (species-independent) parameter, then $\theta_i = A + \varepsilon_i$, where ε_i is the species-specific “departure”
30 from the scaling relationship, assumed to be normally distributed with variance σ_ε^2 . This
31 “scatter” in the inter-species scaling relationship is assumed to have a standard deviation of 1.15
32 = $\ln(3.16)$, so that the un-logarithmically transformed 95% confidence interval spans about 100-
33 fold (i.e., $\exp(2\sigma) = 10$). This implies that 95% of the time, the species-specific scaling
34 parameter is assumed be within 10-fold higher or lower than the “species-independent” value.

1 However, the prior bounds, which generally span a wider range, are maintained so that if the data
 2 strongly imply an extreme species-specific value, it can be accommodated.

3 Therefore, the mouse model gives an initial estimate of “A,” which is used to update the
 4 prior distribution for $\theta_r = A + \varepsilon_r$ in the rat (alternatively, since there is only one species at this
 5 stage, one could think of this as estimating the rat parameter using the mouse parameter, but with
 6 a cross-species variance is twice the allometric scatter variance). The rat and mouse together
 7 then give a “better” estimate of A, which is used to update the prior distribution for $\theta_h = A + \varepsilon_h$ in
 8 the human, with the assumed distribution for ε_h . This approach is implemented by
 9 approximating the posterior distributions by normal distributions, deriving heuristic “data” for
 10 the specific-specific parameters, and then using these pseudo-data to derive updated prior
 11 distributions for the other species parameters. Specifically, the procedure is as follows:

- 12 1. Run the mouse model.
- 13 2. Use the mouse posterior to derive the mouse “pseudo-data” D_m (equal to the posterior
 14 mean) and its uncertainty σ_m^2 (equal to the posterior variance).
- 15 3. Use the D_m as the prior mean for the rat. The prior variance for the rat is $2\sigma_\varepsilon^2 + \sigma_m^2$,
 16 which accounts for two components of species-specific departure from “species-
 17 independence” (one each for mouse and rat), and the mouse posterior uncertainty.
- 18 4. Match the rat posterior mean and variance to the values derived from the normal
 19 approximation (posterior mean= $\{D_m/(2\sigma_\varepsilon^2 + \sigma_m^2) + D_r/\sigma_r^2\} / \{1/(2\sigma_\varepsilon^2 + \sigma_m^2) + 1/\sigma_r^2\}$;
 20 posterior variance= $\{1/(2\sigma_\varepsilon^2 + \sigma_m^2) + 1/\sigma_r^2\}^{-1}$), and solve for the rat “data” D_r and its
 21 uncertainty σ_r^2 .
- 22 5. Use σ_m^2 , and σ_r^2 to derive the updated prior mean and variance for the human model.
 23 For the mean ($=\{D_m/(\sigma_\varepsilon^2 + \sigma_m^2) + D_r/(\sigma_\varepsilon^2 + \sigma_r^2)\} / \{1/(\sigma_\varepsilon^2 + \sigma_m^2) + 1/(\sigma_\varepsilon^2 + \sigma_r^2)\}$), it is the
 24 weighted average of the mouse and rat, with each weight including both posterior
 25 uncertainty and departure from “species-independence.” For the variance ($=\{1/(\sigma_\varepsilon^2 +$
 26 $\sigma_m^2) + 1/(\sigma_\varepsilon^2 + \sigma_r^2)\}^{-1} + \sigma_\varepsilon^2$), it is the variance in the weighted average of the mouse and
 27 rat plus an additional component of species-specific departure from “species-
 28 independence.”

29

30 Formally, then, we can write the probability of θ_i given A as

31

$$32 \quad P(\theta_i | A) = \varphi(\theta_i - A, \sigma_\varepsilon^2) \tag{1}$$

33

34 where $\varphi(x, \sigma^2)$ is the normal density centered on 0 with variance σ^2 . Let D_i be a heuristic
 35 “datum” for species i , so the likelihood given θ_i is adequately approximated by

36

$$1 \quad P(D_i | \theta_i) = \varphi(D_i - \theta_i, \sigma_i^2) \quad (2)$$

2

3 Therefore, considering A to have a uniform prior distribution, then running the mouse model
4 gives a posterior of the form

5

$$6 \quad P(A, \theta_m | D_m) \propto P(A) P(\theta_m | A) P(D_m | \theta_m) \propto \varphi(\theta_m - A, \sigma_\varepsilon^2) \varphi(D_m - \theta_m, \sigma_m^2) \quad (3)$$

7

8 From the MCMC posterior, we identify the values of D_m and σ_m^2 as simply the mean and
9 variance of the scaled parameter θ_m .

10

11 Now, if we add the rat data, then we have

12

$$13 \quad P(A, \theta_m, \theta_r | D_m, D_r) \propto P(A) P(\theta_m | A) P(D_m | \theta_m) P(\theta_r | A) P(D_r | \theta_r) \quad (4)$$

$$14 \quad \propto \varphi(\theta_m - A, \sigma_\varepsilon^2) \varphi(D_m - \theta_m, \sigma_m^2) \varphi(\theta_r - A, \sigma_\varepsilon^2) \varphi(D_r - \theta_r, \sigma_r^2) \quad (5)$$

15

16 We can identify D_r and σ_r^2 by marginalizing first over θ_m and then over A:

17

$$18 \quad \int P(A, \theta_m, \theta_r | D_m, D_r) d\theta_m dA$$

$$19 \quad \propto \left[\int P(A) \left\{ \int P(\theta_m | A) P(D_m | \theta_m) d\theta_m \right\} P(\theta_r | A) dA \right] P(D_r | \theta_r) \quad (5)$$

$$20 \quad = \left[\int P(A) P(D_m | A) P(\theta_r | A) dA \right] P(D_r | \theta_r) \quad (6)$$

$$21 \quad \propto \left[\int P(A | D_m) P(\theta_r | A) dA \right] P(D_r | \theta_r) \quad (7)$$

$$22 \quad = P(\theta_r | D_m) P(D_r | \theta_r) \quad (8)$$

23 So we can identify the $P(\theta_r | D_m)$ as the prior for θ_r based on the mouse data, and $P(D_r | \theta_r)$ as the
24 rat-specific likelihood. The updated prior for the rats is then

$$25 \quad P(\theta_r | D_m) \propto \int \varphi(\theta_m - A, \sigma_\varepsilon^2) \varphi(D_m - \theta_m, \sigma_m^2) \varphi(\theta_r - A, \sigma_\varepsilon^2) d\theta_m dA \quad (9)$$

$$26 \quad = \int \varphi(D_m - A, \sigma_\varepsilon^2 + \sigma_m^2) \varphi(\theta_r - A, \sigma_\varepsilon^2) dA \quad (10)$$

$$27 \quad = \varphi(D_m - \theta_r, 2\sigma_\varepsilon^2 + \sigma_m^2) \quad (11)$$

28

29 Therefore, for the “mouse-based” prior, use the mean D_m from the mouse, and then the variance
30 from the mouse σ_m^2 plus twice the “allometric scatter” variance σ_ε^2 .

31

32 We can now derive the rat “data” and variance, assuming conditional independence of the rat and
33 mouse “pseudo-data,” as

$$34 \quad P(\theta_r | D_m, D_r) \propto P(\theta_r | D_m) P(D_r | \theta_r) \quad (12)$$

$$35 \quad \propto \varphi(D_m - \theta_r, 2\sigma_\varepsilon^2 + \sigma_m^2) \varphi(D_r - \theta_r, \sigma_r^2) \quad (13)$$

1 This distribution is also normal with

$$2 E(\theta_r) = \{D_m/(2\sigma_\epsilon^2 + \sigma_m^2) + D_r/\sigma_r^2\} / \{1/(2\sigma_\epsilon^2 + \sigma_m^2) + 1/\sigma_r^2\} = \text{weighted mean of } D_r \quad (14)$$

$$3 \text{VAR}(\theta_r) = \{1/(2\sigma_\epsilon^2 + \sigma_m^2) + 1/\sigma_r^2\}^{-1} = \text{harmonic mean of variances} \quad (15)$$

4

5 Thus, using the mean and variance of the posterior distribution from the MCMC analysis, D_r and
6 σ_r^2 can be derived.

7

8 Now, D_m , σ_m^2 , D_r , and σ_r^2 are known, so the analogous “mouse+rat” based prior used in the
9 human model can be derived. As with the rat prior, the human prior is based on a normal
10 approximation of the posterior for A, and then incorporates a random term for cross-species
11 variation (allometric scatter).

12

$$13 P(A, \theta_m, \theta_r, \theta_h | D_m, D_r, D_h) \quad (16)$$

$$14 \propto P(A) P(\theta_m | A) P(D_m | \theta_m) P(\theta_r | A) P(D_r | \theta_r) P(\theta_h | A) P(D_h | \theta_h)$$

$$15 \propto \varphi(\theta_m - A, \sigma_\epsilon^2) \varphi(D_m - \theta_m, \sigma_m^2) \varphi(\theta_r - A, \sigma_\epsilon^2) \varphi(D_r - \theta_r, \sigma_r^2) \quad (17)$$

$$16 \varphi(\theta_h - A, \sigma_\epsilon^2) \varphi(D_h - \theta_h, \sigma_h^2)$$

17

18 Consider marginalizing first over θ_m , then over θ_r , and then over A:

$$19 \int P(A, \theta_m, \theta_r, \theta_h | D_m, D_r, D_h) d\theta_m d\theta_r dA$$

$$20 \propto \left[\int P(A) \{ \int P(\theta_m | A) P(D_m | \theta_m) d\theta_m \} \{ \int P(\theta_r | A) P(D_r | \theta_r) d\theta_r \} P(\theta_h | A) dA \right] P(D_h | \theta_h) \quad (18)$$

$$21 = \left[\int P(A) P(D_m | A) P(D_r | A) P(\theta_h | A) dA \right] P(D_h | \theta_h) \quad (19)$$

$$22 \propto \left[\int P(A | D_m D_r) P(\theta_h | A) dA \right] P(D_h | \theta_h) \quad (20)$$

$$23 = P(\theta_h | D_m D_r) P(D_h | \theta_h) \quad (21)$$

24 So we can identify the $P(\theta_h | D_m D_r)$ as the prior for θ_h based on the mouse and rat data, and $P(D_h$
25 $| \theta_h)$ as the human-specific likelihood. The prior we use in the MCMC analysis for the humans,
26 and it is derived to be

$$27 P(\theta_h | D_m D_r) \propto \int \varphi(\theta_m - A, \sigma_\epsilon^2) \varphi(D_m - \theta_m, \sigma_m^2) \varphi(\theta_r - A, \sigma_\epsilon^2) \varphi(D_r - \theta_r, \sigma_r^2) \varphi(\theta_h - A, \sigma_\epsilon^2) \quad (22)$$

$$28 d\theta_m d\theta_r dA$$

$$29 = \int [\varphi(D_m - A, \sigma_\epsilon^2 + \sigma_m^2) \varphi(D_r - A, \sigma_\epsilon^2 + \sigma_r^2)] \varphi(\theta_h - A, \sigma_\epsilon^2) dA \quad (23)$$

$$30 \propto \int \varphi(D_{m+r} - A, \sigma_{m+r}^2) \varphi(\theta_h - A, \sigma_\epsilon^2) dA \quad (24)$$

$$31 = \varphi(D_{m+r} - \theta_h, \sigma_{m+r}^2 + \sigma_\epsilon^2) \quad (25)$$

32

33 where D_{m+r} and σ_{m+r}^2 are the weighted mean and variances of A under the density

$$34 [\varphi(D_m - A, \sigma_\epsilon^2 + \sigma_m^2) \varphi(D_r - A, \sigma_\epsilon^2 + \sigma_r^2)] \quad (26)$$

35

1 which is given by

$$2 \quad D_{m+r} = E(A | D_m D_r) = \{D_m/(\sigma_\varepsilon^2 + \sigma_m^2) + D_r/(\sigma_\varepsilon^2 + \sigma_r^2)\} / \{1/(\sigma_\varepsilon^2 + \sigma_m^2) + 1/(\sigma_\varepsilon^2 + \sigma_r^2)\}$$

3 = weighted mean of D_m and D_r (27)

$$4 \quad \sigma_{m+r}^2 = \text{VAR}(A | D_m D_r) = \{1/(\sigma_\varepsilon^2 + \sigma_m^2) + 1/(\sigma_\varepsilon^2 + \sigma_r^2)\}^{-1} = \text{harmonic mean of variances} \quad (28)$$

5 At this point, these values are used in the normal approximation of the combined rodent
6 posterior, which will be incorporated into the cross-species extrapolation as described in Step 5
7 above.

8 The results of these calculations for the updated prior distributions, are shown in Table
9 A.6. With this methodology for updating the prior distributions, adequate convergence was
10 achieved for the rat and human after 110,000~140,000 iterations.

1

2 **Table A.6. Updated prior distributions for selected parameters in the rat and human.**

Scaling parameter	Initial prior bounds		Updated rat prior		Updated human prior	
	exp(min)	exp(max)	exp(μ)	exp(σ)	exp(μ)	exp(σ)
InDRespC	1.00E-05	1.00E+01	1.22	5.21	1.84	4.18
InPBodTCOGC	1.00E-02	1.00E+02	0.42	5.47	0.81	5.10
InPLivTCOGC	1.00E-02	1.00E+02	1.01	5.31	2.92	4.31
InFracOtherC	1.00E-03	1.00E+03	0.02	6.82	0.14	4.76
InV _{Max} DCVGC	1.00E-02	1.00E+04	2.61	42.52		
InCIDCVGC	1.00E-02	1.00E+04	0.36	15.03		
InV _{Max} KidDCVGC	1.00E-02	1.00E+04	2.56	22.65		
InCIKidDCVGC	1.00E-02	1.00E+04	1.22	15.03		
InV _{Max} LungLivC	3.70E-02	2.70E+01	2.77	6.17	2.80	4.71
InK _M Clara	1.00E-03	1.00E+03	0.01	6.69	0.02	4.85
InFracLungSysC	1.00E-03	1.00E+03	4.39	11.13	3.10	8.08
InV _{Max} TCOHC	1.00E-04	1.00E+04	1.65	5.42		
InCITCOHC	1.00E-05	1.00E+03			0.37	4.44
InK _M TCOH	1.00E-04	1.00E+04	0.93	5.64	4.81	4.53
InV _{Max} GlucC	1.00E-04	1.00E+04	69.41	5.58		
InCIGlucC	1.00E-04	1.00E+02			3.39	4.35
InK _M Gluc	1.00E-03	1.00E+03	30.57	6.11	11.13	4.57
InkMetTCOHC	1.00E-05	1.00E+03	3.35	5.87	2.39	4.62
InkUrnTCAC	1.00E-02	1.00E+02	0.11	5.42	0.09	4.22
InkMetTCAC	1.00E-04	1.00E+02	0.61	5.37	0.45	4.26
InkBileC	1.00E-04	1.00E+02	1.01	5.70	3.39	4.44
InkEHRC	1.00E-04	1.00E+02	0.01	6.62	0.22	4.71
InkUrnTCOGC	1.00E-03	1.00E+03	8.58	6.05	16.12	4.81
InkNATC	1.00E-04	1.00E+02			0.00	6.11
InkKidBioactC	1.00E-04	1.00E+02			0.01	6.49

3 Notes: updated rat prior is based on the mouse posterior; and the updated human priors are based
4 on combining the mouse and rat posteriors, except in the case of InkNATC and InkKidBioactC,
5 which are unidentified in the mouse model. Columns labeled exp(min) and exp(max) are the
6 exponentiated prior bounds; columns labeled exp(μ) and exp(σ) are the exponentiated mean and
7 standard deviation of the updated prior distributions, which are normal distributions truncated at
8 the prior bounds.

9

10

11

12

13 **A.4.2.3. Population Variance: Prior Central Estimates and Uncertainty**

14 The following multi-page Tables A.7aA.7d describe the uncertainty distributions used for the
15 population variability in the PBPK model parameters.

16

1 **Explanatory note for all tables below:** All population variance parameters (V_pname, for parameter “pname”)
 2 have Inverse-Gamma distributions, with the expected value given by CV and coefficient of uncertainty given by CU
 3 (i.e., standard deviation of V_pname divided by expected value of V_pname) (notation the same as Hack et al.
 4 [2006]). Under these conditions, the Inverse-Gamma distribution has a shape parameter is given by $\alpha = 2 + 1/CU^2$
 5 and scale parameter $\beta = (\alpha - 1) CV^2$. In addition, it should be noted that, under a normal distribution and a uniform
 6 prior distribution on the population variance, the posterior distribution for the variance given n data points with a
 7 sample variance s^2 is given by and Inverse-Gamma distribution with $\alpha = (n-1)/2$ and $\beta = \alpha s^2$. Therefore, the
 8 “effective” number of data points is given by $n = 5 + 2/CU^2$ and the “effective” sample variance is $s^2 = CV^2$
 9 $\alpha/(\alpha - 1)$.

10
 11 **Table A.7a. Uncertainty distributions for the population variance of the PBPK model**
 12 **parameters.**

Scaling (Sampled) Parameter	Mouse		Rat		Human		Notes/Source
	CV	CU	CV	CU	CV	CU	
Flows							
InQCC	0.2	2	0.14	2	0.2	2	uu
InVPRC	0.2	2	0.3	2	0.2	2	
InDRespC	0.2	0.5	0.2	0.5	0.2	0.5	
Physiological Blood Flows to Tissues							
QFatC	0.46	0.5	0.46	0.5	0.46	0.5	
QGutC	0.17	0.5	0.17	0.5	0.18	0.5	
QLivC	0.17	0.5	0.17	0.5	0.45	0.5	
QSlwC	0.29	0.5	0.3	0.5	0.32	0.5	
QKidC	0.32	0.5	0.13	0.5	0.12	0.5	
FracPlasC	0.2	0.5	0.2	0.5	0.05	0.5	
Physiological Volumes							
VFatC	0.45	0.5	0.45	0.5	0.45	0.5	
VGutC	0.13	0.5	0.13	0.5	0.08	0.5	
VLivC	0.24	0.5	0.18	0.5	0.23	0.5	
VRapC	0.1	0.5	0.12	0.5	0.08	0.5	
VRespLumC	0.11	0.5	0.18	0.5	0.2	0.5	
VRespEffC	0.11	0.5	0.18	0.5	0.2	0.5	
VKidC	0.1	0.5	0.15	0.5	0.17	0.5	
VBldC	0.12	0.5	0.12	0.5	0.12	0.5	

13
 uu For physiological parameters, CV values generally taken to be equal to the uncertainty SD in the population mean, most of which were based on variability between studies (i.e., not clear whether variability represents uncertainty or variability). Given this uncertainty, CU of 2 assigned to cardiac output and ventilation-perfusion, while CU of 0.5 assigned to the remaining physiological parameters.

1 **Table A.7b. Uncertainty distributions for the population variance of the PBPK model**
 2 **parameters (continued).**

3

Scaling (Sampled) Parameter	Mouse		Rat		Human		Notes/ Source
	CV	CU	CV	CU	CV	CU	
TCE Distribution/Partitioning							
InPBC	0.25	2	0.25	0.333	0.185	0.333	vw
InPFatC	0.3	2	0.3	0.333	0.2	1	
InPGutC	0.4	2	0.4	2	0.4	2	
InPLivC	0.4	2	0.15	0.333	0.4	1.414	
InPRapC	0.4	2	0.4	2	0.4	2	
InPRespC	0.4	2	0.4	2	0.4	2	
InPKidC	0.4	2	0.3	0.577	0.2	1.414	
InPSlwC	0.4	2	0.3	0.333	0.3	1.414	
TCA Distribution/Partitioning							
InPRBCPlasTCAC	0.336	2	0.336	2	0.336	2	ww
InPBodTCAC	0.336	2	0.693	2	0.336	2	
InPLivTCAC	0.336	2	0.693	2	0.336	2	
TCA Plasma Binding							
InkDissocC	1.191	2	0.61	2	0.06	2	
InBMaxkDC	0.495	2	0.47	2	0.182	2	
TCOH and TCOG Distribution/Partitioning							
InPBodTCOHC	0.336	2	0.693	2	0.336	2	
InPLivTCOHC	0.336	2	0.693	2	0.336	2	
InPBodTCOGC	0.4	2	0.4	2	0.4	2	xx
InPLivTCOGC	0.4	2	0.4	2	0.4	2	
DCVG Distribution/Partitioning							
InPeffDCVG	0.4	2	0.4	2	0.4	2	

4

^{vw} As discussed above, it is not clear whether inter-study variability is due to inter-individual or assay variability, so the same central were assigned to the uncertainty in the population mean as to the central estimate of the population variance. In the cases where direct measurements were available, the CU for the uncertainty in the population variance is based on the actual sample n , with the derivation discussed in the notes preceding this table. Otherwise, a CU of 2 was assigned, reflecting high uncertainty.

^{ww} Used value from uncertainty in population in mean in rats for all species with high uncertainty.

^{xx} No data, so assumed CV of 0.4 with high uncertainty.

1 **Table A.7c. Uncertainty distributions for the population variance of the PBPK model**
 2 **parameters (continued).**

Scaling (Sampled) Parameter	Mouse		Rat		Human		Notes/ Source
	CV	CU	CV	CU	CV	CU	
TCE Metabolism							
InV _{Max} C	0.824	1	0.806	1	0.708	0.26	yy
InK _M C	0.270	1	1.200	1			
InCIC					0.944	1.41	
InFracOtherC	0.5	2	0.5	2	0.5	2	zz
InFracTCAC	0.5	2	0.5	2	1.8	2	aaa
InV _{Max} DCVGC	0.5	2	0.5	2			
InCIDCVGC	0.5	2	0.5	2	0.5	2	
InK _M DCVGC					0.5	2	
InV _{Max} KidDCVGC	0.5	2	0.5	2			
InCICidDCVGC	0.5	2	0.5	2	0.5	2	
InK _M KidDCVGC					0.5	2	
InV _{Max} LungLivC	0.5	2	0.5	2	0.5	2	
InK _M Clara	0.5	2	0.5	2	0.5	2	
InFracLungSysC	0.5	2	0.5	2	0.5	2	
TCOH Metabolism							
InV _{Max} TCOHC	0.5	2	0.5	2			
InCITCOHC					0.5	2	
InK _M TCOH	0.5	2	0.5	2	0.5	2	
InV _{Max} GlucC	0.5	2	0.5	2			
InCIGlucC					0.5	2	
InK _M Gluc	0.5	2	0.5	2	0.5	2	
InkMetTCOHC	0.5	2	0.5	2	0.5	2	
TCA Metabolism/Clearance							
InkUrnTCAC	0.5	2	0.5	2	0.5	2	
InkMetTCAC	0.5	2	0.5	2	0.5	2	
TCOG Metabolism/Clearance							
InkBileC	0.5	2	0.5	2	0.5	2	
InkEHRC	0.5	2	0.5	2	0.5	2	
InkUrnTCOGC	0.5	2	0.5	2	0.5	2	

^{yy} For mice and rats, based on variability in results from Lipscomb et al. (1998b) and Elfarra et al. (1998) in microsomes. Since only pooled or mean values are available, CU of 1 was assigned (moderate uncertainty). For humans, based on variability in *individual* samples from Lipscomb et al. (1997) (microsomes), Elfarra et al. (1998) (microsomes) and Lipscomb et al. (1998a) (freshly isolated hepatocytes). High uncertainty in clearance (InCIC) reflects two different methods for scaling concentrations in microsomal preparations to blood concentrations: (1) assuming microsomal concentration equals liver concentration and then using the measured liver: blood partition coefficient to convert to blood and (2) using the measured microsome: air partition coefficient and then using the measured blood: air partition coefficient to convert to blood.

^{zz} No data on variability, so a CV of 0.5 was assigned, with a CU of 2.

^{aaa} For mice and rats, no data on variability, so a CV of 0.5 was assigned, with a CU of 2. For humans, 6-fold variability based on *in vitro* data from Bronley-DeLancy et al. (2006), but with high uncertainty.

1 **Table A.7d. Uncertainty distributions for the population variance of the PBPK model**
 2 **parameters (continued).**

Scaling (Sampled) Parameter	Mouse		Rat		Human		Notes/ Source
	CV	CU	CV	CU	CV	CU	
DCVG Metabolism/Clearance							
InFracKidDCVCC	0.5	2	0.5	2	0.5	2	bbb
InkDCVGC	0.5	2	0.5	2	0.5	2	
DCVC Metabolism/Clearance							
InkNATC	0.5	2	0.5	2	0.5	2	
InkKidBioactC	0.5	2	0.5	2	0.5	2	
Oral Uptake/Transfer Coefficients							
InkTSD	2	2	2	2	2	2	ccc
InkAS	2	2	2	2	2	2	
InkTD	2	2	2	2	2	2	
InkAD	2	2	2	2	2	2	
InkASTCA	2	2	2	2	2	2	
InkASTCOH	2	2	2	2	2	2	

3

4 **A.4.2.4. Prior distributions for residual error estimates**

5 In all cases except one, the likelihood was assumed to be lognormal, which requires
 6 specification of the variance of the “residual error.” This error may include variability due to
 7 measurement error, intra-individual and intra-study heterogeneity, as well as model
 8 misspecification. The available *in vivo* measurements to which the model was calibrated are
 9 listed in Table A.8. The variances for each of the corresponding residual errors were given log-
 10 uniform distributions. For all measurements, the bounds on the log-uniform distribution was
 11 0.01 and 3.3, corresponding to geometric standard deviations bounded by 1.11 and 6.15. The
 12 lower bound was set to prevent “over-fitting,” as was done in Bois (2000a) and Hack et al.
 13 (2006).

14 Non-detects of DCVG from Lash et al. (1999b) were also included in the data, at it was
 15 found that these data were needed to place constraints on the clearance rate of DCVG from
 16 blood. The detection limit reported in the study was $LD = 0.05 \text{ pmol/mL} = 5 \times 10^{-5} \text{ mmol/L}$. It
 17 was assumed, as is standard in analytical chemistry, that the detection limit represents a response
 18 from a blank sample at 3-standard deviations. Because detector responses near the detection
 19 limit are generally normally distributed, the likelihood for observing a non-detect given a model-
 20 predicted value of y_p is equal to $P(\text{ND}|y_p) = \Phi(3 \times \{1 - y_p / LD\})$, where $\Phi(y)$ is the cumulative
 21 standard normal distribution.

bbb No data on variability, so a CV of 0.5 was assigned, with a CU of 2.

ccc No data on variability, so a CV of 2 was assigned (larger than assumed for metabolism due to possible vehicle effects), with a CU of 2.

1 The rat and human models differed from mouse model in terms of the hierarchical
 2 structure of the residual errors. In the mouse model, all the studies were assumed to have the
 3 same residual error, as shown in Figure A.1. This appeared reasonable because there were fewer
 4 studies, and there appeared to be less variation between studies. In the rat and human models,
 5 each of which used a much larger database of *in vivo* studies, residual errors were assumed to be
 6 the same within a study, but may differ between studies. The updated hierarchical structures are
 7 shown in Figure A.6. Initial attempts to use a single set of residual errors led to large residual
 8 errors for some measurements, even though fits to many studies appeared reasonable. Residual
 9 errors were generally reduced when study-specific errors were used, except for some datasets
 10 that appeared to be outliers (discussed below).

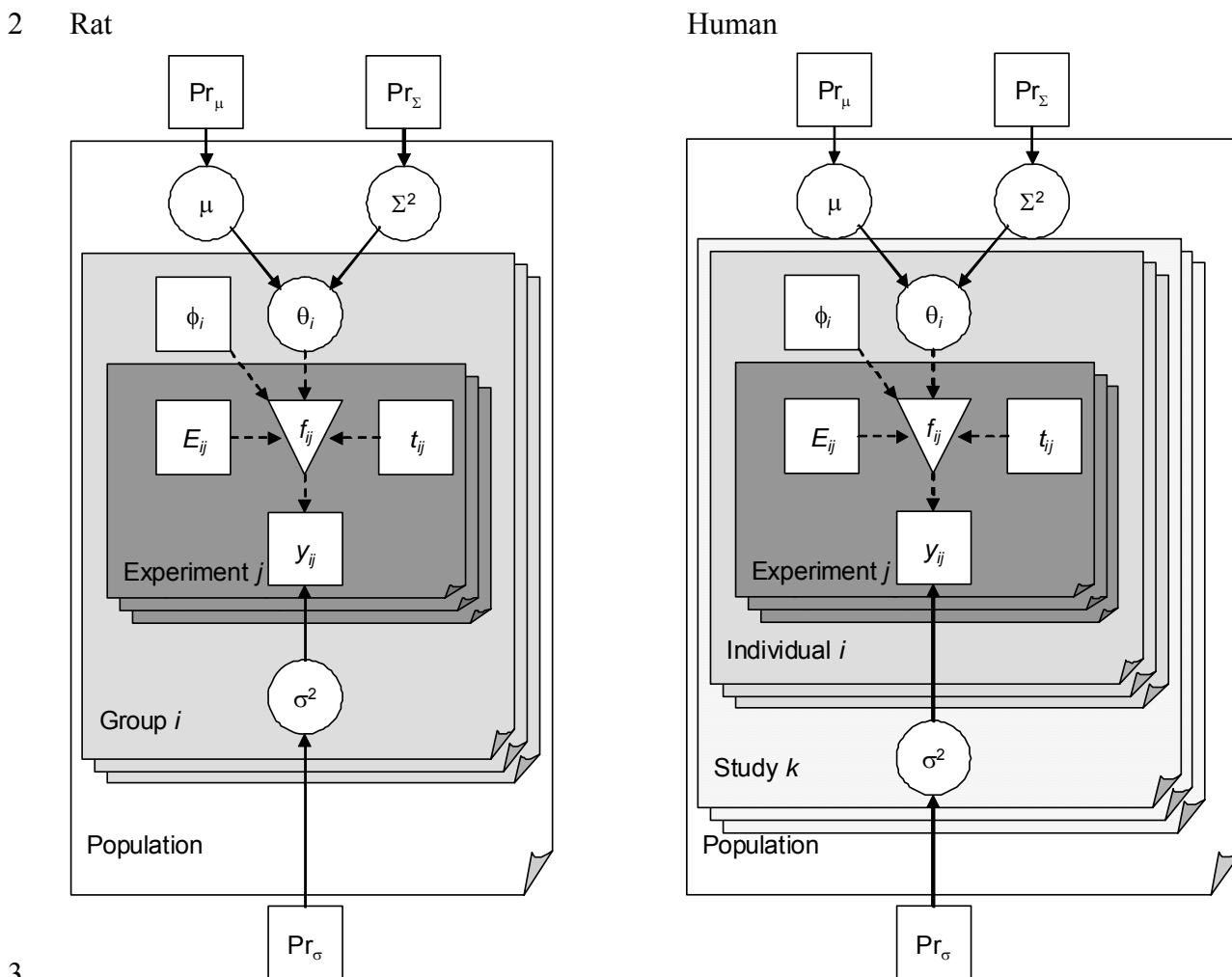
11

12 **Table A.8.** Measurements used for calibration

Measurement Abbreviation	Mouse	Rat	Human	Measurement Description
RetDose			√	Retained TCE dose (mg)
CAIvPPM			√	TCE concentration in alveolar air (ppm)
CIinhPPM	√	√		TCE concentration in closed chamber (ppm)
CArt		√		TCE concentration in arterial blood (mg/L)
CVen	√	√	√	TCE concentration in venous blood (mg/L)
CBldMix	√	√		TCE concentration in mixed arterial and venous blood (mg/L)
CFat	√	√		TCE concentration in fat (mg/L)
CGut		√		TCE concentration in gut (mg/L)
CKid	√	√		TCE concentration in kidney (mg/L)
CLiv	√	√		TCE concentration in liver (mg/L)
CMus		√		TCE concentration in muscle (mg/L)
AExhpost	√	√		Amount of TCE exhaled post-exposure (mg)
CTCOH	√	√	√	Free TCOH concentration in blood (mg/L)
CLivTCOH	√			Free TCOH concentration in liver (mg/L)
CPlasTCA	√	√	√	TCA concentration in plasma (mg/L)
CBldTCA	√	√	√	TCA concentration in blood (mg/L)
CLivTCA	√	√		TCA concentration in liver (mg/L)
AUrnTCA	√	√	√	Cumulative amount of TCA excreted in urine (mg)
AUrnTCA_collect			√	Cumulative amount of TCA collected in urine (non-continuous sampling) (mg)
ABileTCOG		√		Cumulative amount of bound TCOH excreted in bile (mg)
CTCOG		√		Bound TCOH concentration in blood (mg/L)
CTCOGTCOH	√			Bound TCOH concentration in blood in free TCOH equivalents (mg/L)
CLivTCOGTCOH	√			Bound TCOH concentration in liver in free TCOH equivalents (mg/L)
AUrnTCOGTCOH	√	√	√	Cumulative amount of total TCOH excreted in urine (mg)
AUrnTCOGTCOH_collect			√	Cumulative amount of total TCOH collected in urine (non-continuous sampling) (mg)
CDCVGmol			√	DCVG concentration in blood (mmol/L)
CDCVG_ND			√	DCVG non-detects from Lash et al. (1999b)
AUrnNDCVC		√	√	Cumulative amount of NAcDCVC excreted in urine (mg)
AUrnTCTotMole		√		Cumulative amount of TCA+total TCOH excreted in urine (mmol)
TotCTCOH	√	√	√	Total TCOH concentration in blood (mg/L)

13

1 **Figure A.6. Updated hierarchical structure for rat and human models**



4 Symbols have the same meaning as Figure A.1, with modifications for the rat and human. In particular, in the rat,
 5 each “group” consists of animals (usually comprising multiple dose groups) of the same sex, species, and strain
 6 within a study (possibly reported in more than one publication, but reasonably presumed to be of animals in the
 7 same “lot”). Animals within each group are presumed to be “identical,” with the same PBPK model parameters, and
 8 each such group is assigned its own set of “residual” error variances σ^2 . In humans, each “individual” is a single
 9 person, possibly exposed in multiple experiments, and each individual is assigned a set of PBPK model parameters
 10 drawn from the population. However, in humans, “residual” error variances are assigned at the “study” level, rather
 11 than the individual or the population level.

12

13 **A.5. Results of Updated PBPK Model**

14 The evaluation of the updated PBPK model was discussed in Chapter 3. Detailed results
 15 in the form of tables and figures are provided in this section.

1 **A.5.1. Convergence and posterior distributions of sampled parameters**

2 For each sampled parameter (population mean and variance and the variance for residual
3 errors), summary statistics (median, [2.5%, 97.5%] confidence interval) for the posterior
4 distribution are tabulated in Tables A.9A.14 below. In addition, the potential scale reduction
5 factor R , calculated from comparing 4 independent chains, is given.

1 **Table A.9.** Posterior distributions for mouse PBPK model population parameters

Sampled Parameter	Posterior Distributions Reflecting Uncertainty in Population Distribution			
	Population (Geometric) Mean		Population (Geometric) Standard Deviation	
	Median (2.5% , 97.5%)	R	Median (2.5% , 97.5%)	R
InQCC	1.237 (0.8972 , 1.602)	1	1.402 (1.183 , 2.283)	1
InVPRC	0.8076 (0.6434 , 1.022)	1	1.224 (1.108 , 1.63)	1.001
QFatC	1.034 (0.5235 , 1.55)	1	0.436 (0.3057 , 0.6935)	1
QGutC	1.183 (1.002 , 1.322)	1	0.1548 (0.1101 , 0.2421)	1
QLivC	1.035 (0.8002 , 1.256)	1	0.1593 (0.1107 , 0.2581)	1
QSlwC	0.9828 (0.6043 , 1.378)	1	0.275 (0.1915 , 0.4425)	1
InDRspC	1.214 (0.7167 , 2.149)	1.002	1.215 (1.143 , 1.375)	1
QKidC	0.995 (0.5642 , 1.425)	1	0.3001 (0.21 , 0.48)	1
FracPlasC	0.8707 (0.5979 , 1.152)	1.001	0.1903 (0.1327 , 0.3039)	1
VFatC	1.329 (0.8537 , 1.784)	1.002	0.4123 (0.2928 , 0.6414)	1
VGutC	0.9871 (0.817 , 1.162)	1	0.1219 (0.085 , 0.1965)	1
VLivC	0.8035 (0.5609 , 1.093)	1.013	0.2216 (0.1552 , 0.3488)	1
VRapC	0.997 (0.8627 , 1.131)	1	0.09384 (0.06519 , 0.1512)	1
VRespLumC	0.9995 (0.8536 , 1.145)	1	0.1027 (0.07172 , 0.1639)	1
VRespEffC	1 (0.8537 , 1.148)	1.001	0.1032 (0.07176 , 0.1652)	1
VKidC	1.001 (0.8676 , 1.134)	1	0.09365 (0.06523 , 0.1494)	1
VBldC	0.9916 (0.8341 , 1.153)	1.001	0.1126 (0.07835 , 0.1817)	1
InPBC	0.9259 (0.647 , 1.369)	1	1.644 (1.278 , 3.682)	1
InPFatC	0.9828 (0.7039 , 1.431)	1.001	1.321 (1.16 , 2.002)	1.001
InPGutC	0.805 (0.4735 , 1.418)	1	1.375 (1.198 , 2.062)	1
InPLivC	1.297 (0.7687 , 2.039)	1	1.415 (1.21 , 2.342)	1
InPRapC	0.9529 (0.5336 , 1.721)	1	1.378 (1.203 , 2.141)	1
InPRespC	0.9918 (0.5566 , 1.773)	1.001	1.378 (1.2 , 2.066)	1
InPKidC	1.277 (0.7274 , 2.089)	1	1.554 (1.265 , 2.872)	1
InPSlwC	0.92 (0.5585 , 1.586)	1.001	1.411 (1.209 , 2.3)	1.001
InPRBCPlasTCAC	2.495 (1.144 , 5.138)	1.001	1.398 (1.178 , 2.623)	1.001
InPBodTCAC	0.8816 (0.6219 , 1.29)	1.003	1.27 (1.158 , 1.609)	1
InPLivTCAC	0.8003 (0.5696 , 1.15)	1.003	1.278 (1.157 , 1.641)	1.001
InkDissocC	1.214 (0.2527 , 4.896)	1.003	2.71 (1.765 , 8.973)	1
InBMaxkDC	1.25 (0.6793 , 2.162)	1.002	1.474 (1.253 , 2.383)	1
InPBodTCOHC	0.8025 (0.5607 , 1.174)	1	1.314 (1.17 , 1.85)	1.001
InPLivTCOHC	1.526 (0.9099 , 2.245)	1	1.399 (1.194 , 2.352)	1
InPBodTCOGC	0.4241 (0.1555 , 1.053)	1.004	1.398 (1.207 , 2.156)	1
InPLivTCOGC	1.013 (0.492 , 2.025)	1.002	1.554 (1.279 , 2.526)	1
InPeffDCVG	0.9807 (0.008098 , 149.6)	1.041	1.406 (1.206 , 2.379)	1
InkTSD	5.187 (0.3909 , 69.34)	1.001	5.858 (2.614 , 80)	1
InkAS	1.711 (0.3729 , 11.23)	1.001	4.203 (2.379 , 18.15)	1
InkTD	0.1002 (0.01304 , 0.7688)	1	5.16 (2.478 , 60.24)	1
InkAD	0.2665 (0.05143 , 1.483)	1.003	4.282 (2.378 , 20.21)	1
InkASTCA	3.986 (0.1048 , 141.9)	1	5.187 (2.516 , 58.72)	1
InkASTCOH	0.7308 (0.006338 , 89.75)	1.001	5.047 (2.496 , 54.8)	1
InV _{Max} C	0.6693 (0.4093 , 1.106)	1.005	1.793 (1.49 , 2.675)	1
InK _M C	0.07148 (0.0323 , 0.1882)	1	2.203 (1.535 , 4.536)	1.001
InFracOtherC	0.02384 (0.003244 , 0.1611)	1.006	1.532 (1.265 , 2.971)	1
InFracTCAC	0.4875 (0.2764 , 0.8444)	1.002	1.474 (1.258 , 2.111)	1

INTER-AGENCY REVIEW DRAFT–DO NOT CITE OR QUOTE

InV _{Max} DCVGC	1.517 (0.02376 , 1,421)	1.001	1.53 (1.263 , 2.795)	1
InCIDCVGC	0.1794 (0.02333 , 79.69)	1.013	1.528 (1.261 , 2.922)	1
InV _{Max} KidDCVGC	1.424 (0.04313 , 704.9)	1.014	1.533 (1.262 , 2.854)	1
InCIKidDCVGC	0.827 (0.04059 , 167.2)	1.019	1.527 (1.263 , 2.874)	1
InV _{Max} LungLivC	2.903 (0.487 , 12.1)	1.001	4.157 (1.778 , 29.01)	1.018
InK _M Clara	0.01123 (0.001983 , 0.09537)	1.012	1.629 (1.278 , 5.955)	1.003
InFracLungSysC	3.304 (0.2619 , 182.1)	1.011	1.543 (1.266 , 3.102)	1.001
InV _{Max} TCOHC	1.645 (0.6986 , 3.915)	1.005	1.603 (1.28 , 2.918)	1
InK _M TCOH	0.9594 (0.2867 , 2.778)	1.007	1.521 (1.264 , 2.626)	1
InV _{Max} GlucC	65.59 (27.58 , 232.5)	1.018	1.487 (1.254 , 2.335)	1
InK _M Gluc	31.16 (6.122 , 137.3)	1.015	1.781 (1.299 , 5.667)	1.002
InkMetTCOHC	3.629 (0.7248 , 9.535)	1.009	1.527 (1.265 , 2.626)	1
InkUrnTCAC	0.1126 (0.04083 , 0.2423)	1.012	1.757 (1.318 , 3.281)	1.003
InkMetTCAC	0.6175 (0.2702 , 1.305)	1.027	1.508 (1.262 , 2.352)	1.002
InkBileC	0.9954 (0.316 , 3.952)	1.003	1.502 (1.26 , 2.453)	1
InkEHRC	0.01553 (0.001001 , 0.0432)	1.008	1.534 (1.264 , 2.767)	1
InkUrnTCOGC	7.874 (2.408 , 50.28)	1	3.156 (1.783 , 12.18)	1.001
InFracKidDCVCC	1.931 (0.01084 , 113.7)	1.018	1.53 (1.264 , 2.77)	1
InkDCVGC	0.2266 (0.001104 , 16.46)	1.011	1.525 (1.263 , 2.855)	1
InkNATC	0.1175 (0.0008506 , 14.34)	1.024	1.528 (1.264 , 2.851)	1
InkKidBioactC	0.07506 (0.0009418 , 12.35)	1.035	1.527 (1.263 , 2.84)	1.001

1
 2 For natural log transformed parameters (name starting with “In”), values are for the population
 3 geometric means and standard deviations.

4
 5 **Table A.10.** Posterior distributions for mouse residual errors

Measurement	Residual Error Geometric	
	Median (2.5%, 97.5%)	R
CInhPPM	1.177 (1.16 , 1.198)	1.001
CVen	2.678 (2.354 , 3.146)	1.001
CBldMix	1.606 (1.415 , 1.96)	1.001
CFat	2.486 (2.08 , 3.195)	1
CKid	2.23 (1.908 , 2.796)	1
CLiv	1.712 (1.543 , 1.993)	1
AExhpost	1.234 (1.159 , 1.359)	1
CTCOH	1.543 (1.424 , 1.725)	1
CLivTCOH	1.591 (1.454 , 1.818)	1
CPlasTCA	1.396 (1.338 , 1.467)	1.001
CBldTCA	1.488 (1.423 , 1.572)	1.001
CLivTCA	1.337 (1.271 , 1.43)	1
AUrnTCA	1.338 (1.259 , 1.467)	1
CTCOGTCOH	1.493 (1.38 , 1.674)	1.001
CLivTCOGTCOH	1.63 (1.457 , 1.924)	1
AUrnTCOGTCOH	1.263 (1.203 , 1.355)	1
TotCTCOH	1.846 (1.506 , 2.509)	1.002

7

1 **Table A.11.** Posterior distributions for rat PBPK model population parameters

Sampled Parameter	Population (Geometric) Mean		Population (Geometric) Standard Deviation	
	Median (2.5% , 97.5%)	R	Median (2.5% , 97.5%)	R
InQCC	1.195 (0.9285 , 1.448)	1.034	1.298 (1.123 , 2.041)	1.031
InVPRC	0.6304 (0.4788 , 0.8607)	1.012	1.446 (1.247 , 2.011)	1.005
QFatC	1.167 (0.8321 , 1.561)	1	0.4119 (0.2934 , 0.6438)	1
QGutC	1.154 (0.988 , 1.306)	1	0.1613 (0.1132 , 0.2542)	1
QLivC	1.029 (0.8322 , 1.223)	1.002	0.1551 (0.1092 , 0.2483)	1
QSlwC	0.9086 (0.5738 , 1.251)	1.001	0.2817 (0.1968 , 0.4493)	1
InDRespC	2.765 (1.391 , 5.262)	1.018	1.21 (1.142 , 1.358)	1.001
QKidC	1.002 (0.8519 , 1.152)	1.001	0.1185 (0.08284 , 0.1871)	1
FracPlasC	1.037 (0.8071 , 1.259)	1.002	0.1785 (0.1272 , 0.2723)	1
VFatC	0.9728 (0.593 , 1.378)	1	0.4139 (0.2924 , 0.6552)	1.002
VGutC	0.9826 (0.8321 , 1.137)	1	0.1187 (0.08296 , 0.1873)	1
VLivC	0.9608 (0.7493 , 1.19)	1.015	0.1682 (0.1168 , 0.2718)	1.001
VRapC	0.9929 (0.8563 , 1.133)	1.001	0.1093 (0.07693 , 0.175)	1
VRespLumC	1.001 (0.7924 , 1.21)	1	0.1636 (0.116 , 0.2601)	1
VRespEffC	0.999 (0.7921 , 1.208)	1.001	0.1635 (0.1161 , 0.2598)	1
VKidC	0.999 (0.8263 , 1.169)	1	0.1361 (0.09617 , 0.2167)	1
VBldC	1.002 (0.8617 , 1.141)	1	0.1096 (0.07755 , 0.176)	1
InPBC	0.8551 (0.6854 , 1.065)	1.001	1.317 (1.232 , 1.462)	1.001
InPFatC	1.17 (0.8705 , 1.595)	1.003	1.333 (1.247 , 1.481)	1.001
InPGutC	0.8197 (0.5649 , 1.227)	1	1.362 (1.198 , 1.895)	1
InPLivC	1.046 (0.8886 , 1.234)	1.001	1.152 (1.115 , 1.214)	1
InPRapC	1.021 (0.6239 , 1.675)	1.002	1.373 (1.201 , 1.988)	1
InPRespC	0.993 (0.5964 , 1.645)	1.001	1.356 (1.197 , 1.948)	1
InPKidC	0.9209 (0.6728 , 1.281)	1	1.304 (1.201 , 1.536)	1
InPSlwC	1.258 (0.9228 , 1.711)	1.001	1.364 (1.263 , 1.544)	1
InPRBCPlasTCAC	0.9763 (0.6761 , 1.353)	1	1.276 (1.159 , 1.634)	1
InPBodTCAC	1.136 (0.6737 , 1.953)	1.008	1.631 (1.364 , 2.351)	1.003
InPLivTCAC	1.283 (0.6425 , 2.491)	1.008	1.651 (1.356 , 2.658)	1
InkDissocC	1.01 (0.5052 , 2.017)	1.002	1.596 (1.315 , 2.774)	1
InBMaxkDC	0.9654 (0.5716 , 1.733)	1.02	1.412 (1.234 , 2.01)	1
InPBodTCOHC	0.9454 (0.4533 , 1.884)	1.045	1.734 (1.39 , 3.151)	1.002
InPLivTCOHC	0.926 (0.3916 , 2.196)	1.013	1.785 (1.382 , 4.142)	1.003
InPBodTCOGC	1.968 (0.09185 , 14.44)	1.031	1.414 (1.208 , 2.571)	1
InPLivTCOGC	7.484 (2.389 , 26.92)	1.017	1.41 (1.208 , 2.108)	1
InkTSD	3.747 (0.2263 , 62.58)	1.01	6.777 (2.844 , 87.29)	1
InkAS	2.474 (0.2542 , 28.35)	1.004	10.16 (4.085 , 143.7)	1
InkAD	0.1731 (0.04001 , 0.7841)	1.018	4.069 (2.373 , 14.19)	1.009
InkASTCA	1.513 (0.1401 , 17.19)	1.002	4.376 (2.43 , 22.83)	1
InkASTCOH	0.6896 (0.01534 , 25.81)	1.001	4.734 (2.444 , 35.2)	1.001
InV _{Max} C	0.8948 (0.6377 , 1.293)	1.028	1.646 (1.424 , 2.146)	1.021
InK _M C	0.0239 (0.01602 , 0.04993)	1.001	2.402 (1.812 , 4.056)	1.001
InFracOtherC	0.344 (0.0206 , 1.228)	1.442	3 (1.332 , 10.04)	1.353
InFracTCAC	0.2348 (0.122 , 0.4616)	1.028	1.517 (1.264 , 2.393)	1.001
InV _{Max} DCVGC	7.749 (0.2332 , 458.8)	1.088	1.534 (1.262 , 2.804)	1.001
InCIDCVGC	0.3556 (0.06631 , 2.242)	1.018	1.509 (1.261 , 2.553)	1

INTER-AGENCY REVIEW DRAFT–DO NOT CITE OR QUOTE

InV_{Max}KidDCVGC	0.2089 (0.04229 , 1.14)	1.011	1.542 (1.263 , 2.923)	1.001
InCIKidDCVGC	184 (26.29 , 1312)	1.02	1.527 (1.265 , 2.873)	1.001
InV_{Max}LungLivC	2.673 (0.4019 , 14.16)	1.002	4.833 (1.599 , 48.32)	1.002
InK_MClara	0.02563 (0.005231 , 0.197)	1.01	1.66 (1.279 , 18.74)	1.002
InFracLungSysC	2.729 (0.04124 , 63.27)	1.027	1.536 (1.267 , 2.868)	1.001
InV_{Max}TCOHC	1.832 (0.6673 , 6.885)	1.041	1.667 (1.292 , 3.148)	1.002
InK_MTCOH	22.09 (3.075 , 131.9)	1.186	1.629 (1.276 , 3.773)	1.017
InV_{Max}GlucC	28.72 (10.02 , 86.33)	1.225	2.331 (1.364 , 5.891)	1.126
InK_MGluc	6.579 (1.378 , 23.57)	1.119	2.046 (1.309 , 10.3)	1.125
InkMetTCOHC	2.354 (0.3445 , 15.83)	1.287	1.876 (1.283 , 11.82)	1.182
InkUrnTCAC	0.07112 (0.03934 , 0.1329)	1.076	1.513 (1.27 , 2.327)	1.003
InkMetTCAC	0.3554 (0.1195 , 0.8715)	1.036	1.528 (1.263 , 2.444)	1.001
InkBileC	8.7 (1.939 , 26.71)	1.05	1.65 (1.282 , 5.494)	1.017
InkEHRC	1.396 (0.2711 , 6.624)	1.091	1.647 (1.277 , 5.582)	1.005
InkUrnTCOGC	20.65 (2.437 , 138)	1.041	1.595 (1.269 , 5.257)	1.026
InkNATC	0.002035 (0.0004799 , 0.01019)	1.01	1.523 (1.261 , 2.593)	1.001
InkKidBioactC	0.006618 (0.0009409 , 0.0367)	1.039	1.52 (1.261 , 2.674)	1

1

2

1 **Table A.12.** Posterior distributions for rat residual errors
 2

Measurement	Group	Residual Error Geometric Standard Deviation	
		Median (2.5% , 97.5%)	R
CinhPPM	Group 3	1.124 (1.108 , 1.147)	1
	Group 16	1.106 (1.105 , 1.111)	1
CMixExh	Group 2	1.501 (1.398 , 1.65)	1
CArt	Group 2	1.174 (1.142 , 1.222)	1
	Group 6	1.523 (1.321 , 1.918)	1.002
CVen	Group 4	1.22 (1.111 , 1.877)	1
	Group 7	1.668 (1.489 , 1.986)	1.001
	Group 8	1.45 (1.234 , 2.065)	1.014
	Group 9	1.571 (1.426 , 1.811)	1
	Group 10	4.459 (2.754 , 6.009)	1
	Group 11	1.587 (1.347 , 2.296)	1.002
	Group 16	1.874 (1.466 , 2.964)	1.011
	Group 18	1.676 (1.188 , 3.486)	1.003
CBldMix	Group 12	1.498 (1.268 , 2.189)	1
CFat	Group 9	1.846 (1.635 , 2.184)	1
	Group 16	2.658 (1.861 , 4.728)	1.001
CGut	Group 9	1.855 (1.622 , 2.243)	1
CKid	Group 9	1.469 (1.354 , 1.648)	1
CLiv	Group 9	1.783 (1.554 , 2.157)	1
	Group 12	1.744 (1.401 , 2.892)	1
	Group 16	1.665 (1.376 , 2.411)	1.001
CMus	Group 9	1.653 (1.494 , 1.919)	1
AExhpost	Group 6	1.142 (1.108 , 1.239)	1.003
	Group 10	1.117 (1.106 , 1.184)	1.004
	Group 14	1.166 (1.107 , 1.475)	1
	Group 15	1.125 (1.106 , 1.237)	1
CTCOH	Group 6	1.635 (1.455 , 1.983)	1.002
	Group 10	1.259 (1.122 , 1.868)	1.009
	Group 11	1.497 (1.299 , 1.923)	1.01
	Group 13	1.611 (1.216 , 3.556)	1.001
	Group 17	1.45 (1.213 , 2.208)	1.004
	Group 18	1.142 (1.107 , 1.268)	1
CPlasTCA	Group 4	1.134 (1.106 , 1.254)	1
	Group 5	1.141 (1.107 , 1.291)	1
	Group 11	1.213 (1.136 , 1.381)	1
	Group 19	1.201 (1.145 , 1.305)	1
CBldTCA	Group 4	1.134 (1.106 , 1.258)	1
	Group 5	1.14 (1.107 , 1.289)	1
	Group 6	1.59 (1.431 , 1.878)	1.001
	Group 11	1.429 (1.292 , 1.701)	1.001
	Group 17	1.432 (1.282 , 1.675)	1.03
	Group 18	1.193 (1.12 , 1.358)	1.004
	Group 19	1.214 (1.153 , 1.327)	1
CLivTCA	Group 19	1.666 (1.443 , 2.104)	1

INTER-AGENCY REVIEW DRAFT–DO NOT CITE OR QUOTE

AUrnTCA	Group 1	1.498 (1.125 , 2.18)	1.135
	Group 6	1.95 (1.124 , 5.264)	1.003
	Group 8	1.221 (1.146 , 1.375)	1.003
	Group 10	1.18 (1.108 , 1.444)	1.007
	Group 17	1.753 (1.163 , 4.337)	1.001
	Group 19	1.333 (1.201 , 1.707)	1
ABileTCOG	Group 6	2.129 (1.128 , 5.363)	1.003
CTCOG	Group 17	2.758 (1.664 , 5.734)	1.028
AUrnTCOGTCOH	Group 1	1.129 (1.106 , 1.232)	1.004
	Group 6	1.483 (1.113 , 4.791)	1.002
	Group 8	1.115 (1.106 , 1.162)	1
	Group 10	1.145 (1.107 , 1.305)	1
	Group 17	2.27 (1.53 , 4.956)	1.009
AUrnNDCVC	Group 1	1.168 (1.11 , 1.33)	1.002
AUrnTCTotMole	Group 6	1.538 (1.182 , 3.868)	1.002
	Group 7	1.117 (1.106 , 1.153)	1.001
	Group 14	1.121 (1.106 , 1.207)	1
	Group 15	1.162 (1.108 , 1.358)	1
TotCTCOH	Group 17	1.488 (1.172 , 2.366)	1.015

1 The nineteen groups are (1) Bernauer et al., 1996; (2) Dallas et al., 1991; (3) Fisher et al., 1989 females; (4) Fisher et
 2 al., 1991 females; (5) Fisher et al., 1991 males; (6) Green and Prout, 1985, Prout et al., 1985, male OA rats; (7)
 3 Hissink et al., 2002; (8) Kaneko et al., 1994; (9) Keys et al., 2003; (10) Kimmerle and Eben, 1973a; (11) Larson and
 4 Bull, 1992a, b; (12) Lee et al., 2000; (13) Merdink et al., 1999; (14) Prout et al., 1985 AP rats; (15) Prout et al., 1985
 5 OM rats; (16) Simmons et al., 2002; (17) Stenner et al., 1997; (18) Templin et al., 1995; (19) Yu et al., 2000.

6

7 **Table A.13.** Posterior distributions for human PBPK model population parameters

Sampled Parameter	Population (Geometric) Mean		Population (Geometric) Standard Deviation	
	Median (2.5% , 97.5%)	R	Median (2.5% , 97.5%)	R
InQCC	0.837 (0.6761 , 1.022)	1.038	1.457 (1.271 , 1.996)	1.036
InVPRC	1.519 (1.261 , 1.884)	1.007	1.497 (1.317 , 1.851)	1.008
QFatC	0.7781 (0.405 , 1.143)	1.014	0.6272 (0.4431 , 0.9773)	1
QGutC	0.7917 (0.6631 , 0.925)	1.017	0.1693 (0.1199 , 0.2559)	1.019
QLivC	0.5099 (0.1737 , 0.8386)	1.031	0.4167 (0.2943 , 0.6324)	1.009
QSlwC	0.7261 (0.4864 , 0.9234)	1.011	0.3166 (0.2254 , 0.4802)	1.005
InDRespC	0.626 (0.3063 , 1.013)	1.197	1.291 (1.158 , 2.006)	1.083
QKidC	1.007 (0.9137 , 1.103)	1.009	0.1004 (0.07307 , 0.1545)	1
FracPlasC	1.001 (0.9544 , 1.047)	1.01	0.04275 (0.03155 , 0.06305)	1
VFatC	0.788 (0.48 , 1.056)	1.005	0.3666 (0.2696 , 0.5542)	1
VGutC	1 (0.937 , 1.067)	1.007	0.06745 (0.04923 , 0.1038)	1
VLivC	1.043 (0.8683 , 1.23)	1.047	0.1959 (0.1424 , 0.3017)	1.003
VRapC	0.9959 (0.9311 , 1.06)	1.006	0.06692 (0.04843 , 0.1027)	1
VRespLumC	1.003 (0.8461 , 1.164)	1.001	0.1671 (0.1209 , 0.255)	1
VRespEffC	1 (0.8383 , 1.159)	1.001	0.1672 (0.1215 , 0.259)	1
VKidC	0.9965 (0.8551 , 1.14)	1.007	0.1425 (0.1037 , 0.2183)	1
VBldC	1.013 (0.9177 , 1.108)	1.003	0.1005 (0.07265 , 0.1564)	1
InPBC	0.9704 (0.8529 , 1.101)	1.001	1.216 (1.161 , 1.307)	1.002
InPFatC	0.8498 (0.7334 , 0.9976)	1.002	1.188 (1.113 , 1.366)	1.002

INTER-AGENCY REVIEW DRAFT–DO NOT CITE OR QUOTE

InPGutC	1.095 (0.7377 , 1.585)	1.029	1.413 (1.214 , 2.05)	1.002
InPLivC	0.9907 (0.6679 , 1.441)	1.01	1.338 (1.203 , 1.683)	1
InPRapC	0.93 (0.6589 , 1.28)	1.003	1.528 (1.248 , 2.472)	1.001
InPRespC	1.018 (0.6773 , 1.5)	1.015	1.32 (1.192 , 1.656)	1
InPKidC	0.9993 (0.8236 , 1.219)	1.003	1.155 (1.097 , 1.287)	1
InPSlwC	1.157 (0.8468 , 1.59)	1.018	1.69 (1.383 , 3.157)	1.008
InPRBCPlasTCAC	0.3223 (0.04876 , 0.8378)	1.007	5.507 (3.047 , 19.88)	1.003
InPBodTCAC	1.194 (0.929 , 1.481)	1.043	1.327 (1.185 , 1.67)	1.018
InPLivTCAC	1.202 (0.8429 , 1.634)	1.046	1.285 (1.162 , 1.648)	1.007
InkDissocC	0.9932 (0.9387 , 1.053)	1.012	1.043 (1.026 , 1.076)	1.003
InBMaxkDC	0.8806 (0.7492 , 1.047)	1.038	1.157 (1.085 , 1.37)	1.012
InPBodTCOHC	1.703 (1.439 , 2.172)	1.019	1.409 (1.267 , 1.678)	1.011
InPLivTCOHC	1.069 (0.7643 , 1.485)	1.028	1.288 (1.165 , 1.629)	1.002
InPBodTCOGC	0.7264 (0.1237 , 2.54)	1.003	11.98 (5.037 , 185.3)	1.017
InPLivTCOGC	6.671 (1.545 , 24.87)	1.225	5.954 (2.653 , 23.68)	1.052
InPeffDCVGC	0.01007 (0.003264 , 0.03264)	1.004	1.385 (1.201 , 2.03)	1.001
InkASTCA	4.511 (0.04731 , 465.7)	1	5.467 (2.523 , 71.06)	1
InkASTCOH	8.262 (0.0677 , 347.9)	1	5.481 (2.513 , 67.86)	1
InV_{Max}C	0.3759 (0.2218 , 0.5882)	1.026	2.21 (1.862 , 2.848)	1.003
InCIC	12.64 (5.207 , 39.96)	1.028	4.325 (2.672 , 9.003)	1.016
InFracOtherC	0.1186 (0.02298 , 0.2989)	1.061	3.449 (1.392 , 9.146)	1.102
InFracTCAC	0.1315 (0.07115 , 0.197)	1.026	2.467 (1.916 , 3.778)	1.01
InCIDCVGC	2.786 (1.326 , 5.769)	1.08	2.789 (1.867 , 4.877)	1.02
InK_MDCVGC	1.213 (0.3908 , 4.707)	1.029	4.43 (2.396 , 18.56)	1.035
InCIKidDCVGC	0.04538 (0.001311 , 0.1945)	1.204	3.338 (1.295 , 30.46)	1.095
InK_MKidDCVGC	0.2802 (0.1096 , 1.778)	1.097	1.496 (1.263 , 2.317)	1.001
InV_{Max}LungLivC	3.772 (0.8319 , 9.157)	1.035	2.228 (1.335 , 21.89)	1.014
InK_MClara	0.2726 (0.02144 , 1.411)	1.041	11.63 (1.877 , 682.7)	1.041
InFracLungSysC	24.08 (6.276 , 81.14)	1.016	1.496 (1.263 , 2.439)	1.001
InCITCOHC	0.1767 (0.1374 , 0.2257)	1.011	1.888 (1.624 , 2.307)	1.01
InK_MTCOH	2.221 (1.296 , 4.575)	1.02	2.578 (1.782 , 4.584)	1.015
InCIGlucC	0.2796 (0.2132 , 0.3807)	1.056	1.955 (1.583 , 2.418)	1.079
InK_MGluc	133.4 (51.56 , 277.2)	1.02	1.573 (1.266 , 4.968)	1.011
InkMetTCOHC	0.7546 (0.1427 , 2.13)	1.007	5.011 (2.668 , 15.71)	1.002
InkUrnTCAC	0.04565 (0.0324 , 0.06029)	1.005	1.878 (1.589 , 2.48)	1.006
InkMetTCAC	0.2812 (0.1293 , 0.5359)	1.004	2.529 (1.78 , 4.211)	1.002
InkBileC	6.855 (3.016 , 20.69)	1.464	1.589 (1.27 , 3.358)	1.015
InkEHRC	0.1561 (0.09511 , 0.2608)	1.1	1.699 (1.348 , 2.498)	1.015
InkUrnTCOGC	15.78 (6.135 , 72.5)	1.007	9.351 (4.93 , 29.96)	1.003
InkDCVGC	7.123 (5.429 , 9.702)	1.026	1.507 (1.311 , 1.897)	1.008
InkNATC	0.0003157 (0.0001087 , 0.002305)	1.008	1.54 (1.261 , 3.306)	1
InkKidBioactC	0.06516 (0.01763 , 0.1743)	1.001	1.523 (1.262 , 2.987)	1

1

2

1 **Table A.14.** Posterior distributions for human residual errors

2

Measurement	Group	Residual Error Geometric	
		Standard Deviation	R
		Median (2.5% , 97.5%)	
RetDose	Group 4	1.131 (1.106 , 1.25)	1.001
CAIvPPM	Group 1	1.832 (1.509 , 2.376)	1.015
	Group 4	1.515 (1.378 , 1.738)	1
	Group 5	1.44 (1.413 , 1.471)	1
CVen	Group 1	1.875 (1.683 , 2.129)	1.018
	Group 3	1.618 (1.462 , 1.862)	1
	Group 4	1.716 (1.513 , 2.057)	1.001
	Group 5	2.948 (2.423 , 3.8)	1.007
CTCOH	Group 1	1.205 (1.185 , 1.227)	1.012
	Group 3	1.213 (1.187 , 1.247)	1
	Group 5	2.101 (1.826 , 2.571)	1.001
	Group 7	1.144 (1.106 , 2.887)	1.123
CPlasTCA	Group 2	1.117 (1.106 , 1.17)	1.001
	Group 7	1.168 (1.123 , 1.242)	1
CBIdTCA	Group 1	1.138 (1.126 , 1.152)	1.003
	Group 2	1.119 (1.106 , 1.178)	1
	Group 4	1.488 (1.351 , 1.646)	1.018
	Group 5	1.438 (1.367 , 1.537)	1.002
zAUrnTCA	Group 1	1.448 (1.414 , 1.485)	1.001
	Group 2	1.113 (1.105 , 1.149)	1.001
	Group 3	1.242 (1.197 , 1.301)	1.001
	Group 4	1.538 (1.441 , 1.67)	1
	Group 6	1.158 (1.118 , 1.228)	1
	Group 7	1.119 (1.106 , 1.181)	1
zAUrnTCA_collect	Group 3	1.999 (1.178 , 3.903)	1.003
	Group 5	2.787 (2.134 , 4.23)	1.001
AUrnTCOGTCOH	Group 1	1.106 (1.105 , 1.112)	1.001
	Group 3	1.11 (1.105 , 1.125)	1
	Group 4	1.124 (1.107 , 1.151)	1.001
	Group 6	1.117 (1.106 , 1.157)	1.001
	Group 7	1.134 (1.106 , 1.348)	1.003
AUrnTCOGTCOH_collect	Group 3	1.3 (1.111 , 2.333)	1.004
	Group 5	1.626 (1.524 , 1.767)	1
CDCVGmol	Group 1	1.53 (1.436 , 1.656)	1.009
zAUrnNDCVC	Group 6	1.167 (1.124 , 1.244)	1
TotCTCOH	Group 1	1.204 (1.185 , 1.226)	1.011
	Group 4	1.247 (1.177 , 1.366)	1.009
	Group 5	1.689 (1.552 , 1.9)	1.001

3 The seven groups are (1) Fisher et al., 1998; (2) Paycok and Powell, 1945; (3) Kimmerle and Eben, 1973b;
 4 (4) Monster et al., 1976; (5) Chiu et al., 2007; (6) Bernauer et al., 1996; (7) Muller et al., 1974.

5

1 **A.5.2. Comparison of model predictions with data**

2 **A.5.2.1. *Mouse model***

3 **A.5.2.1.1. *Group-specific predictions and calibration data***

4 [See [Appendix.linked.files\AppA.5.2.1.1.Updated.mouse.group.calib.TCE.DRAFT.pdf](#)]

5 **A.5.2.1.2. *Population-based predictions and calibration data***

6 [See [Appendix.linked.files\AppA.5.2.1.2.Updated.mouse.pop.calib.TCE.DRAFT.pdf](#)]

7 **A.5.2.2. *Rat model***

8 **A.5.2.2.1. *Group-specific predictions and calibration data***

9 [See [Appendix.linked.files\AppA.5.2.2.1.Updated.rat.group.calib.TCE.DRAFT.pdf](#)]

10 **A.5.2.2.2. *Population-based predictions and calibration data***

11 [See [Appendix.linked.files\AppA.5.2.2.2.Updated.rat.pop.calib.TCE.DRAFT.pdf](#)]

12 **A.5.2.2.3. *Population-based predictions and additional evaluation data***

13 [See [Appendix.linked.files\AppA.5.2.2.3.Updated.rat.pop.eval.TCE.DRAFT.pdf](#)]

14 **A.5.2.3. *Human model***

15 **A.5.2.3.1. *Individual-specific predictions and calibration data***

16 [See [Appendix.linked.files\AppA.5.2.3.1.Updated.human.indiv.calib.TCE.DRAFT.pdf](#)]

17 **A.5.2.3.2. *Population-based predictions and calibration data***

18 [See [Appendix.linked.files\AppA.5.2.3.2.Updated.human.pop.calib.TCE.DRAFT.pdf](#)]

19 **A.5.2.3.3. *Population-based predictions and additional evaluation data***

20 [See [Appendix.linked.files\AppA.5.2.3.3.Updated.human.pop.eval.TCE.DRAFT.pdf](#)]

21 **A.6. Updated PBPK Model Code**

22 The following pages contain the updated PBPK model code for the MCSim software (version
23 5.0.0). Additional details on baseline parameter derivations are included as inline
24 documentation. Simulation files containing prior distributions and experimental data, and R
25 scripts for data analysis, are available electronically.

26

INTER-AGENCY REVIEW DRAFT-DO NOT CITE OR QUOTE

```

1 # TCE.risk3.1.2.3.3.pop.model -- Updated TCE Risk Assessment Model
2 #
3 # Model code to correspond to the block diagram version of the model
4 # Edited by Deborah Keys to incorporate Lapare et al. 1995 data
5 # Last edited: August 6, 2004
6 # Translated into MCSim from acslXtreme CSL file by Eric Hack, started 31Aug2004
7 # Removed nonessential differential equations (i.e., AUCCbld) for MCMC runs.
8 # Changed QRap and QSlw calculations and added QTot to scale fractional flows
9 # back to 1 after sampling.
10 # Finished translating and verifying results on 15Sep2004.
11 # Changed QSlw calculation and removed QTot 21Sep2004.
12 # Removed diffusion-limited fat uptake 24Sep2004.
13 # Extensively revised by U.S. EPA June 2007-June 2008
14 #   - Fixed hepatic plasma flow for TCA-submodel to include
15 #     portal vein (i.e., QGutLivPlas -- originally was just
16 #     QLivPlas, which was only hepatic artery).
17 #   - Clearer coding and in-line documentation
18 #   - Single model for 3 species
19 #   - Revised physiological parameters, with discussion of
20 #     uncertainty and variability,
21 #   - In vitro data used for default metabolism parameters,
22 #     with discussion of uncertainty and variability
23 #   - added TCE blood compartment
24 #   - added TCE kidney compartment, with GSH metabolism
25 #   - added DCVG compartment
26 #   - added additional outputs available from in vivo data
27 #   - removed DCA compartment
28 #   - added IA and PV dosing (for rats)
29 #   - Version 1.1 -- fixed urinary parameter scaling
30 #     -- fixed VBod in kUrnTCOG (should be VBodTCOH)
31 #   - Version 1.1.1 -- changed some truncation limits (in comments only)
32 #   - Version 1.2 --
33 #     -- removed TB compartment as currently coded
34 #     -- added respiratory oxidative metabolism:
35 #       3 states: AInhResp, AResp, AExhResp
36 #     -- removed clearance from respiratory metabolism
37 #   - Version 1.2.1 -- changed oral dosing to be similar to IV
38 #   - Version 1.2.2 -- fixed default lung metabolism (additional
39 #     scaling by lung/liver weight ratio)
40 #   - Version 1.2.3 -- fixed FracKidDCVC scaling
41 #   - Version 1.2.3.1 -- added output CDCVG_ND (no new dynamics)
42 #     for non-detects of DCVG in blood
43 #   - Version 1.2.3.2 -- Exact version of non-detects likelihood
44 #   - Version 1.2.3.3 -- Error variances changed to "Ve_xxx"
45 # NOTE -- lines with comment "(vrisk)" are used only for
46 #       calculating dose metrics, and are commented out
47 #       when doing MCMC runs.
48 #*****
49 #***      State Variable Specifications      ***
50 #*****
51 States = {
52 #-- TCE uptake

```

```

54 AStom,          # Amount of TCE in stomach
55 ADuod,         # oral gavage absorption -- mice and rats only
56 AExc,         # (vrisk) excreted in feces from gavage (currently 0)
57 AO,          # (vrisk) total absorbed
58 InhDose,     # Amount inhaled
59 #-- TCE in the body
60 ARap,        # Amount in rapidly perfused tissues
61 ASlw,        # Amount in slowly perfused tissues
62 AFat,        # Amount in fat
63 AGut,        # Amount in gut
64 ALiv,        # Amount in liver
65 AKid,        # Amount in Kidney -- previously in Rap tissue
66 ABld,        # Amount in Blood -- previously in Rap tissue
67 AInhResp,   # Amount in respiratory lumen during inhalation
68 AResp,      # Amount in respiratory tissue
69 AExhResp,   # Amount in respiratory lumen during exhalation
70 #-- TCA in the body
71 AOTCA,      # (vrisk)
72 AStomTCA,  # Amount of TCA in stomach
73 APlasTCA,  # Amount of TCA in plasma #comment out for
74 ABodTCA,   # Amount of TCA in lumped body compartment
75 ALivTCA,   # Amount of TCA in liver
76 #-- TCA metabolized
77 AUrnTCA,   # Cumulative Amount of TCA excreted in urine
78 AUrnTCA_sat, # Amount of TCA excreted that during times that had
79             # saturated measurements (for lower bounds)
80 AUrnTCA_collect, # Cumulative Amount of TCA excreted in urine during
81             # collection times (for intermittent collection)
82 #-- TCOH in body
83 AOTCOH,    # (vrisk)
84 AStomTCOH, # Amount of TCOH in stomach
85 ABodTCOH,  # Amount of TCOH in lumped body compartment
86 ALivTCOH,  # Amount of TCOH in liver
87 #-- TCOG in body
88 ABodTCOG,  # Amount of TCOG in lumped body compartment
89 ALivTCOG,  # Amount of TCOG in liver
90 ABileTCOG, # Amount of TCOG in bile (incl. gut)
91 ARecircTCOG, # (vrisk)
92 #-- TCOG excreted
93 AUrnTCOG, # Amount of TCOG excreted in urine
94 AUrnTCOG_sat, # Amount of TCOG excreted that during times that had
95             # saturated measurements (for lower bounds)
96 AUrnTCOG_collect, # Cumulative Amount of TCA excreted in urine during
97             # collection times (for intermittent collection)
98 #-- DCVG in body
99 ADCVGIn,   # (vrisk)
100 ADCVGmol,  # Amount of DCVG in body in mmoles
101 AMetDCVG,  # (vrisk)
102 #-- DCVC in body
103 ADCVCIn,   # (vrisk)
104 ADCVC,     # Amount of DCVC in body
105 ABioactDCVC, # (vrisk)
106 #-- NAcDCVC excreted

```

INTER-AGENCY REVIEW DRAFT-DO NOT CITE OR QUOTE

```

1      AUrnNDCVC,      # Amount of NAcDCVC excreted
2  ##-- Other states for TCE
3      ACh,           # Amount in closed chamber -- mice and rats only
4      AExh,          # Amount exhaled
5      AExhExp,      # Amount exhaled during expos [to calc. retention]
6  ##-- Metabolism
7      AMetLiv1,     #(vrisk) Amount metabolized by P450 in liver
8      AMetLiv2,     #(vrisk) Amount metabolized by GSH conjugation in liver
9      AMetLng,      #(vrisk) Amount metabolized in the lung
10     AMetKid,       #(vrisk)
11     AMetTCOHTCA,   #(vrisk) Amount of TCOH metabolized to TCA
12     AMetTCOHGluc, #(vrisk) Amount of TCOH glucuronidated
13     AMetTCOHOther, #(vrisk)
14     AMetTCA,      #(vrisk) Amount of TCA metabolized
15  ##-- Other Dose metrics
16     AUCCBld,      #(vrisk)
17     AUCCLiv,      #(vrisk)
18     AUCCKid,      #(vrisk)
19     AUCCRap,      #(vrisk)
20     AUCCTCOH,     #(vrisk)
21     AUCCBodTCOH, #(vrisk)
22     AUCTotCTCOH, #(vrisk)
23     AUCPlasTCAFree, #(vrisk)
24     AUCPlasTCA,   #(vrisk)
25     AUCLivTCA,    #(vrisk)
26     AUCCDCVG     #(vrisk)
27  };
28
29  *****
30  ***          Input Variable Specifications          ***
31  *****
32
33  Inputs = {
34  ##-- TCE dosing
35     Conc,          # Inhalation exposure conc. (ppm)
36     IVDose,        # IV dose (mg/kg)
37     PDose,         # Oral gavage dose (mg/kg)
38     Drink,         # Drinking water dose (mg/kg/day)
39     IADose,        # Inter-arterial
40     PVDose,        # Portal Vein
41  ##-- TCA dosing
42     IVDoseTCA,    # IV dose (mg/kg) of TCA
43     PODoseTCA,    # Oral dose (mg/Kg) of TCA
44  ##-- TCOH dosing
45     IVDoseTCOH,   # IV dose (mg/kg) of TCOH
46     PODoseTCOH,   # Oral dose (mg/kg) of TCOH
47  ##-- Potentially time-varying parameters
48     QPmeas,       # Measured value of Alveolar ventilation QP
49     TCAUrnSat,    # Flag for saturated TCA urine
50     TCOGUrnSat,   # Flag for saturated TCOG urine
51     UrnMissing    # Flag for missing urine collection times
52  };
53
54  *****
55  ***          Output Variable Specifications          ***
56  *****
57  Outputs = {
58  *****
59  *** Outputs for mass balance check
60  MassBaltTCE,
61  TotDose,
62  TotTissue,
63  MassBaltCOH,
64  TotTCOHIn,
65  TotTCOHDose,
66  TotTissueTCOH,
67  TotMetabTCOH,
68  MassBaltTCA,
69  TotTCAIn,
70  TotTissueTCA,
71  MassBaltCOG,
72  TotTCOGIn,
73  TotTissueTCOG,
74  MassBalDCVG,
75  MassBalDCVC,
76  AUrnNDCVCequiv,
77
78  *****
79  *** Outputs that are potential dose metrics
80     TotMetab,     #(vrisk) Total metabolism
81     TotMetabBW34, #(vrisk) Total metabolism/BW^3/4
82     ATotMetLiv,   #(vrisk) Total metabolism in liver
83     AMetLivLiv,   #(vrisk) Total oxidation in liver/liver volume
84     AMetLivOther, #(vrisk) Total "other" oxidation in liver
85     AMetLivOtherLiv, #(vrisk) Total "other" oxidation in liver/liver vol
86     AMetLngResp, #(vrisk) oxiation in lung/respiratory tissue volume
87     AMetGSH,      #(vrisk) total GSH conjugation
88     AMetGSHBW34, #(vrisk) total GSH conjugation/BW^3/4
89     ABioactDCVCKid, #(vrisk) Amount of DCVC bioactivated/kidney volume
90  # NEW
91     TotDoseBW34, #(vrisk2) mg intake / BW^3/4
92     AMetLiv1BW34, #(vrisk2) mg hepatic oxidative metabolism / BW^3/4
93     TotOxMetabBW34, #(vrisk2) mg oxidative metabolism / BW^3/4
94     TotTCAInBW,  #(vrisk2) TCA production / BW
95  *****
96  *** Outputs for comparison to in vivo data
97  # TCE
98  RetDose, # human - = (InhDose - AExhExp)
99  CALv,   # needed for CALvPPM
100 CALvPPM, # human
101 CInhPPM, # mouse, rat
102 CInh,    # needed for CMixExh
103 CMixExh, # rat - Mixed exhaled breath (mg/l)
104 CArT,    # rat, human - Arterial blood concentration
105 CVen,    # mouse, rat, human
106 CBldMix, # rat - Concentration in mixed arterial+venous blood

```

INTER-AGENCY REVIEW DRAFT-DO NOT CITE OR QUOTE

1 # (used for cardiac puncture)
2 CFat, # mouse, rat - Concentration in fat
3 CGut, # rat
4 CRap, # needed for unlumped tissues
5 CSLw, # needed for unlumped tissues
6 CHrt, # rat - Concentration in heart tissue [use CRap]
7 CKid, # mouse, rat - Concentration in kidney
8 CLiv, # mouse, rat - Concentration in liver
9 CLung, # mouse, rat - Concentration in lung [use CRap]
10 CMus, # rat - Concentration in muscle [use CSLw]
11 CSpl, # rat - Concentration in spleen [use CRap]
12 CBrn, # rat - Concentration in brain [use CRap]
13 zAExh, # mouse
14 zAExhpost, # rat - Amount exhaled post-exposure (mg)
15
16 # TCOH
17 CTCOH, # mouse, rat, human - TCOH concentration in blood
18 CKidTCOH, # mouse - TCOH concentration in kidney
19 CLivTCOH, # mouse - TCOH concentration in liver
20 CLungTCOH, # mouse - TCOH concentration in lung
21
22 # TCA
23 CPlasTCA, # mouse, rat, human - TCA concentration in plasma
24 CBldTCA, # mouse, rat, human - TCA concentration in blood
25 CBodTCA, # needed for CKidTCA and CLungTCA
26 CKidTCA, # mouse - TCA concentration in kidney
27 CLivTCA, # mouse, rat - TCA concentration in liver
28 CLungTCA, # mouse - TCA concentration in lung
29 zAUrnTCA, # mouse, rat, human - Cumulative Urinary TCA
30 zAUrnTCA_collect, # human - TCA measurements for intermittent collection
31 zAUrnTCA_sat, # human - Saturated TCA measurements
32
33 # TCOG
34 zABileTCOG, # rat - Amount of TCOG in bile (mg)
35 CTCOG, # needed for CTCOGTCOH
36 CTCOGTCOH, # mouse - TCOG concentration in blood (in TCOH-equiv)
37 CKidTCOGTCOH, # mouse - TCOG concentration in kidney (in TCOH-equiv)
38 CLivTCOGTCOH, # mouse - TCOG concentration in liver (in TCOH-equiv)
39 CLungTCOGTCOH, # mouse - TCOG concentration in lung (in TCOH-equiv)
40 AUrnTCOGTCOH, # mouse, rat, human - Cumulative Urinary TCOG (in TCOH-equiv)
41 AUrnTCOGTCOH_collect, # human - TCOG (in TCOH-equiv) measurements for
42 # intermittent collection
43 AUrnTCOGTCOH_sat, # human - Saturated TCOG (in TCOH-equiv) measurements
44
45 # Other
46 CDCVGmol, # concentration of DCVG (mmol/l)
47 CDCVGmol0, # Dummy variable without likelihood (for plotting)#(v1.2.3.1)
48 CDCVG_ND, # Non-detect of DCVG (<0.05 pmol/ml= 5e-5 mmol/l)#(v1.2.3.1)
49 # Output -ln(likelihood)#(v1.2.3.1)
50 zAUrnNDCVC, # rat, human - Cumulative urinary NAcDVCV
51 AUrnTCTotMole, # rat, human - Cumulative urinary TCOH+TCA in nmoles
52 TotCTCOH, # mouse, human - TCOH+TCOG Concentration (in TCOH-equiv)
53 TotCTCOHcomp, # ONLY FOR COMPARISON WITH HACK

54 ATCOG, # ONLY FOR COMPARISON WITH HACK
55 QPsamp, # human - sampled value of alveolar ventilation rate
56
57 ## PARAMETERS #(vrisk3)
58
59 QCNOW, # (vrisk3) #Cardiac output (L/hr)
60 QP, # (vrisk3) #Alveolar ventilation (L/hr)
61 QFatCtmp, # (vrisk3) #Scaled fat blood flow
62 QGutCtmp, # (vrisk3) #Scaled gut blood flow
63 QLivCtmp, # (vrisk3) #Scaled liver blood flow
64 QSlwCtmp, # (vrisk3) #Scaled slowly perfused blood flow
65 QRapCtmp, # (vrisk3) #Scaled rapidly perfused blood flow
66 QKidCtmp, # (vrisk3) #Scaled kidney blood flow
67 DResp, # (vrisk3) #Respiratory lumen:tissue diffusive clearance rate
68 VFatCtmp, # (vrisk3) #Fat fractional compartment volume
69 VGutCtmp, # (vrisk3) #Gut fractional compartment volume
70 VLivCtmp, # (vrisk3) #Liver fractional compartment volume
71 VRapCtmp, # (vrisk3) #Rapidly perfused fractional compartment volume
72 VRespLumCtmp, # (vrisk3) # Fractional volume of respiratory lumen
73 VRespEffCtmp, # (vrisk3) #Effective fractional volume of respiratory tissue
74 VKidCtmp, # (vrisk3) #Kidney fractional compartment volume
75 VBldCtmp, # (vrisk3) #Blood fractional compartment volume
76 VSlwCtmp, # (vrisk3) #Slowly perfused fractional compartment volume
77 VPlasCtmp, # (vrisk3) #Plasma fractional compartment volume
78 VBodCtmp, # (vrisk3) #TCA Body fractional compartment volume [not incl.
79 blood+liver]
80 VBodTCOHctmp, # (vrisk3) #TCOH/G Body fractional compartment volume [not incl.
81 liver]
82 PB, # (vrisk3) #TCE Blood/air partition coefficient
83 PFat, # (vrisk3) #TCE Fat/Blood partition coefficient
84 PGut, # (vrisk3) #TCE Gut/Blood partition coefficient
85 PLiv, # (vrisk3) #TCE Liver/Blood partition coefficient
86 PRap, # (vrisk3) #TCE Rapidly perfused/Blood partition coefficient
87 PResp, # (vrisk3) #TCE Respiratory tissue:air partition coefficient
88 PKid, # (vrisk3) #TCE Kidney/Blood partition coefficient
89 PSlw, # (vrisk3) #TCE Slowly perfused/Blood partition coefficient
90 TCAPlas, # (vrisk3) #TCA blood/plasma concentration ratio
91 PBodTCA, # (vrisk3) #Free TCA Body/blood plasma partition coefficient
92 PLivTCA, # (vrisk3) #Free TCA Liver/blood plasma partition coefficient
93 kDissoc, # (vrisk3) #Protein/TCA dissociation constant (umole/L)
94 BMax, # (vrisk3) #Maximum binding concentration (umole/L)
95 PBodTCOH, # (vrisk3) #TCOH body/blood partition coefficient
96 PLivTCOH, # (vrisk3) #TCOH liver/body partition coefficient
97 PBodTCOG, # (vrisk3) #TCOG body/blood partition coefficient
98 PLivTCOG, # (vrisk3) #TCOG liver/body partition coefficient
99 VDCVG, # (vrisk3) #DCVG effective volume of distribution
100 kAS, # (vrisk3) #TCE Stomach absorption coefficient (/hr)
101 kTSD, # (vrisk3) #TCE Stomach-duodenum transfer coefficient (/hr)
102 kAD, # (vrisk3) #TCE Duodenum absorption coefficient (/hr)
103 kTD, # (vrisk3) #TCE Duodenum-feces transfer coefficient (/hr)
104 kASTCA, # (vrisk3) #TCA Stomach absorption coefficient (/hr)
105 kASTCOH, # (vrisk3) #TCOH Stomach absorption coefficient (/hr)
106 VMax, # (vrisk3) #VMax for hepatic TCE oxidation (mg/hr)

INTER-AGENCY REVIEW DRAFT-DO NOT CITE OR QUOTE

1
2
3
4
5
6
7
8
9
10
11
12
13
14
15
16
17
18
19
20
21
22
23
24
25
26
27
28
29
30
31
32
33
34
35
36
37
38
39
40
41
42
43
44
45
46
47
48
49
50
51
52
53

```

KM, # (vrisk3) #KM for hepatic TCE oxidation (mg/L)
FracOther, # (vrisk3) #Fraction of hepatic TCE oxidation not to TCA+TCOH
FracTCA, # (vrisk3) #Fraction of hepatic TCE oxidation to TCA
VMaxDCVG, # (vrisk3) #VMax for hepatic TCE GSH conjugation (mg/hr)
KMDCVG, # (vrisk3) #KM for hepatic TCE GSH conjugation (mg/L)
VMaxKidDCVG, # (vrisk3) #VMax for renal TCE GSH conjugation (mg/hr)
KMKidDCVG, # (vrisk3) #KM for renal TCE GSH conjugation (mg/L)
FracKidDCVC, # (vrisk3) #Fraction of renal TCE GSH conj. "directly" to DCVC
# (vrisk3) #(i.e., via first pass)

VMaxClara, # (vrisk3) #VMax for Tracheo-bronchial TCE oxidation (mg/hr)
KMClara, # (vrisk3) #KM for Tracheo-bronchial TCE oxidation (mg/L)
FracLungSys, # (vrisk3) #Fraction of respiratory metabolism to systemic circ.
VMaxTCOH, # (vrisk3) #VMax for hepatic TCOH->TCA (mg/hr)
KMTCOH, # (vrisk3) #KM for hepatic TCOH->TCA (mg/L)
VMaxGluc, # (vrisk3) #VMax for hepatic TCOH->TCOG (mg/hr)
KMGluc, # (vrisk3) #KM for hepatic TCOH->TCOG (mg/L)
kMetTCOH, # (vrisk3) #Rate constant for hepatic TCOH->other (/hr)
kUrnTCA, # (vrisk3) #Rate constant for TCA plasma->urine (/hr)
kMetTCA, # (vrisk3) #Rate constant for hepatic TCA->other (/hr)
kBile, # (vrisk3) #Rate constant for TCOG liver->bile (/hr)
kEHR, # (vrisk3) #Lumped rate constant for TCOG bile->TCOH liver (/hr)
kUrnTCOG, # (vrisk3) #Rate constant for TCOG->urine (/hr)
kDCVG, # (vrisk3) #Rate constant for hepatic DCVG->DCVC (/hr)
kNAT, # (vrisk3) #Lumped rate constant for DCVC->Urinary NAcDCVC (/hr)
kKidBioact, # (vrisk3) #Rate constant for DCVC bioactivation (/hr)

## Misc
RUrnTCA, # (vrisk3)
RUrnTCOGTCOH, # (vrisk3)
RUrnNDCVC, # (vrisk3)
RAO,
CVenMole,
CPlasTCAMole,
CPlasTCAFreeMole
};

#####
***          Global Constants          ***
#####

# Molecular Weights
      MWTCE = 131.39;      # TCE
      MWDCA = 129.0;      # DCA
      MWDCVC = 216.1;      # DCVC
      MWTCA = 163.5;      # TCA
      MWChlor = 147.5;      # Chloral
      MWTCOH = 149.5;      # TCOH
      MWTCOHGluc = 325.53;      # TCOH-Gluc
      MWNADCVC = 258.8;      # N Acetyl DCVC

# Stoichiometry
StochChlorTCE = MWChlor / MWTCE;
StochTCATCE = MWTCA / MWTCE;

```

54
55
56
57
58
59
60
61
62
63
64
65
66
67
68
69
70
71
72
73
74
75
76
77
78
79
80
81
82
83
84
85
86
87
88
89
90
91
92
93
94
95
96
97
98
99
100
101
102
103
104
105
106

```

StochTCATCOH = MWTCA / MWTCE;
StochTCOHTCE = MWTCE / MWTCE;
StochGlucTCOH = MWTCOHGluc / MWTCE;
StochTCOHGluc = MWTCE / MWTCOHGluc;
StochTCEGluc = MWTCE / MWTCOHGluc;
StochDCVCTCE = MWDCVC / MWTCE;
      StochN = MWNADCVC / MWDCVC;
StochDCATCE = MWDCA / MWTCE;

#####
***          Global Model Parameters          ***
#####
# These are the actual model parameters used in "dynamics."
# Values that are assigned in the "initialize" section,
# are all set to 1 to avoid confusion.

#####
# Flows
QC      = 1;      # Cardiac output (L/hr)
QPsamp  = 1;      # Alveolar ventilation (L/hr)
VPR     = 1;      # Alveolar ventilation-perfusion ratio
QFatCtmp = 1;      # Scaled fat blood flow
QGutCtmp = 1;      # Scaled gut blood flow
QLivCtmp = 1;      # Scaled liver blood flow
QSlwCtmp = 1;      # Scaled slowly perfused blood flow
DResptmp = 1;      # Respiratory lumen:tissue diffusive clearance rate (L/hr)
[scaled to QP]
QKidCtmp = 1;      # Scaled kidney blood flow
FracPlas = 1;      # Fraction of blood that is plasma (1-hematocrit)
#####
# Volumes
VFat    = 1;      # Fat compartment volume (L)
VGut    = 1;      # Gut compartment volume (L)
VLiv    = 1;      # Liver compartment volume (L)
VRap    = 1;      # Rapidly perfused compartment volume (L)
VRespLum = 1;      # Volume of respiratory lumen (L air)
VRespEfftmp = 1;      # (vrisk) volume for respiratory tissue (L)
VRespEff = 1;      # Effective volume for respiratory tissue (L air) = V(tissue) *
Resp:Air partition coefficient
VKid    = 1;      # Kidney compartment volume (L)
VBld    = 1;      # Blood compartment volume (L)
VSlw    = 1;      # Slowly perfused compartment volume (L)
VPlas   = 1;      # Plasma compartment volume [fraction of blood] (L)
VBod    = 1;      # TCA Body compartment volume [not incl. blood+liver] (L)
VBodTCOH = 1;      # TCOH/G Body compartment volume [not incl. liver] (L)
#####
# Distribution/partitioning
PB      = 1;      # TCE Blood/air partition coefficient
PFat    = 1;      # TCE Fat/Blood partition coefficient
PGut    = 1;      # TCE Gut/Blood partition coefficient
PLiv    = 1;      # TCE Liver/Blood partition coefficient
PRap    = 1;      # TCE Rapidly perfused/Blood partition coefficient
PResp   = 1;      # TCE Respiratory tissue:air partition coefficient

```

INTER-AGENCY REVIEW DRAFT-DO NOT CITE OR QUOTE

```

1 PKid = 1; # TCE Kidney/Blood partition coefficient
2 PSlw = 1; # TCE Slowly perfused/Blood partition coefficient
3 TCAPlas = 1; # TCA blood/plasma concentration ratio
4 PBodTCA = 1; # Free TCA Body/blood plasma partition coefficient
5 PLivTCA = 1; # Free TCA Liver/blood plasma partition coefficient
6 kDissoc = 1; # Protein/TCA dissociation constant (umole/L)
7 BMax = 1; # Protein concentration (UNITS?)
8 PBodTCOH = 1; # TCOH body/blood partition coefficient
9 PLivTCOH = 1; # TCOH liver/body partition coefficient
10 PBodTCOG = 1; # TCOG body/blood partition coefficient
11 PLivTCOG = 1; # TCOG liver/body partition coefficient
12 VDCVG = 1; # DCVG effective volume of distribution
13 *****
14 # Oral absorption
15 kTSD = 1.4; # TCE Stomach-duodenum transfer coefficient (/hr)
16 kAS = 1.4; # TCE Stomach absorption coefficient (/hr)
17 kTD = 0.1; # TCE Duodenum-feces transfer coefficient (/hr)
18 kAD = 0.75; # TCE Duodenum absorption coefficient (/hr)
19 kASTCA = 0.75; # TCA Stomach absorption coefficient (/hr)
20 kASTCOH = 0.75; # TCOH Stomach absorption coefficient (/hr)
21 *****
22 # TCE Metabolism
23 VMax = 1; # VMax for hepatic TCE oxidation (mg/hr)
24 KM = 1; # KM for hepatic TCE oxidation (mg/L)
25 FracOther = 1; # Fraction of hepatic TCE oxidation not to TCA+TCOH
26 FracTCA = 1; # Fraction of hepatic TCE oxidation to TCA
27 VMaxDCVG = 1; # VMax for hepatic TCE GSH conjugation (mg/hr)
28 KMDCVG = 1; # KM for hepatic TCE GSH conjugation (mg/L)
29 VMaxKidDCVG = 1; # VMax for renal TCE GSH conjugation (mg/hr)
30 KMKidDCVG = 1; # KM for renal TCE GSH conjugation (mg/L)
31 VMaxClara = 1; # VMax for Tracheo-bronchial TCE oxidation (mg/hr)
32 KMClara = 1; # KM for Tracheo-bronchial TCE oxidation (mg/L)
33 # but in units of air concentration
34 FracLungSys = 1; # Fraction of respiratory oxidative metabolism that
35 enters systemic circulation
36 *****
37 # TCOH metabolism
38 VMaxTCOH = 1; # VMax for hepatic TCOH->TCA (mg/hr)
39 KMTCOH = 1; # KM for hepatic TCOH->TCA (mg/L)
40 VMaxGluc = 1; # VMax for hepatic TCOH->TCOG (mg/hr)
41 KMGluc = 1; # KM for hepatic TCOH->TCOG (mg/L)
42 kMetTCOH = 1; # Rate constant for hepatic TCOH->other (/hr)
43 *****
44 # TCA metabolism/clearance
45 kUrnTCA = 1; # Rate constant for TCA plasma->urine (/hr)
46 kMetTCA = 1; # Rate constant for hepatic TCA->other (/hr)
47 *****
48 # TCOG metabolism/clearance
49 kBile = 1; # Rate constant for TCOG liver->bile (/hr)
50 kEHR = 1; # Lumped rate constant for TCOG bile->TCOH liver (/hr)
51 kUrnTCOG = 1; # Rate constant for TCOG->urine (/hr)
52 *****
53

```

```

54 # DCVG metabolism
55 kDCVG = 1; # Rate constant for hepatic DCVG->DCVC (/hr)
56 FracKidDCVC = 1; # Fraction of renal TCE GSH conj. "directly" to DCVC
57 (i.e., via first pass)
58 *****
59 # DCVC metabolism/clearance
60 kNAT = 1; # Lumped rate constant for DCVC->Urinary NAcDCVC (/hr)
61 kKidBioact = 1; # Rate constant for DCVC bioactivation (/hr)
62 *****
63 # Closed chamber and other exposure parameters
64 Rodents = 1; # Number of rodents in closed chamber data
65 VCh = 1; # Chamber volume for closed chamber data
66 kLoss = 1; # Rate constant for closed chamber air loss
67 CC = 0.0; # Initial chamber concentration (ppm)
68 TChng = 0.003; # IV infusion duration (hour)
69 *****
70 ## Flag for species, sex -- these are global parameters
71 BW = 0.0; # Species-specific defaults during initialization
72 BW75 = 0.0; # (vrisk) Variable for BW^3/4
73 Male = 1.0; # 1 = male, 0 = female
74 Species = 1.0; # 1 = human, 2 = rat, 3 = mouse
75 *****
76 #*** Potentially measured covariates (constants) ***
77 *****
78 BWmeas = 0.0; # Body weight
79 VFatCmeas = 0.0; # Fractional volume fat
80 PBmeas = 0.0; # Measured blood-air partition coefficient
81 Hematocritmeas = 0.0; # Measured hematocrit -- used for FracPlas = 1 - HCT
82 CDCVGmolLD = 5e-5; # Detection limit of CDCVGmol#(v1.2.3.1)
83 *****
84 #*** Global Sampling Parameters ***
85 *****
86 # These parameters are potentially sampled/calibrated in the MCMC or MC
87 # analyses. The default values here are used if no sampled value is given.
88 # M_ indicates population mean parameters used only in MC sampling
89 # V_ indicates a population variance parameter used in MC and MCMC sampling
90 *****
91 # Flow Rates
92 lnQCC = 0.0; # Scaled by BW^0.75 and species-specific central estimates
93 lnVPRC = 0.0; # Scaled to species-specific central estimates
94 *****
95 # Fractional Blood Flows to Tissues (fraction of cardiac output)
96 QFatC = 1.0; # Scaled to species-specific central estimates
97 QGutC = 1.0; # Scaled to species-specific central estimates
98 QLivC = 1.0; # Scaled to species-specific central estimates
99 QSlwC = 1.0; # Scaled to species-specific central estimates
100 QKidC = 1.0; # Scaled to species-specific central estimates
101 FracPlasC = 1.0; # Scaled to species-specific central estimates
102 lnDRespC = 0.0; # Scaled to alveolar ventilation rate in dynamics
103 *****
104 # Fractional Tissue Volumes (fraction of BW)
105 *****
106

```

INTER-AGENCY REVIEW DRAFT-DO NOT CITE OR QUOTE

1 VFatC = 1.0; # Scaled to species-specific central estimates
 2 VGutC = 1.0; # Scaled to species-specific central estimates
 3 VLivC = 1.0; # Scaled to species-specific central estimates
 4 VRapC = 1.0; # Scaled to species-specific central estimates
 5 VRespLumC = 1.0; # Scaled to species-specific central estimates
 6 VRespEffC = 1.0; # Scaled to species-specific central estimates
 7
 8 VKidC = 1.0; # Scaled to species-specific central estimates
 9 VBldC = 1.0; # Scaled to species-specific central estimate
 10
 11 # Partition Coefficients for TCE
 12 lnPBC = 0.0; # Scaled to species-specific central estimates
 13 lnPFatC = 0.0; # Scaled to species-specific central estimates
 14 lnPGutC = 0.0; # Scaled to species-specific central estimates
 15 lnPLivC = 0.0; # Scaled to species-specific central estimates
 16 lnPRapC = 0.0; # Scaled to species-specific central estimates
 17 lnPRespC = 0.0; # Scaled to species-specific central estimates
 18 lnPKidC = 0.0; # Scaled to species-specific central estimates
 19 lnPSlwC = 0.0; # Scaled to species-specific central estimates
 20
 21 # Partition Coefficients for TCA
 22 lnPRBCPlasTCAC = 0.0; # Scaled to species-specific central estimates
 23 lnPBodTCAC = 0.0; # Scaled to species-specific central estimates
 24 lnPLivTCAC = 0.0; # Scaled to species-specific central estimates
 25
 26 # Plasma Binding for TCA
 27 lnkDissocC = 0.0; # Scaled to species-specific central estimates
 28 lnBMaxkDC = 0.0; # Scaled to species-specific central estimates
 29
 30 # Partition Coefficients for TCOH and TCOG
 31 lnPBodTCOHC = 0.0; # Scaled to species-specific central estimates
 32 lnPLivTCOHC = 0.0; # Scaled to species-specific central estimates
 33 lnPBodTCOGC = 0.0; # Scaled to species-specific central estimates
 34 lnPLivTCOGC = 0.0; # Scaled to species-specific central estimates
 35 lnPeffDCVG = 0.0; # Scaled to species-specific central estimates
 36
 37 # Oral Absorption rates
 38 lnkTSD = 0.336;
 39 lnkAS = 0.336;
 40 lnkTD = -2.303;
 41 lnkAD = -0.288;
 42 lnkASTCA = -0.288;
 43 lnkASTCOH = -0.288;
 44
 45 # TCE Metabolism
 46 lnVMaxC = 0.0; # Scaled by liver weight and species-specific central estimates
 47 lnKMC = 0.0; # Scaled to species-specific central estimates
 48 lnClC = 0.0; # Scaled to species-specific central estimates
 49 lnFracOtherC = 0.0; # Ratio of DCA to non-DCA
 50 lnFracTCAC = 0.0; # Ratio of TCA to TCOH
 51 lnVMaxDCVGC = 0.0; # Scaled by liver weight and species-specific central
 52 estimates
 53 lnClDCVGC = 0.0; # Scaled to species-specific central estimates

54 lnKMDCVGC = 0.0; # Scaled to species-specific central estimates
 55 lnVMaxKidDCVGC = 0.0; # Scaled by kidney weight and species-specific central
 56 estimates
 57 lnClKidDCVGC = 0.0; # Scaled to species-specific central estimates
 58 lnKMKidDCVGC = 0.0; # Scaled to species-specific central estimates
 59 lnVMaxLungLivC = 0.0; # Ratio of lung Vmax to liver Vmax,
 60 # Scaled to species-specific central estimates
 61 lnKMClara = 0.0; # now in units of air concentration
 62
 63 # Clearance in lung
 64 lnFracLungSysC = 0.0; # ratio of systemic to local clearance of lung
 65 oxidation
 66
 67 # TCOH Metabolism
 68 lnVMaxTCOHC = 0.0; # Scaled by BW^{0.75}
 69 lnClTCOHC = 0.0; # Scaled by BW^{0.75}
 70 lnKMTCOH = 0.0; #
 71 lnVMaxGlucC = 0.0; # Scaled by BW^{0.75}
 72 lnClGlucC = 0.0; # Scaled by BW^{0.75}
 73 lnKMGluc = 0.0; #
 74 lnkMetTCOHC = 0.0; # Scaled by BW^{-0.25}
 75
 76 # TCA Metabolism/clearance
 77 lnkUrnTCAC = 0.0; # Scaled by (plasma volume)⁻¹ and species-specific
 78 central estimates
 79 lnkMetTCAC = 0.0; # Scaled by BW^{-0.25}
 80
 81 # TCOG excretion and reabsorption
 82 lnkBileC = 0.0; # Scaled by BW^{-0.25}
 83 lnkEHRC = 0.0; # Scaled by BW^{-0.25}
 84 lnkUrnTCOGC = 0.0; # Scaled by (blood volume)⁻¹ and species-specific
 85 central estimates
 86
 87 # DCVG metabolism
 88 lnFracKidDCVCC = 0.0; # Ratio of "directly" to DCVC to systemic DCVG
 89 lnkDCVGC = 0.0; # Scaled by BW^{-0.25}
 90
 91 # DCVC metabolism
 92 lnkNATC = 0.0; # Scaled by BW^{-0.25}
 93 lnkKidBioactC = 0.0; # Scaled by BW^{-0.25}
 94
 95 # Closed chamber parameters
 96 NRodents = 1; #
 97 VChC = 1; #
 98 lnkLossC = 0; #
 99
 100 *****
 101 # Population means
 102 #
 103 # These are given truncated normal or uniform distributions, depending on
 104 # what prior information is available. Note that these distributions
 105 # reflect uncertainty in the population mean, not inter-individual
 106 # variability. Normal distributions are truncated at 2, 3, or 4 SD.

INTER-AGENCY REVIEW DRAFT-DO NOT CITE OR QUOTE

```

1 #           For fractional volumes and flows, 2xSD
2 #           For plasma fraction, 3xSD
3 #           For cardiac output and ventilation-perfusion ratio, 4xSD
4 #           For all others, 3xSD
5 #           For uniform distributions, range of 1e2 to 1e8 fold, centered on
6 #           central estimate.
7 #
8 M_lnQCC = 1.0;
9 M_lnVPRC = 1.0;
10 M_QFatC = 1.0;
11 M_QGutC = 1.0;
12 M_QLivC = 1.0;
13 M_QSlwC = 1.0;
14 M_QKidC = 1.0;
15 M_FracPlasC = 1.0;
16 M_lnDRespC = 1.0;
17 M_VFatC = 1.0;
18 M_VGutC = 1.0;
19 M_VLivC = 1.0;
20 M_VRapC = 1.0;
21 M_VRespLumC = 1.0;
22 M_VRespEffC = 1.0;
23 M_VKidC = 1.0;
24 M_VBldC = 1.0;
25 M_lnPBC = 1.0;
26 M_lnPFatC = 1.0;
27 M_lnPGutC = 1.0;
28 M_lnPLivC = 1.0;
29 M_lnPRapC = 1.0;
30 M_lnPRespC = 1.0;
31 M_lnPKidC = 1.0;
32 M_lnPSlwC = 1.0;
33 M_lnPRBCPlasTCAC = 1.0;
34 M_lnPBodTCAC = 1.0;
35 M_lnPLivTCAC = 1.0;
36 M_lnkDissoc = 1.0;
37 M_lnBMaxkDC = 1.0;
38 M_lnPBodTCOHC = 1.0;
39 M_lnPLivTCOHC = 1.0;
40 M_lnPBodTCOGC = 1.0;
41 M_lnPLivTCOGC = 1.0;
42 M_lnPeffDCVG = 1.0;
43 M_lnkTSD = 1.0;
44 M_lnkAS = 1.0;
45 M_lnkTD = 1.0;
46 M_lnkAD = 1.0;
47 M_lnkASTCA = 1.0;
48 M_lnkASTCOH = 1.0;
49 M_lnVMaxC = 1.0;
50 M_lnkMC = 1.0;
51 M_lnC1c = 1.0;
52 M_lnFracOtherC = 1.0;
53 M_lnFracTCAC = 1.0;

```

```

54 M_lnVMaxDCVGC = 1.0;
55 M_lnC1DCVGC = 1.0;
56 M_lnkMDCVGC = 1.0;
57 M_lnVMaxKidDCVGC = 1.0;
58 M_lnC1KidDCVGC = 1.0;
59 M_lnkMKidDCVGC = 1.0;
60 M_lnVMaxLungLivC = 1.0;
61 M_lnkMClara = 1.0;
62 M_lnFracLungSysC = 1.0;
63 M_lnVMaxTCOHC = 1.0;
64 M_lnC1TCOHC = 1.0;
65 M_lnkMTCOH = 1.0;
66 M_lnVMaxGlucC = 1.0;
67 M_lnC1GlucC = 1.0;
68 M_lnkMGluc = 1.0;
69 M_lnkMetTCOHC = 1.0;
70 M_lnkUrnTCAC = 1.0;
71 M_lnkMetTCAC = 1.0;
72 M_lnkBileC = 1.0;
73 M_lnkEHRC = 1.0;
74 M_lnkUrnTCOGC = 1.0;
75 M_lnFracKidDCVCC = 1.0;
76 M_lnkDCVGC = 1.0;
77 M_lnkNATC = 1.0;
78 M_lnkKidBioactC = 1.0;
79
80
81 #*****
82 # Population Variances
83 #
84 # These are given InvGamma(alpha,beta) distributions. The parameterization
85 # for alpha and beta is given by:
86 # alpha = (n-1)/2
87 # beta = s^2*(n-1)/2
88 # where n = number of data points, and s^2 is the sample variance
89 # Sum(x_i^2)/n - <x>^2.
90 # Generally, for parameters for which there is no direct data, assume a
91 # value of n = 5 (alpha = 2). For a sample variance s^2, this gives
92 # an expected value for the standard deviation <sigma> = 0.9*s,
93 # a median [2.5%,97.5%] of 1.1*s [0.6*s,2.9*s].
94 #
95 V_lnQCC = 1.0;
96 V_lnVPRC = 1.0;
97 V_QFatC = 1.0;
98 V_QGutC = 1.0;
99 V_QLivC = 1.0;
100 V_QSlwC = 1.0;
101 V_QKidC = 1.0;
102 V_FracPlasC = 1.0;
103 V_lnDRespC = 1.0;
104 V_VFatC = 1.0;
105 V_VGutC = 1.0;
106 V_VLivC = 1.0;

```

INTER-AGENCY REVIEW DRAFT-DO NOT CITE OR QUOTE

1 V_VRapC = 1.0;
 2 V_VRespLumC = 1.0;
 3 V_VRespEffC = 1.0;
 4 V_VKidC = 1.0;
 5 V_VBldC = 1.0;
 6 V_lnPBC = 1.0;
 7 V_lnPFatC = 1.0;
 8 V_lnPGutC = 1.0;
 9 V_lnPLivC = 1.0;
 10 V_lnPRapC = 1.0;
 11 V_lnPRespC = 1.0;
 12 V_lnPKidC = 1.0;
 13 V_lnPSlwC = 1.0;
 14 V_lnPRBCPlasTCAC = 1.0;
 15 V_lnPBodTCAC = 1.0;
 16 V_lnPLivTCAC = 1.0;
 17 V_lnkDissocC = 1.0;
 18 V_lnBMaxkDC = 1.0;
 19 V_lnPBodTCOHC = 1.0;
 20 V_lnPLivTCOHC = 1.0;
 21 V_lnPBodTCOGC = 1.0;
 22 V_lnPLivTCOGC = 1.0;
 23 V_lnPeffDCVG = 1.0;
 24 V_lnkTSD = 1.0;
 25 V_lnkAS = 1.0;
 26 V_lnkTD = 1.0;
 27 V_lnkAD = 1.0;
 28 V_lnkASTCA = 1.0;
 29 V_lnkASTCOH = 1.0;
 30 V_lnVMaxC = 1.0;
 31 V_lnKMC = 1.0;
 32 V_lnClC = 1.0;
 33 V_lnFracOtherC = 1.0;
 34 V_lnFracTCAC = 1.0;
 35 V_lnVMaxDCVGC = 1.0;
 36 V_lnClDCVGC = 1.0;
 37 V_lnKMDCVGC = 1.0;
 38 V_lnVMaxKidDCVGC = 1.0;
 39 V_lnClKidDCVGC = 1.0;
 40 V_lnKMKidDCVGC = 1.0;
 41 V_lnVMaxLungLivC = 1.0;
 42 V_lnKMClara = 1.0;
 43 V_lnFracLungSysC = 1.0;
 44 V_lnVMaxTCOHC = 1.0;
 45 V_lnClTCOHC = 1.0;
 46 V_lnkMTCOH = 1.0;
 47 V_lnVMaxGlucC = 1.0;
 48 V_lnClGlucC = 1.0;
 49 V_lnkMGluc = 1.0;
 50 V_lnkMetTCOHC = 1.0;
 51 V_lnkUrnTCAC = 1.0;
 52 V_lnkMetTCAC = 1.0;
 53 V_lnkBileC = 1.0;

54 V_lnkEHRC = 1.0;
 55 V_lnkUrnTCOGC = 1.0;
 56 V_lnFracKidDCVCC = 1.0;
 57 V_lnkDCVGC = 1.0;
 58 V_lnkNATC = 1.0;
 59 V_lnkKidBioactC = 1.0;
 60
 61 #*****
 62 # Measurement error variances for output
 63
 64 Ve_RetDose = 1;
 65 Ve_CALv = 1;
 66 Ve_CALvPPM = 1;
 67 Ve_CInhPPM = 1;
 68 Ve_CInh = 1;
 69 Ve_CMixExh = 1;
 70 Ve_CArt = 1;
 71 Ve_CVen = 1;
 72 Ve_CBldMix = 1;
 73
 74 Ve_CFat = 1;
 75 Ve_CGut = 1;
 76 Ve_CRap = 1;
 77 Ve_CSlw = 1;
 78 Ve_CHrt = 1;
 79 Ve_CKid = 1;
 80 Ve_CLiv = 1;
 81 Ve_CLung = 1;
 82 Ve_CMus = 1;
 83 Ve_CSpl = 1;
 84 Ve_CBrn = 1;
 85 Ve_zAExh = 1;
 86 Ve_zAExhpost = 1;
 87
 88
 89 Ve_CTCOH = 1;
 90 Ve_CKidTCOH = 1;
 91 Ve_CLivTCOH = 1;
 92 Ve_CLungTCOH = 1;
 93
 94
 95 Ve_CPlasTCA = 1;
 96 Ve_CBldTCA = 1;
 97 Ve_CBodTCA = 1;
 98 Ve_CKidTCA = 1;
 99 Ve_CLivTCA = 1;
 100 Ve_CLungTCA = 1;
 101 Ve_zAurnTCA = 1;
 102 Ve_zAurnTCA_collect = 1;
 103 Ve_zAurnTCA_sat = 1;
 104
 105
 106 Ve_zABileTCOG = 1;

INTER-AGENCY REVIEW DRAFT-DO NOT CITE OR QUOTE

```

1 Ve_CTCOG = 1;
2 Ve_CTCOGTCOH = 1;
3 Ve_CKidTCOGTCOH = 1;
4 Ve_CLivTCOGTCOH = 1;
5 Ve_CLungTCOGTCOH = 1;
6 Ve_AUrnTCOGTCOH = 1;
7 Ve_AUrnTCOGTCOH_collect = 1;
8
9 Ve_AUrnTCOGTCOH_sat = 1;
10
11
12 Ve_CDCVGmol = 1;
13 Ve_zAUrnNDCVC = 1;
14 Ve_AUrnTCTotMole = 1;
15 Ve_TotCTCOH = 1;
16 Ve_QPsamp = 1;
17
18
19 *****
20 *** Defaults for input parameters ***
21 *****
22 ##-- TCE dosing
23     Conc = 0.0;      # Inhalation exposure conc. (ppm)
24     IVDose = 0.0;    # IV dose (mg/kg)
25     PDose = 0.0;     # Oral gavage dose (mg/kg)
26     Drink = 0.0;     # Drinking water dose (mg/kg/day)
27     IADose = 0.0;    # Intraarterial dose (mg/kg)
28     PVDose = 0.0;    # Portal vein dose (mg/kg)
29
30 ##-- TCA dosing
31     IVDoseTCA = 0.0;# IV dose (mg/kg) of TCA
32     PODoseTCA = 0.0;# Oral dose (mg/kg) of TCA
33
34 ##-- TCOH dosing
35     IVDoseTCOH = 0.0;# IV dose (mg/kg) of TCOH
36     PODoseTCOH = 0.0;# Oral dose (mg/kg) of TCOH
37
38 ##-- Potentially time-varying parameters
39     QPmeas = 0.0;    # Measured value of Alveolar ventilation QP
40     TCAUrnSat = 0.0;# Flag for saturated TCA urine
41     TCOGUrnSat = 0.0;# Flag for saturated TCOG urine
42     UrnMissing = 0.0;# Flag for missing urine collection times
43
44 Initialize {
45
46 *****
47 *** Parameter Initialization and Scaling ***
48 *****
49 # Model Parameters (used in dynamics):
50 #     QC          Cardiac output (L/hr)
51 #     VPR         Ventilation-perfusion ratio
52 #     QPsamp      Alveolar ventilation (L/hr)
53 #     QFatCtmp    Scaled fat blood flow
54 #     QGutCtmp    Scaled gut blood flow
55 #     QLivCtmp    Scaled liver blood flow
56 #     QSlwCtmp    Scaled slowly perfused blood flow
57 #     DResptmp    Respiratory lumen:tissue diffusive clearance rate

```

```

54 #     QKidCtmp    Scaled kidney blood flow
55 #     FracPlas    Fraction of blood that is plasma (1-hematocrit)
56 #     VFat        Fat compartment volume (L)
57 #     VGut        Gut compartment volume (L)
58 #     VLiv        Liver compartment volume (L)
59 #     VRap        Rapidly perfused compartment volume (L)
60 #     VRespLum    Volume of respiratory lumen (L air)
61 #     VRespEff    Effective volume of respiratory tissue (L air)
62 #     VKid        Kidney compartment volume (L)
63 #     VBld        Blood compartment volume (L)
64 #     VSlw        Slowly perfused compartment volume (L)
65 #     VPlas       Plasma compartment volume [fraction of blood] (L)
66 #     VBod        TCA Body compartment volume [not incl. blood+liver]
67 (L)
68 #     VBodTCOH   TCOH/G Body compartment volume [not incl. liver] (L)
69 #     PB          TCE Blood/air partition coefficient
70 #     PFat        TCE Fat/Blood partition coefficient
71 #     PGut        TCE Gut/Blood partition coefficient
72 #     PLiv        TCE Liver/Blood partition coefficient
73 #     PRap        TCE Rapidly perfused/Blood partition coefficient
74 #     PResp       TCE Respiratory tissue:air partition coefficient
75 #     PKid        TCE Kidney/Blood partition coefficient
76 #     PSlw        TCE Slowly perfused/Blood partition coefficient
77 #     TCAPlas    TCA blood/plasma concentration ratio
78 #     PBodTCA    Free TCA Body/blood plasma partition coefficient
79 #     PLivTCA    Free TCA Liver/blood plasma partition coefficient
80 #     kDissoc     Protein/TCA dissociation constant (umole/L)
81 #     BMax        Maximum binding concentration (umole/L)
82 #     PBodTCOH   TCOH body/blood partition coefficient
83 #     PLivTCOH   TCOH liver/body partition coefficient
84 #     PBodTCOG   TCOG body/blood partition coefficient
85 #     PLivTCOG   TCOG liver/body partition coefficient
86 #     kAS         TCE Stomach absorption coefficient (/hr)
87 #     kTSD        TCE Stomach-duodenum transfer coefficient (/hr)
88 #     kAD         TCE Duodenum absorption coefficient (/hr)
89 #     kTD         TCE Duodenum-feces transfer coefficient (/hr)
90 #     kASTCA     TCA Stomach absorption coefficient (/hr)
91 #     kASTCOH    TCOH Stomach absorption coefficient (/hr)
92 #     VMax        VMax for hepatic TCE oxidation (mg/hr)
93 #     KM          KM for hepatic TCE oxidation (mg/L)
94 #     FracOther   Fraction of hepatic TCE oxidation not to TCA+TCOH
95 #     FracTCA     Fraction of hepatic TCE oxidation to TCA
96 #     VMaxDCVG    VMax for hepatic TCE GSH conjugation (mg/hr)
97 #     KMDCVG     KM for hepatic TCE GSH conjugation (mg/L)
98 #     VMaxKidDCVG VMax for renal TCE GSH conjugation (mg/hr)
99 #     KMKidDCVG  KM for renal TCE GSH conjugation (mg/L)
100 #     VMaxClara  VMax for Tracheo-bronchial TCE oxidation (mg/hr)
101 #     KMClara    KM for Tracheo-bronchial TCE oxidation (mg/L)
102 #     FracLungSys Fraction of respiratory metabolism to systemic circ.
103 #     VMaxTCOH   VMax for hepatic TCOH->TCA (mg/hr)
104 #     KMTCOH     KM for hepatic TCOH->TCA (mg/L)
105 #     VMaxGluc   VMax for hepatic TCOH->TCOG (mg/hr)
106 #     KMGluc     KM for hepatic TCOH->TCOG (mg/L)

```

INTER-AGENCY REVIEW DRAFT-DO NOT CITE OR QUOTE

```

1 # kMetTCOH Rate constant for hepatic TCOH->other (/hr)
2 # kUrnTCA Rate constant for TCA plasma->urine (/hr)
3 # kMetTCA Rate constant for hepatic TCA->other (/hr)
4 # kBile Rate constant for TCOG liver->bile (/hr)
5 # kEHR Lumped rate constant for TCOG bile->TCOH liver (/hr)
6 # kUrnTCOG Rate constant for TCOG->urine (/hr)
7 # kDCVG Rate constant for hepatic DCVG->DCVC (/hr)
8 # FracKidDCVC Fraction of renal TCE GSH conj. "directly" to DCVC
9 # (i.e., via first pass)
10 # VDCVG DCVG effective volume of distribution
11 # kNAT Lumped rate constant for DCVC->Urinary NAcDCVC (/hr)
12 # kKidBioact Rate constant for DCVC bioactivation (/hr)
13 # Rodents Number of rodents in closed chamber data
14 # VCh Chamber volume for closed chamber data
15 # kLoss Rate constant for closed chamber air loss
16 # Parameters used (not assigned here)
17 # BW Body weight in kg
18 # Species 1 = human (default), 2 = rat, 3 = mouse
19 # Male 0 = female, 1 (default) = male
20 # CC Closed chamber initial concentration
21 # Sampling/scaling parameters (assigned or sampled)
22 # lnQCC
23 # lnVPRC
24 # lnDRespC
25 # QFatC
26 # QGutC
27 # QLivC
28 # QSlwC
29 # QKidC
30 # FracPlasC
31 # VFatC
32 # VGutC
33 # VLivC
34 # VRapC
35 # VRespLumC
36 # VRespEffC
37 # VKidC
38 # VBldC
39 # lnPBC
40 # lnPFatC
41 # lnPGutC
42 # lnPLivC
43 # lnPRapC
44 # lnPSlwC
45 # lnPRespC
46 # lnPKidC
47 # lnPRBCPlasTCAC
48 # lnPBodTCAC
49 # lnPLivTCAC
50 # lnkDissocC
51 # lnBMaxkDC
52 # lnPBodTCOHC
53 # lnPLivTCOHC
54 # lnPBodTCOGC
55 # lnPLivTCOGC
56 # lnPeffDCVG
57 # lnkTSD
58 # lnkAS
59 # lnkTD
60 # lnkAD
61 # lnkASTCA
62 # lnkASTCOH
63 # lnVMaxC
64 # lnKMC
65 # lnClC
66 # lnFracOtherC
67 # lnFracTCAC
68 # lnVMaxDCVGC
69 # lnClDCVGC
70 # lnKMDCVGC
71 # lnVMaxKidDCVGC
72 # lnClKidDCVGC
73 # lnKMKidDCVGC
74 # lnVMaxLungLivC
75 # lnKMClara
76 # lnFracLungSysC
77 # lnVMaxTCOHC
78 # lnClTCOHC
79 # lnKMTCOH
80 # lnVMaxGlucC
81 # lnClGlucC
82 # lnKMGluc
83 # lnkMetTCOHC
84 # lnkUrnTCAC
85 # lnkMetTCAC
86 # lnkBileC
87 # lnkEHRC
88 # lnkUrnTCOGC
89 # lnFracKidDCVCC
90 # lnkDCVGC
91 # lnkNATC
92 # lnkKidBioactC
93 # NRodents
94 # VChC
95 # lnkLossC
96 # Input parameters
97 # none
98 # Notes:
99 #*****
100 # use measured value of > 0, otherwise use 0.03 for mouse,
101 # 0.3 for rat, 60 for female human, 70 for male human
102 BW = (BWmeas > 0.0 ? BWmeas : (Species == 3 ? 0.03 : (Species == 2 ? 0.3 :
103 (Male == 0 ? 60.0 : 70.0) )));
104
105 BW75 = pow(BW, 0.75);
106 BW25 = pow(BW, 0.25);

```

INTER-AGENCY REVIEW DRAFT-DO NOT CITE OR QUOTE

```

1
2 # Cardiac Output and alveolar ventilation (L/hr)
3   QC = exp(lnQCC) * BW75 *      # Mouse, Rat, Human (default)
4     (Species == 3 ? 11.6 : (Species == 2 ? 13.3 : 16.0 ));
5   # Mouse: CO=13.98 +/- 2.85 ml/min, BW=30 g (Brown et al. 1997, Tab. 22)
6   #   Uncertainty CV is 0.20
7   # Rat: CO=110.4 ml/min +/- 15.6, BW=396 g (Brown et al. 1997, Tab. 22,
8     #   p 441). Uncertainty CV is 0.14.
9   # Human: Average of Male CO=6.5 l/min, BW=73 kg
10  #   and female CO= 5.9 l/min, BW=60 kg (ICRP #89, sitting at rest)
11  #   From Price et al. 2003, estimates of human perfusion rate were
12  #   4.7~6.5 for females and 5.5~7.1 l/min for males (note
13  #   portal blood was double-counted, and subtracted off here)
14  #   Thus for uncertainty use CV of 0.2, truncated at 4xCV
15  #   Variability from Price et al. (2003) had CV of 0.14~0.20,
16  #   so use 0.2 as central estimate
17  VPR = exp(lnVPRC)*
18     (Species == 3 ? 2.5 : (Species == 2 ? 1.9 : 0.96 ));
19  # Mouse: QP/BW=116.5 ml/min/100 g (Brown et al. 1997, Tab. 31), VPR=2.5
20  #   Assume uncertainty CV of 0.2 similar to QC, truncated at 4xCV
21  #   Consistent with range of QP in Tab. 31
22  # Rat: QP/BW=52.9 ml/min/100 g (Brown et al. 1997, Tab. 31), VPR=1.9
23  #   Assume uncertainty CV of 0.3 similar to QC, truncated at 4xCV
24  #   Used larger CV because Tab. 31 shows a very large range of QP
25  # Human: Average of Male VE=9 l/min, resp. rate=12 /min,
26  #   dead space=0.15 l (QP=7.2 l/min), and Female
27  #   VE=6.5 l/min, resp. rate=14 /min, dead space=0.12 l
28  #   (QP=4.8 l/min), VPR = 0.96
29  #   Assume uncertainty CV of 0.2 similar to QC, truncated at 4xCV
30  #   Consistent with range of QP in Tab. 31
31  QPsamp = QC*VPR;
32
33 #   Respiratory diffusion flow rate
34 #   Will be scaled by QP in dynamics
35 #   Use log-uniform distribution from 1e-5 to 10
36   DResptmp = exp(lnDRespC);
37
38 # Fractional Flows scaled to the appropriate species
39 # Fat = Adipose only
40 # Gut = GI tract + pancreas + spleen (all drain to portal vein)
41 # Liv = Liver, hepatic artery
42 # Slw = Muscle + Skin
43 # Kid = Kidney
44 # Rap = Rapidly perfused (rest of organs, plus bone marrow, lymph, etc.),
45 #   derived by difference in dynamics
46 #
47 # Mouse and rat data from Brown et al. (1997). Human data from
48 #   ICRP-89 (2002), and is sex-specific.
49
50   QFatCtmp = QFatC*
51   (Species == 3 ? 0.07 : (Species == 2 ? 0.07 : (Male == 0 ? 0.085 : 0.05)
52   ));
53   QGutCtmp = QGutC*

```

```

54   (Species == 3 ? 0.141 : (Species == 2 ? 0.153 : (Male == 0 ? 0.21 : 0.19)
55   ));
56   QLivCtmp = QLivC*
57   (Species == 3 ? 0.02 : (Species == 2 ? 0.021 : 0.065 ));
58   QSlwCtmp = QSlwC*
59   (Species == 3 ? 0.217 : (Species == 2 ? 0.336 : (Male == 0 ? 0.17 : 0.22)
60   ));
61   QKidCtmp = QKidC*
62   (Species == 3 ? 0.091 : (Species == 2 ? 0.141 : (Male == 0 ?
63   0.17 : 0.19) ));
64
65 # Plasma Flows to Tissues (L/hr)
66 ## Mice and rats from Hejtmancik et al. 2002,
67 ##   control F344 rats and B6C3F1 mice at 19 weeks of age
68 ## However, there appear to be significant strain differences in rodents, so
69 ##   assume uncertainty CV=0.2 and variability CV=0.2.
70 ## Human central estimate from ICRP. Well measured in humans,
71 ##   from Price et al. (2003),
72 ##   human SD in hematocrit was 0.029 in females, 0.027 in males,
73 ##   corresponding to FracPlas CV of 0.047 in females and
74 ##   0.048 in males. Use rounded CV = 0.05 for both uncertainty and
75 variability
76 ## Use measured 1-hematocrit if available
77 ## Truncate distributions at 3xCV to encompass clinical "normal range"
78   FracPlas = (Hematocritmeas > 0.0 ? (1-Hematocritmeas) : (FracPlasC *
79   (Species == 3 ? 0.52 : (Species == 2 ? 0.53 : (Male == 0 ? 0.615 :
80   0.567))));
81
82 # Tissue Volumes (L)
83 # Fat = Adipose only
84 # Gut = GI tract (not contents) + pancreas + spleen (all drain to portal vein)
85 # Liv = Liver
86 # Rap = Brain + Heart + (Lungs-TB) + Bone marrow + "Rest of the body"
87 # VResp = Tracheobronchial region (trachea+bronchial basal+
88 #   bronchial secretory+bronchiolar)
89 # Kid = Kidney
90 # Bld = Blood
91 # Slw = Muscle + Skin, derived by difference
92 # residual (assumed unperfused) = (Bone-Marrow)+GI contents+other
93 #
94 # Mouse and rat data from Brown et al. (1997). Human data from
95 #   ICRP-89 (2002), and is sex-specific.
96
97   VFat = BW * (VFatCmeas > 0.0 ? VFatCmeas : (VFatC * (Species == 3 ? 0.07 :
98   (Species == 2 ? 0.07 : (Male == 0 ? 0.317 : 0.199) ))));
99   VGut = VGutC * BW *
100  (Species == 3 ? 0.049 : (Species == 2 ? 0.032 : (Male == 0 ? 0.022 :
101  0.020) ));
102   VLiv = VLivC * BW *
103  (Species == 3 ? 0.055 : (Species == 2 ? 0.034 : (Male == 0 ? 0.023 :
104  0.025) ));
105   VRap = VRapC * BW *

```

INTER-AGENCY REVIEW DRAFT-DO NOT CITE OR QUOTE

1 (Species == 3 ? 0.100 : (Species == 2 ? 0.088 : (Male == 0 ? 0.093 :
2 0.088)));
3 VRespLum = VRespLumC * BW *
4 (Species == 3 ? (0.00014/0.03) : (Species == 2 ? (0.0014/0.3) : (0.167/70)
5)); # Lumenal volumes from Styrene model (Saragapani et al. 2003)
6 VRespEfftmp = VRespEffC * BW *
7 (Species == 3 ? 0.0007 : (Species == 2 ? 0.0005 : 0.00018));
8 # Respiratory tract volume is TB region
9 # will be multiplied by partition coef. below
10 VKid = VKidC * BW *
11 (Species == 3 ? 0.017 : (Species == 2 ? 0.007 : (Male == 0 ? 0.0046 :
12 0.0043)));
13 VBld = VBldC * BW *
14 (Species == 3 ? 0.049 : (Species == 2 ? 0.074 : (Male == 0 ? 0.068 :
15 0.077)));
16 VSlw = (Species == 3 ? 0.8897 : (Species == 2 ? 0.8995 : (Male == 0 ?
17 0.85778 : 0.856))) * BW
18 - VFat - VGut - VLiv - VRap - VRespEfftmp - VKid - VBld;
19 # Slowly perfused:
20 # Baseline mouse: 0.8897-0.049-0.017-0.0007-0.1-0.055-0.049-0.07= 0.549
21 # Baseline rat: 0.8995 -0.074-0.007-0.0005-0.088-0.034-0.032-0.07= 0.594
22 # Baseline human F: 0.85778-0.068-0.0046-0.00018-0.093-0.023-0.022-0.317= 0.33
23 # Baseline human M: 0.856-0.077-0.0043-0.00018-0.088-0.025-0.02-0.199= 0.4425
24
25 VPlas = FracPlas * VBld;
26 VBod = VFat + VGut + VRap + VRespEfftmp + VKid + VSlw; # For TCA
27 VBodTCOH = VBod + VBld; # for TCOH and TCOG -- body without liver
28
29 # Partition coefficients
30 PB = (PBmeas > 0.0 ? PBmeas : (exp(lnPBC) * (Species == 3 ? 15. : (Species ==
31 2 ? 22. : 9.5)))); # Blood-air
32 # Mice: pooling Abbas and Fisher 1997, Fisher et al. 1991
33 # each a single measurement, with overall CV = 0.07.
34 # Given small number of measurements, and variability
35 # in rat, use CV of 0.25 for uncertainty and variability.
36 # Rats: pooling Sato et al. 1977, Gargas et al. 1989,
37 Barton et al. 1995, Simmons et al. 2002, Koizumi 1989,
38 Fisher et al. 1989. Fisher et al. measurement substantially
39 smaller than others (15 vs. 21-26). Recent article
40 by Rodriguez et al. 2007 shows significant change with
41 age (13.1 at PND10, 17.5 at adult, 21.8 at aged), also seems
42 to favor lower values than previously reported. Therefore
43 use CV = 0.25 for uncertainty and variability.
44 # Humans: pooling Sato and Nakajima 1979, Sato et al. 1977,
45 Gargas et al. 1989, Fiserova-Bergerova et al. 1984,
46 Fisher et al. 1998, Koizumi 1989
47 # Overall variability CV = 0.185. Consistent with
48 # within study inter-individual variability CV = 0.07-0.22.
49 # Study-to-study, sex-specific means range 8.1-11, so
50 # uncertainty CV = 0.2.
51
52 PFat = exp(lnPFatC) * # Fat/blood
53 (Species == 3 ? 36. : (Species == 2 ? 27. : 67.));
Mice: Abbas and Fisher 1997. Single measurement. Use

54 # rat uncertainty of CV = 0.3.
55 # Rats: Pooling Barton et al. 1995, Sato et al. 1977,
56 # Fisher et al. 1989. Recent article by Rodriguez et al.
57 (2007) shows higher value of 36., so assume uncertainty
58 # CV of 0.3.
59 # Humans: Pooling Fiserova-Bergerova et al. 1984, Fisher et al. 1998,
60 # Sato et al. 1977. Variability in Fat:Air has CV = 0.07.
61 # For uncertainty, dominated by PB uncertainty CV = 0.2
62 # For variability, add CVs in quadrature for
63 sqrt(0.07^2+0.185^2)=0.20
64 PGut = exp(lnPGutC) * # Gut/blood
65 (Species == 3 ? 1.9 : (Species == 2 ? 1.4 : 2.6));
66 # Mice: Geometric mean of liver, kidney
67 # Rats: Geometric mean of liver, kidney
68 # Humans: Geometric mean of liver, kidney
69 # Uncertainty of CV = 0.4 due to tissue extrapolation
70 PLiv = exp(lnPLivC) * # Liver/blood
71 (Species == 3 ? 1.7 : (Species == 2 ? 1.5 : 4.1));
72 # Mice: Fisher et al. 1991, single datum, so assumed uncert CV = 0.4
73 # Rats: Pooling Barton et al. 1995, Sato et al. 1977,
74 # Fisher et al. 1989, with little variation (range 1.3-1.7).
75 # Recent article by Rodriguez et al. reports 1.34. Use
76 # uncertainty CV = 0.15.
77 # Humans: Pooling Fiserova-Bergerova et al. 1984, Fisher et al. 1998
78 # almost 2-fold difference in Liver:Air values, so uncertainty
79 # CV = 0.4
80 PRap = exp(lnPRapC) * # Rapidly perfused/blood
81 (Species == 3 ? 1.9 : (Species == 2 ? 1.3 : 2.6));
82 # Mice: Similar to liver, kidney. Uncertainty CV = 0.4 due to
83 # tissue extrapolation
84 # Rats: Use brain values Sato et al. 1977. Recent article by
85 # Rodriguez et al. (2007) reports 0.99 for brain. Uncertainty
86 # CV of 0.4 due to tissue extrapolation.
87 # Humans: Use brain from Fiserova-Bergerova et al. 1984
88 # Uncertainty of CV = 0.4 due to tissue extrapolation
89 PResp = exp(lnPRespC) * # Resp/blood =
90 (Species == 3 ? 2.6 : (Species == 2 ? 1.0 : 1.3));
91 # Mice: Abbas and Fisher 1997, single datum, so assumed uncert CV = 0.4
92 # Rats: Sato et al. 1977, single datum, so assumed uncert CV = 0.4
93 # Humans: Pooling Fiserova-Bergerova et al. 1984, Fisher et al. 1998
94 # > 2-fold difference in lung:air values, so uncertainty
95 # CV = 0.4
96 VRespEff = VRespEfftmp * PResp * PB; # Effective air volume
97 PKid = exp(lnPKidC) * # Slowly perfused/blood
98 (Species == 3 ? 2.1 : (Species == 2 ? 1.3 : 1.6));
99 # Mice: Abbas and Fisher 1997, single datum, so assumed uncert CV = 0.4
100 # Rats: Pooling Barton et al. 1995, Sato et al. 1977. Recent article
101 # by Rodriguez et al. (2007) reports 1.01, so use uncertainty
102 # CV of 0.3. Pooled variability CV = 0.39.
103 # Humans: Pooling Fiserova-Bergerova et al. 1984, Fisher et al. 1998
104 # For uncertainty, dominated by PB uncertainty CV = 0.2
105 # Variability in kidney:air CV = 0.23, so add to PB variability
106 # in quadrature sqrt(0.23^2+0.185^2)=0.30

INTER-AGENCY REVIEW DRAFT-DO NOT CITE OR QUOTE

1
2
3
4
5
6
7
8
9
10
11
12
13
14
15
16
17
18
19
20
21
22
23
24
25
26
27
28
29
30
31
32
33
34
35
36
37
38
39
40
41
42
43
44
45
46
47
48
49
50
51
52
53

```

PSlw = exp(lnPSlwC) * # Slowly perfused/blood
      (Species == 3 ? 2.4 : (Species == 2 ? 0.58 : 2.1 ));
# Mice: Muscle - Abbas and Fisher 1997, single datum, so assumed
#   uncert CV = 0.4
# Rats: Pooling Barton et al. 1995, Sato et al. 1977,
#   Fisher et al. 1989. Recent article by Rodriguez et al. (2007)
#   reported 0.72, so use uncertainty CV of 0.25. Variability
#   in Muscle:air and muscle:blood ~ CV = 0.3
# Humans: Pooling Fiserova-Bergerova et al. 1984, Fisher et al. 1998
#   Range of values 1.4-2.4, so uncertainty CV = 0.3
#   Variability in muscle:air CV = 0.3, so add to PB variability
#   in quadrature sqrt(0.3^2+0.185^2)=0.35

# TCA partitioning
TCAPlas = FracPlas + (1 - FracPlas) * 0.5 * exp(lnPRBCPlasTCAC);
#   Blood/Plasma concentration ratio. Note dependence
#   on fraction of blood that is plasma. Here
#   exp(lnPRBCPlasTCA) = partition coefficient
#   C(blood minus plasma)/C(plasma)
#   Default of 0.5, corresponding to Blood/Plasma
#   concentration ratio of 0.76 in
#   rats (Schultz et al 1999)
#   For rats, Normal uncertainty with GSD = 1.4
#   For mice and humans, diffuse prior uncertainty of
#   100-fold up/down
PBodTCA = TCAPlas * exp(lnPBodTCAC) *
      (Species == 3 ? 0.88 : (Species == 2 ? 0.88 : 0.52 ));
# Note -- these were done at 10-20 microg/ml (Abbas and Fisher 1997),
#   which is 1.635-3.27 mmol/ml (1.635-3.27 x 10^6 microM).
#   At this high concentration, plasma binding should be
#   saturated -- e.g., plasma albumin concentration was
#   measured to be P=190-239 microM in mouse, rat, and human
#   plasma by Lumpkin et al. 2003, or > 6800 molecules of
#   TCA per molecule of albumin. So the measured partition
#   coefficients should reflect free blood-tissue partitioning.
# Used muscle values, multiplied by blood:plasma ratio to get
#   Body:Plasma partition coefficient
# Rats = mice from Abbas and Fisher 1997
# Humans from Fisher et al. 1998
#   Uncertainty in mice, humans GSD = 1.4
#   For rats, GSD = 2.0, based on difference between mice
#   and humans.
PLivTCA = TCAPlas * exp(lnPLivTCAC) *
      (Species == 3 ? 1.18 : (Species == 2 ? 1.18 : 0.66 ));
# Multiplied by blood:plasma ratio to get Liver:Plasma
# Rats = mice from Abbas and Fisher 1997
# Humans from Fisher et al. 1998
#   Uncertainty in mice, humans GSD = 1.4
#   For rats, GSD = 2.0, based on difference between mice
#   and humans.

# Binding Parameters for TCA
# GM of Lumpkin et al. 2003; Schultz et al. 1999;

```

54
55
56
57
58
59
60
61
62
63
64
65
66
67
68
69
70
71
72
73
74
75
76
77
78
79
80
81
82
83
84
85
86
87
88
89
90
91
92
93
94
95
96
97
98
99
100
101
102
103
104
105
106

```

#   Templin et al. 1993, 1995; Yu et al. 2000
# Protein/TCA dissociation constant (umole/L)
#   note - GSD = 3.29, 1.84, and 1.062 for mouse, rat, human
kDissoc = exp(lnkDissocC) *
      (Species == 3 ? 107. : (Species == 2 ? 275. : 182. ));
# BMax = NSites * Protein concentration. Sampled parameter is
#   BMax/kD (determines binding at low concentrations)
#   note - GSD = 1.64, 1.60, 1.20 for mouse, rat, human
BMax = kDissoc * exp(lnBMaxkDC) *
      (Species == 3 ? 0.88 : (Species == 2 ? 1.22 : 4.62 ));

# TCOH partitioning
# Data from Abbas and Fisher 1997 (mouse) and Fisher et al.
#   1998 (human). For rat, used mouse values.
#   Uncertainty in mice, humans GSD = 1.4
#   For rats, GSD = 2.0, based on difference between mice
#   and humans.
PBodTCOH = exp(lnPBodTCOHC) *
      (Species == 3 ? 1.11 : (Species == 2 ? 1.11 : 0.91 ));
PLivTCOH = exp(lnPLivTCOHC) *
      (Species == 3 ? 1.3 : (Species == 2 ? 1.3 : 0.59 ));

# TCOG partitioning
# Use TCOH as a proxy, but uncertainty much greater
# (e.g., use uniform prior, 100-fold up/down)
PBodTCOG = exp(lnPBodTCOGC) *
      (Species == 3 ? 1.11 : (Species == 2 ? 1.11 : 0.91 ));
PLivTCOG = exp(lnPLivTCOGC) *
      (Species == 3 ? 1.3 : (Species == 2 ? 1.3 : 0.59 ));

# DCVG distribution volume
# exp(lnPeffDCVG) is the effective partition coefficient for
# the "body" (non-blood) compartment
# Diffuse prior distribution: loguniform 1e-3 to 1e3
VDCVG = VBld + # blood plus body (with "effective" PC)
      exp(lnPeffDCVG) * (VBod + VLiv);

# Absorption Rate Constants (/hr)
# All priors are diffuse (log)uniform distributions
# transfer from stomach centered on 1.4/hr, range up or down 100-fold,
#   based on human stomach half-time of 0.5 hr.
kTSD = exp(lnkTSD);
# stomach absorption centered on 1.4/hr, range up or down 1000-fold
kAS = exp(lnkAS);
# assume no fecal excretion -- 100% absorption
kTD = 0.0 * exp(lnkTD);
# intestinal absorption centered on 0.75/hr, range up or down
#   1000-fold, based on human transit time of small intestine
#   of 4 hr (95% throughput in 4 hr)
kAD = exp(lnkAD);
kASTCA = exp(lnkASTCA);
kASTCOH = exp(lnkASTCOH);

```

INTER-AGENCY REVIEW DRAFT-DO NOT CITE OR QUOTE

1
2
3
4
5
6
7
8
9
10
11
12
13
14
15
16
17
18
19
20
21
22
23
24
25
26
27
28
29
30
31
32
33
34
35
36
37
38
39
40
41
42
43
44
45
46
47
48
49
50
51
52
53

```
# TCE Oxidative Metabolism Constants
# For rodents, in vitro microsomal data define priors (pooled).
# For human, combined in vitro microsomal+hepatocellular individual data
#   define priors.
# All data from Elfarra et al. 1998; Lipscomb et al. 1997, 1998a,b
# For VMax, scaling from in vitro data were (Barter et al. 2007):
#   32 mg microsomal protein/g liver
#   99 x 1e6 hepatocytes/g liver
# Here, human data assumed representative of mouse and rats.
# For KM, two different scaling methods were used for microsomes:
#   Assume microsomal concentration = liver concentration, and
#   use central estimate of liver:blood PC (see above)
#   Use measured microsome:air partition coefficient (1.78) and
#   central estimate of blood:air PC (see above)
# For human KM from hepatocytes, used measured human hepatocyte:air
#   partition coefficient (21.62, Lipscomb et al. 1998b), and
#   central estimate of blood:air PC.
# Note that to that the hepatocyte:air PC is similar to that
#   found in liver homogenates (human: 29.4+/-5.1 from Fiserova-
#   Bergerova et al. 1984, and 54 for Fisher et al. 1998; rat:
#   27.2+/-3.4 from Gargas et al. 1989, 62.7 from Koisumi 1989,
#   43.6 from Sato et al. 1977; mouse: 23.2 from Fisher et al. 1991).
# For humans, sampled parameters are VMax and CLC (VMax/KM), due to
#   improved convergence. VMax is kept as a parameter because it
#   appears less uncertain (i.e., more consistent across microsomal
#   and hepatocyte data).

# Central estimate of VMax is 342, 76.2, and 32.3 (micromol/min/
#   kg liver) for mouse, rat, human. Converting to /hr by
#   * (60 min/hr * 0.1314 mg/micromol) gives
#   2700, 600, and 255 mg/hr/kg liver
# Observed variability of about 2-fold GSD. Assume 2-fold GSD for
#   both uncertainty and variability
VMax = Vliv*exp(lnVMaxC)*
      (Species == 3 ? 2700. : (Species == 2 ? 600. : 255.));

# For mouse and rat central estimates for KM are 0.068-1.088 and
#   0.039-0.679 mmol/l in blood, depending on the scaling
#   method used. Taking the geometric mean, and converting
#   to mg/l by 131.4 mg/mmol gives 36. and 21. mg/l in blood.
# For human, central estimate
#   for CL are 0.306-3.95 l/min/kg liver. Taking the geometric
#   mean and converting to /hr gives a central estimate of
#   66. l/hr/kg.
#   KM is then derived from KM = VMax/(CL*Vliv) (central estimate
#   of
# Note uncertainty due to scaling is about 4-fold.
#   Variability is about 3-fold in mice, 1.3-fold in rats, and
#   2- to 4- fold in humans (depending on scaling).
KM = (Species == 3 ? 36.*exp(lnKMC) : (Species == 2 ? 21.*exp(lnKMC) :
VMax/(Vliv*66.*exp(lnCLC))));
```

54
55
56
57
58
59
60
61
62
63
64
65
66
67
68
69
70
71
72
73
74
75
76
77
78
79
80
81
82
83
84
85
86
87
88
89
90
91
92
93
94
95
96
97
98
99
100
101
102
103
104
105
106

```
# Oxidative metabolism splits
# Fractional split of TCE to DCA
# exp(lnFracOtherC) = ratio of DCA to non-DCA
# Diffuse prior distribution: loguniform 1e-4 to 1e2
FracOther = exp(lnFracOtherC)/(1+exp(lnFracOtherC));
# Fractional split of TCE to TCA
# exp(lnFracTCAC) = ratio of TCA to TCOH
# TCA/TCOH = 0.1 from Lipscomb et al. 1998b using fresh hepatocytes,
# but TCA/TCOH ~ 1 from Bronley-DeLancey et al 2006
# GM = 0.32, GSD = 3.2
FracTCA = 0.32*exp(lnFracTCAC)*(1-FracOther)/(1+0.32*exp(lnFracTCAC));

# TCE GSH Metabolism Constants
# Human in vitro data from Lash et al. 1999a, define human priors.
#
#           VMax (nmol/min/      KM (mM)           CLeff (ml/min/
#           g tissue)                g tissue)
# -----
#           [high affinity pathway only] [total]
# Human liver cytosol:      ~423           0.0055-0.023       21.2-87.0
# Human liver cytosol+      ~211           --                --
#   microsomes
#           [total]           [total]           [total]
# Human hepatocytes*       12-30**        0.012-0.039***     0.2-0.5****
# Human kidney cytosol:     81            0.0164-0.0263      3.08-4.93
#
# * estimated visually from Fig 1, Lash et al. 1999a
# ** Fig 1A, data from 50-500 ppm headspace at 60 min
#   and Fig 1B, data at 100-5000 ppm in headspace for 120 min
# *** Fig 1B, 30-100 ppm headspace, converted to blood concentration
#   using blood:air PC of 9.5
# **** Fig 1A, data at 50 ppm headspace at 120 min and Fig 1B, data at
#   25 and 50 ppm headspace at 120 min.
# Overall, human liver hepatocytes are probably most like the
#   intact liver (e.g., accounting for the competition between
#   GSH conjugation and oxidation). So central estimates based
#   on those: CLeff ~ 0.32 ml/min/g tissue, KM ~ 0.022 mM in blood.
# CLeff converted to 19 l/hr/kg; KM converted to 2.9 mg/l in blood
# However, uncertainty in CLeff is large (values in cytosol
# ~100-fold larger). Moreover, Green et al. 1997 reported
# DCVG formation in cytosol that was ~30,000-fold smaller
# than Lash et al. (1998) in cytosol, which would be a VMax
# ~300-fold smaller than Lash et al. (1998) in hepatocytes.
# Uncertainty in KM appears smaller (~4-fold)
# CLC: GM = 19., GSD = 100; KM: GM = 2.9., GSD = 4.
# In addition, at a single concentration, the variability
# in human liver cytosol samples had a GSD=1.3.
# For the human kidney, the kidney cytosol values are used, with the same
# uncertainty as for the liver. Note that the DCVG formation rates
# in rat kidney cortical cells and rat cytosol are quite similar
# (see below).
# CLC: GM = 230., GSD = 100; KM: GM = 2.7., GSD = 4.
# Rat and mouse in vitro data from Lash et al. 1995,1998 define rat and mouse
# priors. However, rats and mice are only assayed at 1 and 2 mM
# providing only a bound on VMax and very little data on KM.
```

INTER-AGENCY REVIEW DRAFT-DO NOT CITE OR QUOTE

```

1 #
2 # Rate at 2 mM Equivalent CLeff
3 # at 2 mM
4 # (nmol/min/ (ml/min/
5 # g tissue) g tissue)
6 # -----
7 # Rat hepatocytes: 4.4-16 2.0 0.0022-0.0079
8 # liver cytosol: 8.0-12 1.7-2.0 0.0040-0.0072
9 # kidney cells: 0.79-1.1 2.2 0.00036-0.00049
10 # kidney cytosol: 0.53-0.75 1.1-2.0 0.00027-0.00068
11 # Mouse liver cytosol: 36-40 1.1-2.0 0.018-0.036
12 # kidney cytosol: 6.2-9.3 0.91-2.0 0.0031-0.0102
13 #
14 # In most cases, rates were increased over the same sex/species at 1 mM,
15 # indicating VMax has not yet been reached. The values between cells
16 # and cytosol are more much consistent that in the human data.
17 # These data therefore put a lower bound on VMax and a lower bound
18 # on CLC. To account for in vitro-in vivo uncertainty, the lower
19 # bound of the prior distribution is set 100-fold below the central
20 # estimate of the measurements here. In addition, Green et al.
21 # (1997) found values 100-fold smaller than Lash et al. 1995, 1998.
22 # Therefore diffuse prior distributions set to 1e-2-1e4.
23 # Rat liver: Bound on VMax of 4.4-16, with GM of 8.4. Converting to
24 # mg/hr/kg tissue (* 131.4 ng/nmol * 60 min/hr * 1e3 g/kg / 1e6 mg/ng)
25 # gives a central estimate of 66. mg/hr/kg tissue. Bound on CL of
26 # 0.0022-0.0079, with GM of 0.0042. Converting to l/hr/kg tissue
27 # (* 60 min/hr) gives 0.25 l/hr/kg tissue.
28 # Rat kidney: Bound on VMax of 0.53-1.1, with GM of 0.76. Converting
29 # to mg/hr/kg tissue gives a central estimate of 6.0 mg/hr/kg.
30 # Bound on CL of 0.00027-0.00068, with GM of 0.00043. Converting
31 # to l/hr/kg tissue gives 0.026 l/hr/kg tissue.
32 # Mouse liver: Bound on VMax of 36-40, with GM of 38. Converting
33 # to mg/hr/kg tissue gives a central estimate of 300. mg/hr/kg.
34 # Bound on CL of 0.018-0.036, with GM of 0.025. Converting
35 # to l/hr/kg tissue gives 1.53 l/hr/kg tissue.
36 # Mouse kidney: Bound on VMax of 6.2-9.3, with GM of 7.6. Converting
37 # to mg/hr/kg tissue gives a central estimate of 60. mg/hr/kg.
38 # Bound on CL of 0.0031-0.0102, with GM of 0.0056. Converting
39 # to l/hr/kg tissue gives 0.34 l/hr/kg tissue.
40
41 VMaxDCVG = Vliv*(Species == 3 ? (300.*exp(lnVMaxDCVGC)) : (Species == 2 ?
42 (66.*exp(lnVMaxDCVGC)) : (2.9*19.*exp(lnClDCVGC+lnKMDCVGC))));
43 KMDCVG = (Species == 3 ? (VMaxDCVG/(Vliv*1.53*exp(lnClDCVGC))) : (Species ==
44 2 ? (VMaxDCVG/(Vliv*0.25*exp(lnClDCVGC))) : 2.9*exp(lnKMDCVGC));
45 VMaxKidDCVG = VKid*(Species == 3 ? (60.*exp(lnVMaxKidDCVGC)) : (Species ==
46 2 ? (6.0*exp(lnVMaxKidDCVGC)) : (2.7*230.*exp(lnClKidDCVGC+lnKMKidDCVGC))));
47 KMKidDCVG = (Species == 3 ? (VMaxKidDCVG/(VKid*0.34*exp(lnClKidDCVGC))) :
48 (Species == 2 ? (VMaxKidDCVG/(VKid*0.026*exp(lnClKidDCVGC))) :
49 2.7*exp(lnKMKidDCVGC));
50
51 # TCE Metabolism Constants for Chloral Kinetics in Lung (mg/hr)
52 # Scaled to liver VMax using data from Green et al. (1997)
53 # in microsomal preparations (nmol/min/mg protein) at ~1 mM.
54 # For humans, used detection limit of 0.03

```

```

54 # Additional scaling by lung/liver weight ratio
55 # from Brown et al. (1997) Table 21 (mouse and rat) or
56 # ICRP Pub 89 Table 2.8 (Human female and male)
57 # Uncertainty ~ 3-fold truncated at 3 GSD
58 # VMaxClara = exp(lnVMaxLungLivC) * VMax *
59 # (Species == 3 ? (1.03/1.87*0.7/5.5):(Species == 2 ?
60 (0.08/0.82*0.5/3.4):(0.03/0.33*(Male == 0 ? (0.42/1.4) : (0.5/1.8))));
61 KMClara = exp(lnKMClara);
62 # Fraction of Respiratory Metabolism that goes to system circulation
63 # (translocated to the liver)
64 # FracLungSys = exp(lnFracLungSysC)/(1 + exp(lnFracLungSysC));
65
66 # TCOH Metabolism Constants (mg/hr)
67 # No in vitro data. So use diffuse priors of
68 # 1e-4 to 1e4 mg/hr/kg^0.75 for VMax
69 # (4e-5 to 4000 mg/hr for rat),
70 # 1e-4 to 1e4 mg/l for KM,
71 # and 1e-5 to 1e3 l/hr/kg^0.75 for CL
72 # (2e-4 to 2.4e4 l/hr for human)
73 VMaxTCOH = BW75*
74 # (Species == 3 ? (exp(lnVMaxTCOHC)) : (Species == 2 ?
75 (exp(lnVMaxTCOHC)) : (exp(lnClTCOHC+lnKMTCOH))));
76 KMTCOH = exp(lnKMTCOH);
77 VMaxGluc = BW75*
78 # (Species == 3 ? (exp(lnVMaxGlucC)) : (Species == 2 ?
79 (exp(lnVMaxGlucC)) : (exp(lnClGlucC+lnKMGluc))));
80 KMGluc = exp(lnKMGluc);
81 # No in vitro data. So use diffuse priors of
82 # 1e-5 to 1e3 kg^0.25/hr (3.5e-6/hr to 3.5e2/hr for human)
83 kMetTCOH = exp(lnkMetTCOHC) / BW25;
84
85 # TCA kinetic parameters
86 # Central estimate based on GFR clearance per unit body weight
87 # 10.0, 8.7, 1.8 ml/min/kg for mouse, rat, human
88 # (= 0.6, 0.522, 0.108 l/hr/kg) from Lin 1995.
89 # = CL_GFR / BW (BW=0.02 for mouse, 0.265 for rat, 70 for human)
90 kUrn = CL_GFR / VPlas
91 # Diffuse prior with uncertainty of up,down 100-fold
92 kUrnTCA = exp(lnkUrnTCAC) * BW / VPlas *
93 # (Species == 3 ? 0.6 : (Species == 2 ? 0.522 : 0.108));
94 # No in vitro data. So use diffuse priors of
95 # 1e-4 to 1e2 /hr/kg^0.25 (0.3/hr to 35/hr for human)
96 kMetTCA = exp(lnkMetTCAC) / BW25;
97
98 # TCOG kinetic parameters
99 # No in vitro data. So use diffuse priors of
100 # 1e-4 to 1e2 /hr/kg^0.25 (0.3/hr to 35/hr for human)
101 kBile = exp(lnkBileC) / BW25;
102 kEHR = exp(lnkEHRC) / BW25;
103 # Central estimate based on GFR clearance per unit body weight
104 # 10.0, 8.7, 1.8 ml/min/kg for mouse, rat, human
105 # (= 0.6, 0.522, 0.108 l/hr/kg) from Lin 1995.
106 # = CL_GFR / BW (BW=0.02 for mouse, 0.265 for rat, 70 for human)

```

INTER-AGENCY REVIEW DRAFT-DO NOT CITE OR QUOTE

```

1      #      kUrn = CL_GFR / VBld
2      #      Diffuse prior with Uncertainty of up,down 1000-fold
3      kUrnTCOG = exp(lnkUrnTCOGC) * BW / (VBodTCOH * PBodTCOG) *
4              (Species == 3 ? 0.6 : (Species == 2 ? 0.522 : 0.108));
5
6      # DCVG Kinetics (/hr)
7      # Fraction of renal TCE GSH conj. "directly" to DCVC via "first pass"
8      # exp(lnFracOtherCC) = ratio of direct/non-direct
9      # Diffuse prior distribution: loguniform 1e-3 to 1e3
10     # FIXED in v1.2.3
11     # In ".in" files, set to 1, so that all kidney GSH conjugation
12     # is assumed to directly produce DCVC (model lacks identifiability
13     # otherwise).
14     FracKidDCVC = exp(lnFracKidDCVCC)/(1 + exp(lnFracKidDCVCC));
15     # No in vitro data. So use diffuse priors of
16     #      1e-4 to 1e2 /hr/kg^0.25 (0.3/hr to 35/hr for human)
17     kDCVG = exp(lnkDCVGC) / BW25;
18
19     # DCVC Kinetics in Kidney (/hr)
20     # No in vitro data. So use diffuse priors of
21     #      1e-4 to 1e2 /hr/kg^0.25 (0.3/hr to 35/hr for human)
22     kNAT = exp(lnkNATC) / BW25;
23     kKidBioact = exp(lnkKidBioactC) / BW25;
24
25     # CC data initialization
26     Rodents = (CC > 0 ? NRodents : 0.0); # Closed chamber simulation
27     VCh = (CC > 0 ? VChC - (Rodents * BW) : 1.0);
28     # Calculate net chamber volume
29     kLoss = (CC > 0 ? exp(lnkLossC) : 0.0);
30
31     #*****
32     ***      State Variable Initialization and Scaling      ***
33     #*****
34     # NOTE: All State Variables are automatically set to 0 initially,
35     # unless re-initialized here
36
37     Ach = (CC * VCh * MWTCE) / 24450.0; # Initial amount in chamber
38
39 };
40 ##### End of Initialization #####
41
42 Dynamics{
43
44     #*****
45     ***      Dynamic physiological parameter scaling      ***
46     #*****
47     # State Variables with dynamics:
48     #      none
49     # Input Variables:
50     #      QPmeas
51     # Other State Variables and Global Parameters:
52     #      QC
53     #      VPR
54     #      DResptmp
55     #      QPsamp
56     #      QFatCtmp
57     #      QGutCtmp
58     #      QLivCtmp
59     #      QSlwCtmp
60     #      QKidCtmp
61     #      FracPlas
62     # Temporary variables used:
63     #      none
64     # Temporary variables assigned:
65     #      QP
66     #      DResp
67     #      QCnow
68     #      QFat
69     #      QGut
70     #      QLiv
71     #      QSlw
72     #      QKid
73     #      QGutLiv
74     #      QRap
75     #      QCPlas
76     #      QBodPlas
77     #      QGutLivPlas
78     # Notes:
79     #*****
80     # QP uses QPmeas if value is > 0, otherwise uses sampled value
81     QP = (QPmeas > 0 ? QPmeas : QPsamp);
82     DResp = DResptmp * QP;
83
84     # QCnow uses QPmeas/VPR if QPmeas > 0, otherwise uses sampled value
85     QCnow = (QPmeas > 0 ? QPmeas/VPR : QC);
86
87     # These done here in dynamics in case QCnow changes
88     # Blood Flows to Tissues (L/hr)
89     QFat = (QFatCtmp) * QCnow; #
90     QGut = (QGutCtmp) * QCnow; #
91     QLiv = (QLivCtmp) * QCnow; #
92     QSlw = (QSlwCtmp) * QCnow; #
93
94     QKid = (QKidCtmp) * QCnow; #
95     QGutLiv = QGut + QLiv; #
96     QRap = QCnow - QFat - QGut - QLiv - QSlw - QKid;
97     QRapCtmp = QRap/QCnow; #(vrisk3)
98     QBod = QCnow - QGutLiv;
99
100    # Plasma Flows to Tissues (L/hr)
101    QCPlas = FracPlas * QCnow; #
102    QBodPlas = FracPlas * QBod; #
103    QGutLivPlas = FracPlas * QGutLiv; #
104
105    #*****
106

```

INTER-AGENCY REVIEW DRAFT-DO NOT CITE OR QUOTE

```

1  ***          Exposure and Absorption calculations          ***
2  #*****
3  # State Variables with dynamics:
4  #     AStom
5  #     ADuod
6  #     AStomTCA
7  #     AStomTCOH
8  # Input Variables:
9  #     IVDose
10 #     PDose
11 #     Drink
12 #     Conc
13 #     IVDoseTCA
14 #     PODoseTCA
15 #     IVDoseTCOH
16 #     PODoseTCOH
17 # Other State Variables and Global Parameters:
18 #     ACh
19 #     CC
20 #     VCh
21 #     MWTCE
22 #     BW
23 #     TChng
24 #     kAS
25 #     kTSD
26 #     kAD
27 #     kTD
28 #     kASTCA
29 #     kASTCOH
30 # Temporary variables used:
31 #     none
32 # Temporary variables assigned:
33 #     kIV - rate into CVen
34 #     kIA - rate into CArt
35 #     kPV - rate into portal vein
36 #     kStom - rate into stomach
37 #     kDrink - incorporated into RAO
38 #     RAO - rate into gut (oral absorption - both gavage and drinking water)
39 #     CInh - inhalation exposure concentration
40 #     kIVTCA - rate into blood
41 #     kStomTCA - rate into stomach
42 #     kPOTCA - rate into liver (oral absorption)
43 #     kIVTCOH - rate into blood
44 #     kStomTCOH - rate into stomach
45 #     kPOTCOH - rate into liver (oral absorption)
46 # Notes:
47 # For oral dosing, using "Spikes" for instantaneous inputs
48 # Inhalation Concentration (mg/L)
49 #     CInh uses Conc when open chamber (CC=0) and
50 #     ACh/VCh when closed chamber CC>0.
51 #*****
52 ##### TCE DOSING
53

```

```

54 ## IV route
55 kIV = (IVDose * BW) / TChng; # IV infusion rate (mg/hr)
56 # (IVDose constant for duration TChng)
57
58 kIA = (IADose * BW) / TChng; # IA infusion rate (mg/hr)
59
60 kPV = (PVDose * BW) / TChng; # PV infusion rate (mg/hr)
61
62 kStom = (PDose * BW) / TChng; # PO dose rate (into stomach) (mg/hr)
63
64 ## Oral route
65 # Amount of TCE in stomach -- for oral dosing only (mg)
66 dt(AStom) = kStom - AStom * (kAS + kTSD);
67
68 # Amount of TCE in duodenum -- for oral dosing only (mg)
69 dt(ADuod) = (kTSD * AStom) - (kAD + kTD) * ADuod;
70
71 # Rate of absorption from drinking water
72 kDrink = (Drink * BW) / 24.0; # Ingestion rate via drinking water (mg/hr)
73
74 # Total rate of absorption including gavage and drinking water
75 RAO = kDrink + (kAS * AStom) + (kAD * ADuod);
76
77 ## Inhalation route
78 CInh = (CC > 0 ? ACh/VCh : Conc*MWTCE/24450.0); # in mg/l
79
80 ##### TCA Dosing
81 kIVTCA = (IVDoseTCA * BW) / TChng; # TCA IV infusion rate (mg/hr)
82 kStomTCA = (PODoseTCA * BW) / TChng; # TCA PO dose rate into stomach
83 dt(AStomTCA) = kStomTCA - AStomTCA * kASTCA;
84 kPOTCA = AStomTCA * kASTCA; # TCA oral absorption rate (mg/hr)
85
86 ##### TCOH Dosing
87 kIVTCOH = (IVDoseTCOH * BW) / TChng; # TCOH IV infusion rate (mg/hr)
88 kStomTCOH = (PODoseTCOH * BW) / TChng; # TCOH PO dose rate into stomach
89 dt(AStomTCOH) = kStomTCOH - AStomTCOH * kASTCOH;
90 kPOTCOH = AStomTCOH * kASTCOH; # TCOH oral absorption rate (mg/hr)
91
92 #*****
93 #***          TCE Model          ***
94 #*****
95 # State Variables with dynamics:
96 #     ARap, # Amount in rapidly perfused tissues
97 #     ASlw, # Amount in slowly perfused tissues
98 #     AFat, # Amount in fat
99 #     AGut, # Amount in gut
100 #     ALiv, # Amount in liver
101 #     AInhResp,
102 #     AResp,
103 #     AExhResp,
104 #     AKid, # Amount in Kidney -- currently in Rap tissue
105 #     ABld, # Amount in Blood -- currently in Rap tissue
106 #     ACh, # Amount of TCE in closed chamber
107
108 # Input Variables:
109 #     none
110 # Other State Variables and Global Parameters:
111 #     VRap
112 #     PRap
113 #     VSlw

```

INTER-AGENCY REVIEW DRAFT-DO NOT CITE OR QUOTE

```

1 # PSlw
2 # VFat
3 # PFat
4 # VGut
5 # PGut
6 # VLiv
7 # PLiv
8 # VRespLum
9 # VRespEff
10 # FracLungSys
11 # VKid
12 # PKid
13 # VBld
14 # VMaxClara
15 # KMClara
16 # PB
17 # Rodents
18 # VCh
19 # kLoss
20 # VMax
21 # KM
22 # VMaxDCVG
23 # KMDCVG
24 # VMaxKidDCVG
25 # KMKidDCVG
26 # Temporary variables used:
27 # QM
28 # QFat
29 # QGutLiv
30 # QSlw
31 # QRap
32 # QKid
33 # kIV
34 # QCnow
35 # CInh
36 # QP
37 # RAO
38 # Temporary variables assigned:
39 # QM
40 # CRap
41 # CSLw
42 # CFat
43 # CGut
44 # CLiv
45 # CInhResp
46 # CResp
47 # CExhResp
48 # ExhFactor
49 # CMixExh
50 # CKid
51 # CVRap
52 # CVSlw
53 # CVFat

```

```

54 # CVGut
55 # CVLiv
56 # CVTB
57 # CVKid
58 # CVen
59 # RAMetLng
60 # CArt_tmp
61 # CArt
62 # CALv
63 # RAMetLiv1
64 # RAMetLiv2
65 # RAMetKid
66 # Notes:
67 #*****
68 #
69 #
70 #****Blood (venous)*****
71 # Tissue Concentrations (mg/L)
72   CRap = ARap/VRap;
73   CSLw = ASlw/VSlw;
74   CFat = AFat/VFat;
75   CGut = AGut/VGut;
76   CLiv = ALiv/VLiv;
77   CKid = AKid/VKid;
78 # Venous Concentrations (mg/L)
79   CVRap = CRap / PRap;
80   CVSlw = CSLw / PSlw;
81   CVFat = CFat / PFat;
82   CVGut = CGut / PGut;
83   CVLiv = CLiv / PLiv;
84   CVKid = CKid / PKid;
85 # Concentration of TCE in mixed venous blood (mg/L)
86   CVen = ABld/VBld;
87 # Dynamics for blood
88   dt(ABld) = (QFat*CVFat + QGutLiv*CVLiv + QSlw*CVSlw +
89             QRap*CVRap + QKid*CVKid + kIV) - CVen * QCnow;
90 #****Gas exchange and Respiratory Metabolism*****
91 #
92 #
93   QM = QP/0.7; # Minute-volume
94   CInhResp = AInhResp/VRespLum;
95   CResp = AResp/VRespEff;
96   CExhResp = AExhResp/VRespLum;
97   dt(AInhResp) = (QM*CInh + DResp*(CResp-CInhResp) - QM*CInhResp);
98   RAMetLng = VMaxClara * CResp/(KMClara + CResp);
99   dt(AResp) = (DResp*(CInhResp + CExhResp - 2*CResp) - RAMetLng);
100   CArt_tmp = (QCnow*CVen + QP*CInhResp)/(QCnow + (QP/PB));
101   dt(AExhResp) = (QM*(CInhResp-CExhResp) + QP*(CArt_tmp/PB-CInhResp) +
102                 DResp*(CResp-CExhResp));
103   CMixExh = (CExhResp > 0 ? CExhResp : 1e-15); # mixed exhaled breath
104 # Concentration in alveolar air (mg/L)
105 # Correction factor for exhaled air to account for
106

```

INTER-AGENCY REVIEW DRAFT-DO NOT CITE OR QUOTE

```

1      # absorption/desorption/metabolism in respiratory tissue
2      # = 1 if DResp = 0
3      ExhFactor_den = (QP * CArt_tmp / PB + (QM-QP)*CInhResp);
4      ExhFactor = (ExhFactor_den > 0) ? (
5          QM * CMixExh / ExhFactor_den) : 1;
6      # End-exhaled breath (corrected for absorption/
7      # desorption/metabolism in respiratory tissue)
8      CALv = CArt_tmp / PB * ExhFactor;
9      # Concentration in arterial blood entering circulation (mg/L)
10     CArt = CArt_tmp + kIA/QCnow; # add inter-arterial dose
11
12     #****Other dynamics for inhalation/exhalation *****
13     # Dynamics for amount of TCE in closed chamber
14     dt(ACh) = (Rodents * (QM * CMixExh - QM * ACh/VCh)) - (kLoss * ACh);
15
16     #**** Non-metabolizing tissues *****
17     # Amount of TCE in rapidly perfused tissues (mg)
18     dt(ARap) = QRap * (CArt - CVRap);
19     # Amount of TCE in slowly perfused tissues
20     dt(ASlw) = QSlw * (CArt - CVSlw);
21     # Amount of TCE in fat tissue (mg)
22     dt(AFat) = QFat*(CArt - CVFat);
23     # Amount of TCE in gut compartment (mg)
24     dt(AGut) = (QGut * (CArt - CVGut)) + RAO;
25
26     #**** Liver *****
27     # Rate of TCE oxidation by P450 to TCA, TCOH, and other (DCA) in liver (mg/hr)
28     RAMetLiv1 = (VMax * CVLiv) / (KM + CVLiv);
29     # Rate of TCE metabolized to DCVG in liver (mg)
30     RAMetLiv2 = (VMaxDCVG * CVLiv) / (KMDCVG + CVLiv);
31     # Dynamics for amount of TCE in liver (mg)
32     dt(ALiv) = (QLiv * (CArt - CVLiv)) + (QGut * (CVGut - CVLiv))
33         - RAMetLiv1 - RAMetLiv2 + kPV; # added PV dose
34
35     #**** Kidney *****
36     # Rate of TCE metabolized to DCVG in kidney (mg) #
37     RAMetKid = (VMaxKidDCVG * CVKid) / (KMKidDCVG + CVKid);
38     # Amount of TCE in kidney compartment (mg)
39     dt(AKid) = (QKid * (CArt - CVKid)) - RAMetKid;
40
41     #*****
42     #***          TCOH Sub-model          ***
43     #*****
44     # State Variables with dynamics:
45     #     ABodTCOH
46     #     ALivTCOH
47     # Input Variables:
48     #     none
49     # Other State Variables and Global Parameters:
50     #     ABileTCOG
51     #     kEHR
52     #     VBodTCOH
53     #     PBodTCOH
54     #     VLiv
55     #     PLivTCOH
56     #     VMaxTCOH
57     #     KMTCOH
58     #     VMaxGluc
59     #     KMGluc
60     #     kMetTCOH - hepatic metabolism of TCOH (e.g., to DCA)
61     #     FracOther
62     #     FracTCA
63     #     StochTCOHTCE
64     #     StochTCOHGluc
65     #     FracLungSys
66     # Temporary variables used:
67     #     QBod
68     #     QGutLiv
69     #     QCnow
70     #     kPOTCOH
71     #     RAMetLiv1
72     #     RAMetLng
73     # Temporary variables assigned:
74     #     CVBodTCOH
75     #     CVLivTCOH
76     #     CTCOH
77     #     RAMetTCOHTCA
78     #     RAMetTCOHGluc
79     #     RAMetTCOH
80     #     RAREcircTCOG
81     # Notes:
82     #*****
83     #**** Blood (venous=arterial) *****
84     # Venous Concentrations (mg/L)
85     CVBodTCOH = ABodTCOH / VBodTCOH / PBodTCOH;
86     CVLivTCOH = ALivTCOH / VLiv / PLivTCOH;
87     CTCOH = (QBod * CVBodTCOH + QGutLiv * CVLivTCOH + kIVTCOH)/QCnow;
88
89     #**** Body *****
90     # Amount of TCOH in body
91     dt(ABodTCOH) = QBod * (CTCOH - CVBodTCOH);
92
93     #**** Liver *****
94
95     # Rate of oxidation of TCOH to TCA (mg/hr)
96     RAMetTCOHTCA = (VMaxTCOH * CVLivTCOH) / (KMTCOH + CVLivTCOH);
97     # Amount of glucuronidation to TCOG (mg/hr)
98     RAMetTCOHGluc = (VMaxGluc * CVLivTCOH) / (KMGluc + CVLivTCOH);
99     # Amount of TCOH metabolized to other (e.g., DCA)
100    RAMetTCOH = kMetTCOH * ALivTCOH;
101    # Amount of TCOH-Gluc recirculated (mg)
102    RAREcircTCOG = kEHR * ABileTCOG;
103    # Amount of TCOH in liver (mg)
104    dt(ALivTCOH) = kPOTCOH + QGutLiv * (CTCOH - CVLivTCOH)
105        - RAMetTCOH - RAMetTCOHTCA - RAMetTCOHGluc
106        + ((1.0 - FracOther - FracTCA) * StochTCOHTCE *

```

INTER-AGENCY REVIEW DRAFT-DO NOT CITE OR QUOTE

```

1      (RAMetLiv1 + FracLungSys*RAMetLng))
2      + (StochTCOHGluc * RAREcircTCOG);
3
4
5
6
7
8
9
10
11
12
13
14
15
16
17
18
19
20
21
22
23
24
25
26
27
28
29
30
31
32
33
34
35
36
37
38
39
40
41
42
43
44
45
46
47
48
49
50
51
52
53
#*****
#***          TCA Sub-model          ***
#*****
# State Variables with dynamics:
#   APlasTCA
#   ABodTCA
#   ALivTCA
#   AUrnTCA
#   AUrnTCA_sat
#   AUrnTCA_collect
# Input Variables:
#   TCAUrnSat
#   UrnMissing
# Other State Variables and Global Parameters:
#   VPlas
#   MWTCA
#   kDissoc
#   BMax
#   kMetTCA -- hepatic metabolism of TCA (e.g., to DCA)
#   VBod
#   PBodTCA
#   PLivTCA
#   kUrnTCA
#   FracTCA
#   StochTCATCE
#   StochTCATCOH
#   FracLungSys
# Temporary variables used:
#   kIVTCA
#   kPOTCA
#   QBodPlas
#   QGutLivPlas
#   QCPlas
#   RAMetLiv1
#   RAMetTCOHTCA
#   RAMetLng
# Temporary variables assigned:
#   CPlasTCA
#   CPlasTCAMole
#   a, b, c
#   CPlasTCAFreeMole
#   CPlasTCAFree
#   APlasTCAFree
#   CPlasTCABnd
#   CBodTCAFree
#   CLivTCAFree
#   CBodTCA
#   CLivTCA
#   CVBodTCA
#   CVLivTCA

```

```

54 #   RUrnTCA
55 #   RAMetTCA
56 # Notes:
57 #*****
58 #*** Plasma *****
59 # Concentration of TCA in plasma (umoles/L)
60   CPlasTCA = (APlasTCA<1.0e-15 ? 1.0e-15 : APlasTCA/VPlas);
61 # Concentration of free TCA in plasma in (umoles/L)
62   CPlasTCAMole = (CPlasTCA / MWTCA) * 1000.0;
63   a = kDissoc+BMax-CPlasTCAMole;
64   b = 4.0*kDissoc*CPlasTCAMole;
65   c = (b < 0.01*a*a ? b/2.0/a : sqrt(a*a+b)-a);
66   CPlasTCAFreeMole = 0.5*c;
67 # Concentration of free TCA in plasma (mg/L)
68   CPlasTCAFree = (CPlasTCAFreeMole * MWTCA) / 1000.0;
69   APlasTCAFree = CPlasTCAFree * VPlas;
70 # Concentration of bound TCA in plasma (mg/L)
71   CPlasTCABnd = (CPlasTCA-CPlasTCAFree ? 0 : CPlasTCA-CPlasTCAFree);
72 # Concentration in body and liver
73   CBodTCA = (ABodTCA<0 ? 0 : ABodTCA/VBod);
74   CLivTCA = (ALivTCA<1.0e-15 ? 1.0e-15 : ALivTCA/VLiv);
75 # Total concentration in venous plasma (free+bound)
76   CVBodTCAFree = (CBodTCA / PBodTCA); # free in equilibrium
77   CVBodTCA = CPlasTCABnd + CVBodTCAFree;
78   CVLivTCAFree = (CLivTCA / PLivTCA);
79   CVLivTCA = CPlasTCABnd + CVLivTCAFree; # free in equilibrium
80 # Rate of urinary excretion of TCA
81   RUrnTCA = kUrnTCA * APlasTCAFree;
82 # Dynamics for amount of total (free+bound) TCA in plasma (mg)
83   dt(APlasTCA) = kIVTCA + (QBodPlas*CVBodTCA) + (QGutLivPlas*CVLivTCA)
84     - (QCPlas * CPlasTCA) - RUrnTCA;
85
86 #*** Body *****
87 # Dynamics for amount of TCA in the body (mg)
88   dt(ABodTCA) = QBodPlas * (CPlasTCAFree - CVBodTCAFree);
89
90 #*** Liver *****
91 # Rate of metabolism of TCA
92   RAMetTCA = kMetTCA * ALivTCA;
93 # Dynamics for amount of TCA in the liver (mg)
94   dt(ALivTCA) = kPOTCA + QGutLivPlas*(CPlasTCAFree - CVLivTCAFree)
95     - RAMetTCA + (FracTCA * StochTCATCE *
96     (RAMetLiv1 + FracLungSys*RAMetLng))
97     + (StochTCATCOH * RAMetTCOHTCA);
98
99 #*** Urine *****
100 # Dynamics for amount of TCA in urine (mg)
101   dt(AUrnTCA) = RUrnTCA;
102   dt(AUrnTCA_sat) = TCAUrnSat*(1-UrnMissing)* RUrnTCA;
103     # Saturated, but not missing collection times
104   dt(AUrnTCA_collect) = (1-TCAUrnSat)*(1-UrnMissing)*RUrnTCA;
105     # Not saturated and not missing collection times
106

```

INTER-AGENCY REVIEW DRAFT-DO NOT CITE OR QUOTE

```

1 *****
2 #***                               TCOG Sub-model                               ***
3 *****
4 # State Variables with dynamics:
5 #     ABodTCOG
6 #     ALivTCOG
7 #     ABileTCOG
8 #     AUrnTCOG
9 #     AUrnTCOG_sat
10 #     AUrnTCOG_collect
11 # Input Variables:
12 #     TCOGUrnSat
13 #     UrnMissing
14 # Other State Variables and Global Parameters:
15 #     VBodTCOH
16 #     VLiv
17 #     PBodTCOG
18 #     PLivTCOG
19 #     kUrnTCOG
20 #     kBile
21 #     StochGlucTCOH
22 # Temporary variables used:
23 #     QBod
24 #     QGutLiv
25 #     QCnow
26 #     RAMetTCOHGluc
27 #     RAREcircTCOG
28 # Temporary variables assigned:
29 #     CVBodTCOG
30 #     CVLivTCOG
31 #     CTCOG
32 #     RUrnTCOG
33 #     RBileTCOG
34 # Notes:
35 *****
36 #*** Blood (venous=arterial) *****
37 # Venous Concentrations (mg/L)
38     CVBodTCOG = ABodTCOG / VBodTCOH / PBodTCOG;
39     CVLivTCOG = ALivTCOG / VLiv / PLivTCOG;
40     CTCOG = (QBod * CVBodTCOG + QGutLiv * CVLivTCOG)/QCnow;
41 #*** Body *****
42 # Amount of TCOG in body
43     RUrnTCOG = kUrnTCOG * ABodTCOG;
44     dt(ABodTCOG) = QBod * (CTCOG - CVBodTCOG) - RUrnTCOG;
45     RUrnTCOGTCOH = RUrnTCOG*StochTCOHGluc; #(vrisk3)
46 #*** Liver *****
47 # Amount of TCOG in liver (mg)
48     RBileTCOG = kBile * ALivTCOG;
49     dt(ALivTCOG) = QGutLiv * (CTCOG - CVLivTCOG)
50         + (StochGlucTCOH * RAMetTCOHGluc) - RBileTCOG;
51
52 #*** Bile *****
53 # Amount of TCOH-Gluc excreted into bile (mg)

```

```

54     dt(ABileTCOG) = RBileTCOG - RAREcircTCOG;
55
56 #*** Urine *****
57 # Amount of TCOH-Gluc excreted in urine (mg)
58     dt(AUrnTCOG) = RUrnTCOG;
59     dt(AUrnTCOG_sat) = TCOGUrnSat*(1-UrnMissing)*RUrnTCOG;
60         # Saturated, but not missing collection times
61     dt(AUrnTCOG_collect) = (1-TCOGUrnSat)*(1-UrnMissing)*RUrnTCOG;
62         # Not saturated and not missing collection times
63
64 *****
65 #***                               DCVG Sub-model                               ***
66 *****
67 # State Variables with dynamics:
68 #     ADCVGmol
69 # Input Variables:
70 #     none
71 # Other State Variables and Global Parameters:
72 #     kDCVG
73 #     FracKidDCVC      # Fraction of kidney DCVG going to DCVC in first pass
74 #     VDCVG
75 # Temporary variables used:
76 #     RAMetLiv2
77 #     RAMetKid
78 # Temporary variables assigned:
79 #     RAMetDCVGmol
80 #     CDCVGmol
81 # Notes:
82 #     Assume negligible GGT activity in liver as compared to kidney,
83 #     supported by in vitro data on GGT (even accounting for 5x
84 #     greater liver mass relative to kidney mass), as well as lack
85 #     of DCVC detected in blood.
86 #     "FracKidDCVC" Needed to account for "first pass" in
87 #     kidney (TCE->DCVG->DCVC without systemic circulation of DCVG).
88 *****
89 # Rate of metabolism of DCVG to DCVC
90     RAMetDCVGmol = kDCVG * ADCVGmol;
91 # Dynamics for DCVG in blood
92     dt(ADCVGmol) = (RAMetLiv2 + RAMetKid*(1-FracKidDCVC)) / MWTCE
93         - RAMetDCVGmol;
94 # Concentration of DCVG in blood (in mmoles/l)
95     CDCVGmol = ADCVGmol / VDCVG;
96
97 *****
98 #***                               DCVC Sub-model                               ***
99 *****
100 # State Variables with dynamics:
101 #     ADCVC
102 #     AUrnNDCVC
103 # Input Variables:
104 #     none
105 # Other State Variables and Global Parameters:
106 #     MWDCVC

```

INTER-AGENCY REVIEW DRAFT-DO NOT CITE OR QUOTE

```

1 # FracKidDCVC
2 # StochDCVCTCE
3 # kNAT
4 # kKidBioact
5 # StochN
6 # Temporary variables used:
7 # RAMetDCVGmol
8 # RAMetKid
9 # Temporary variables assigned:
10 # RAUrnDCVC
11 # Notes:
12 # Cannot detect DCVC in blood, so assume all is locally generated
13 # and excreted or bioactivated in kidney.
14 #*****
15 # Amount of DCVC in kidney (mg)
16 dt(ADCVC) = RAMetDCVGmol * MWDCVC
17 + RAMetKid * FracKidDCVC * StochDCVCTCE
18 - ((kNAT + kKidBioact) * ADCVC);
19 # Rate of NAcDCVC excretion into urine (mg)
20 RAUrnDCVC = kNAT * ADCVC;
21 # Dynamics for amount of N Acetyl DCVC excreted (mg)
22 dt(AUrnNDCVC) = StochN * RAUrnDCVC;
23 RUrnNDCVC = StochN * RAUrnDCVC; #(vrisk3)
24 #*****
25 #*** Total Mass Balance ***
26 #*****
27 #**** Mass Balance for TCE *****
28 # Total intake from inhalation (mg)
29 Rinhdose = QM * CInh;
30 dt(Inhdose) = Rinhdose;
31 # Amount of TCE absorbed by non-inhalation routes (mg)
32 dt(AO) = RAO + kIV + kIA + kPV; #(vrisk)
33 # Total dose
34 TotDose = InhDose + AO; #(vrisk)
35 # Total in tissues
36 TotTissue = #(vrisk)
37 ARap + ASlw + AFat + AGut + ALiv + AKid + ABld + #(vrisk)
38 AInhResp + AResp + AExhResp; #(vrisk)
39 # Total metabolized
40 dt(AMetLng) = RAMetLng; #(vrisk)
41 dt(AMetLiv1) = RAMetLiv1; #(vrisk)
42 dt(AMetLiv2) = RAMetLiv2; #(vrisk)
43 dt(AMetKid) = RAMetKid; #(vrisk)
44 ATotMetLiv = AMetLiv1 + AMetLiv2; #(vrisk)
45 TotMetab = AMetLng + ATotMetLiv + AMetKid; #(vrisk)
46 AMetLivOther = AMetLiv1 * FracOther; #(vrisk)
47 AMetGSH = AMetLiv2 + AMetKid; #(vrisk)
48 # Amount of TCE excreted in feces (mg)
49 RAExc = kTD * ADuod; #(vrisk)
50 dt(AExc) = RAExc; #(vrisk)
51 # Amount exhaled (mg)
52 RAExh = QM * CMixExh;
53 dt(AExh) = RAExh;

```

```

54 # Mass balance
55 TCEDiff = TotDose - TotTissue - TotMetab; #(vrisk)
56 MassBaltCE = TCEDiff - AExc - AExh; #(vrisk)
57
58 #**** Mass Balance for TCOH *****
59 # Total production/intake of TCOH
60 dt(ARecircTCOG) = RARecircTCOG; #(vrisk)
61 dt(AOTCOH) = kPOTCOH + kIVTCOH; #(vrisk)
62 TotTCOHIn = AOTCOH + ((1.0 - FracOther - FracTCA) * #(vrisk)
63 StochTCOHTCE * (AMetLiv1 + FracLungSys*AMetLng)) + #(vrisk)
64 (StochTCOHGluc * ARecircTCOG); #(vrisk)
65 TotTCOHDose = AOTCOH + ((1.0 - FracOther - FracTCA) * #(vrisk)
66 StochTCOHTCE * (AMetLiv1 + FracLungSys*AMetLng)); #(vrisk)
67 # Total in tissues
68 TotTissueTCOH = ABodTCOH + ALivTCOH; #(vrisk)
69 # Total metabolism of TCOH
70 dt(AMetTCOHTCA) = RAMetTCOHTCA; #(vrisk)
71 dt(AMetTCOHGluc) = RAMetTCOHGluc; #(vrisk)
72 dt(AMetTCOHOther) = RAMetTCOH; #(vrisk)
73 TotMetabTCOH = AMetTCOHTCA + AMetTCOHGluc + AMetTCOHOther; #(vrisk)
74 # Mass balance
75 MassBaltTCOH = TotTCOHIn - TotTissueTCOH - TotMetabTCOH; #(vrisk)
76
77 #**** Mass Balance for TCA *****
78 # Total production/intake of TCA
79 dt(AOTCA) = kPOTCA + kIVTCA; #(vrisk)
80 TotTCAIn = AOTCA + (FracTCA*StochTCATCE*(AMetLiv1 + #(vrisk)
81 FracLungSys*AMetLng)) + (StochTCATCOH*AMetTCOHTCA); #(vrisk)
82 # Total in tissues
83 TotTissueTCA = APlasTCA + ABodTCA + ALivTCA; #(vrisk)
84 # Total metabolism of TCA
85 dt(AMetTCA) = RAMetTCA; #(vrisk)
86 # Mass balance
87 TCADiff = TotTCAIn - TotTissueTCA - AMetTCA; #(vrisk)
88 MassBaltTCA = TCADiff - AUrnTCA; #(vrisk)
89
90 #**** Mass Balance for TCOG *****
91 # Total production of TCOG
92 TotTCOGIn = StochGlucTCOH * AMetTCOHGluc; #(vrisk)
93 # Total in tissues
94 TotTissueTCOG = ABodTCOG + ALivTCOG + ABileTCOG; #(vrisk)
95 # Mass balance
96 MassBaltTCOG = TotTCOGIn - TotTissueTCOG - #(vrisk)
97 ARecircTCOG - AUrnTCOG; #(vrisk)
98
99 #**** Mass Balance for DCVG *****
100 # Total production of DCVG
101 dt(ADCVGIn) = (RAMetLiv2 + RAMetKid*(1-FracKidDCVC)) / MWTC; #(vrisk)
102 # Metabolism of DCVG
103 dt(AMetDCVG) = RAMetDCVGmol; #(vrisk)
104 # Mass balance
105 MassBalDCVG = ADCVGIn - ADCVGmol - AMetDCVG; #(vrisk)
106

```

INTER-AGENCY REVIEW DRAFT-DO NOT CITE OR QUOTE

```

1  **** Mass Balance for DCVC *****
2  # Total production of DCVC
3      dt(ADCVCIn) = RAMetDCVGmol * MWDCVC  #(vrisk)
4                  + RAMetKid * FracKidDCVC * StochDCVCTCE;#(vrisk)
5  # Bioactivation of DCVC
6      dt(ABioactDCVC) = (kKidBioact * ADCVC);#(vrisk)
7  # Mass balance
8      AUrnNDCVCequiv = AUrnNDCVC/StochN;
9      MassBalDCVC = ADCVCIn - ADCVC - ABioactDCVC - AUrnNDCVCequiv;#(vrisk)
10
11 *****
12 ****          Dynamic Outputs          ****
13 *****
14 # Amount exhaled during exposure (mg)
15     dt(AExhExp) = (CInh > 0 ? RAExh : 0);
16
17 *****
18 ****          Dose Metrics          ****
19 *****
20 **** AUCs in mg-hr/L unless otherwise noted *****
21 #AUC of TCE in arterial blood
22     dt(AUCCBld) = CArt; #(vrisk)
23 #AUC of TCE in liver
24     dt(AUCCLiv) = CLiv; #(vrisk)
25 #AUC of TCE in kidney
26     dt(AUCCKid) = CKid; #(vrisk)
27 #AUC of TCE in rapidly perfused
28     dt(AUCCRap) = CRap; #(vrisk)
29 #AUC of TCOH in blood
30     dt(AUCCTCOH) = CTCOH; #(vrisk)
31 #AUC of TCOH in body
32     dt(AUCCBodTCOH) = ABodTCOH / VBodTCOH; #(vrisk)
33 #AUC of free TCA in the plasma (mg/L * hr)
34     dt(AUCPlasTCAFree) = CPlasTCAFree; #(vrisk)
35 #AUC of total TCA in plasma (mg/L * hr)
36     dt(AUCPlasTCA) = CPlasTCA; #(vrisk)
37 #AUC of TCA in liver (mg/L * hr)
38     dt(AUCLivTCA) = CLivTCA; #(vrisk)
39 #AUC of total TCOH (free+gluc) in TCOH-equiv in blood (mg/L * hr)
40     dt(AUCTotTCOH) = CTCOH + CTCOGTCOH; #(vrisk)
41 #AUC of DCVG in blood (mmol/L * hr) -- NOTE moles, not mg
42     dt(AUCCDCVG) = CDCVGMol; #(vrisk)
43 };
44 ##### End of Dynamics #####
45
46 CalcOutputs{
47
48 **** Static outputs for comparison to data *****
49 # TCE
50     RetDose = ((InhDose-AExhExp) > 0 ? (InhDose - AExhExp) : 1e-15);
51     CALvPPM = (CALv < 1.0e-15 ? 1.0e-15 : CALv * (24450.0 / MWTCE));
52     CInhPPM = (ACh < 1.0e-15 ? 1.0e-15 : ACh/Vch*24450.0/MWTCE);
53

```

```

54     # CInhPPM Only used for CC inhalation
55     CArt = (CArt < 1.0e-15 ? 1.0e-15 : CArt);
56     CVen = (CVen < 1.0e-15 ? 1.0e-15 : CVen);
57     CBldMix = (CArt+CVen)/2;
58     CFat = (CFat < 1.0e-15 ? 1.0e-15 : CFat);
59     CGut = (CGut < 1.0e-15 ? 1.0e-15 : CGut);
60     CRap = (CRap < 1.0e-15 ? 1.0e-15 : CRap);
61     CSLw = (CSlw < 1.0e-15 ? 1.0e-15 : CSLw);
62     CHrt = CRap;
63     CKid = (CKid < 1.0e-15 ? 1.0e-15 : CKid);
64     CLiv = (CLiv < 1.0e-15 ? 1.0e-15 : CLiv);
65     CLung = CRap;
66     CMus = (CSlw < 1.0e-15 ? 1.0e-15 : CSLw);
67     CSpl = CRap;
68     CBrn = CRap;
69     zAExh = (AExh < 1.0e-15 ? 1.0e-15 : AExh);
70     zAExhpost = ((AExh - AExhExp) < 1.0e-15 ? 1.0e-15 : AExh - AExhExp);
71 # TCOH
72     CTCOH = (CTCOH < 1.0e-15 ? 1.0e-15 : CTCOH);
73     CBodTCOH = (ABodTCOH < 1.0e-15 ? 1.0e-15 : ABodTCOH/VBodTCOH);
74     CKidTCOH = CBodTCOH;
75     CLivTCOH = (ALivTCOH < 1.0e-15 ? 1.0e-15 : ALivTCOH/VLiv);
76     CLungTCOH = CBodTCOH;
77 # TCA
78     CPlasTCA = (CPlasTCA < 1.0e-15 ? 1.0e-15 : CPlasTCA);
79     CBldTCA = CPlasTCA*TCAPlas;
80     CBodTCA = (CBodTCA < 1.0e-15 ? 1.0e-15 : CBodTCA);
81     CLivTCA = (CLivTCA < 1.0e-15 ? 1.0e-15 : CLivTCA);
82     CKidTCA = CBodTCA;
83     CLungTCA = CBodTCA;
84     zAUrnTCA = (AUrnTCA < 1.0e-15 ? 1.0e-15 : AUrnTCA);
85     zAUrnTCA_sat = (AUrnTCA_sat < 1.0e-15 ? 1.0e-15 : AUrnTCA_sat);
86     zAUrnTCA_collect = (AUrnTCA_collect < 1.0e-15 ? 1.0e-15 :
87 AUrnTCA_collect);
88 # TCOG
89     zABileTCOG = (ABileTCOG < 1.0e-15 ? 1.0e-15 : ABileTCOG);
90     # Concentrations are in TCOH-equivalents
91     CTCOG = (CTCOG < 1.0e-15 ? 1.0e-15 : CTCOG);
92     CTCOGTCOH = (CTCOG < 1.0e-15 ? 1.0e-15 : StochTCOHGluc*CTCOG);
93     CBodTCOGTCOH = (ABodTCOG < 1.0e-15 ? 1.0e-15 :
94 StochTCOHGluc*ABodTCOG/VBodTCOH);
95     CKidTCOGTCOH = CBodTCOGTCOH;
96     CLivTCOGTCOH = (ALivTCOG < 1.0e-15 ? 1.0e-15 :
97 StochTCOHGluc*ALivTCOG/VLiv);
98     CLungTCOGTCOH = CBodTCOGTCOH;
99     AUrnTCOGTCOH = (AUrnTCOG < 1.0e-15 ? 1.0e-15 : StochTCOHGluc*AUrnTCOG);
100     AUrnTCOGTCOH_sat = (AUrnTCOG_sat < 1.0e-15 ? 1.0e-15 :
101 StochTCOHGluc*AUrnTCOG_sat);
102     AUrnTCOGTCOH_collect = (AUrnTCOG_collect < 1.0e-15 ? 1.0e-15 :
103 StochTCOHGluc*AUrnTCOG_collect);
104 # Other
105     CDCVGMol = (CDCVGMol < 1.0e-15 ? 1.0e-15 : CDCVGMol);
106     CDCVGMol0 = CDCVGMol; #(v1.2.3.2)

```

INTER-AGENCY REVIEW DRAFT-DO NOT CITE OR QUOTE

```

1      CDCVG_NDtmp = CDFNormal(3*(1-CDCVGMol/CDCVGMolLD));
2      # Assuming LD = 3*sigma_blank, Normally distributed
3      CDCVG_ND = ( CDCVG_NDtmp < 1.0 ? ( CDCVG_NDtmp >= 1e-100 ? -
4      log(CDCVG_NDtmp) : -log(1e-100)) : 1e-100 );
5      #(v1.2.3.2)
6      zAUrnNDCVC =(AUrnNDCVC < 1.0e-15 ? 1.0e-15 : AUrnNDCVC);
7      AUrnTCTotMole = zAUrnTCA / MWTCA + AUrnTCOGTCOH / MWTCOH;
8      TotCTCOH = CTCOH + CTCOGTCOH;
9      TotCTCOHcomp = CTCOH + CTCOG; # ONLY FOR COMPARISON WITH HACK
10     ATCOG = ABodTCOG + ALivTCOG; # ONLY FOR COMPARISON WITH HACK
11     # Misc
12     CVenMole = CVen / MWTCE;
13     CPlasTCAMole = (CPlasTCAMole < 1.0e-15 ? 1.0e-15 : CPlasTCAMole);
14     CPlasTCAFreeMole = (CPlasTCAFreeMole < 1.0e-15 ? 1.0e-15 :
15     CPlasTCAFreeMole);
16
17     #**** Additional Dose Metrics ****
18     #
19
20     TotTCAInBW = TotTCAIn/BW;#(vrisk2)
21
22     # Scaled by BW^3/4
23     TotMetabBW34 = TotMetab/BW75;#(vrisk)
24     AMetGSHBW34 = AMetGSH/BW75;#(vrisk)
25     TotDoseBW34 = TotDose/BW75;#(vrisk2)
26     AMetLivlBW34 = AMetLivl/BW75;#(vrisk2)
27     TotOxMetabBW34 = (AMetLng+AMetLivl)/BW75;#(vrisk2)
28
29     # Scaled by tissue volume
30     AMetLivlLiv = AMetLivl/VLiv; #(vrisk)
31     AMetLivOtherLiv = AMetLivOther/VLiv; #(vrisk)
32     AMetLngResp = AMetLng/VRespEfftmp; #(vrisk)
33     ABioactDCVCKid = ABioactDCVC/VKid;#(vrisk)
34
35     #**** Fractional Volumes
36
37     VFatCtmp = VFat/BW; #(vrisk3)
38     VGutCtmp = VGut/BW; #(vrisk3)
39     VLivCtmp = VLiv/BW; #(vrisk3)
40     VRapCtmp = VRap/BW; #(vrisk3)
41     VRespLumCtmp = VRespLum/BW; #(vrisk3)
42     VRespEffCtmp = VRespEfftmp/BW; #(vrisk3)
43     VKidCtmp = VKid/BW; #(vrisk3)
44     VBldCtmp = VBld/BW; #(vrisk3)
45     VSlwCtmp = VSlw/BW; #(vrisk3)
46     VPlasCtmp = VPlas/BW; #(vrisk3)
47     VBodCtmp = VBod/BW; #(vrisk3)
48     VBodTCOHctmp = VBodTCOH/BW; #(vrisk3)
49
50 };
51
52

```

1 **References**

- 2 Abbas RR, Seckel CS, Kidney JK, Fisher JW. (1996). Pharmacokinetic analysis of chloral
3 hydrate and its metabolism in B6C3F1 mice. *Drug Metab Dispos.* **24**:1340–6.
- 4 Abbas R, Fisher JW. (1997). physiologically based pharmacokinetic model for trichloroethylene
5 and its metabolites, chloral hydrate, trichloroacetate, dichloroacetate, trichloroethanol,
6 and trichloroethanol glucuronide in B6C3F1 mice. *Toxicol Appl Pharmacol.* **147**:15–30.
- 7 Andersen, M. E., Gargas, M. L., Clewell, H. J., 3rd, and Severyn, K. M. (1987). Quantitative
8 evaluation of the metabolic interactions between trichloroethylene and 1,1-
9 dichloroethylene in vivo using gas uptake methods. *Toxicol Appl Pharmacol*
10 **89**, 149–157.
- 11 Araki, S. (1978). The effects of water restriction and water loading on urinary excretion of lead,
12 delta-aminolevulinic acid and coproporphyrin. *Br J Ind Med.* 35(4):312–7.
- 13 Barter, Z. E., Bayliss, M. K., Beaune, P. H., Boobis, A. R., Carlile, D. J., Edwards, R. J.,
14 Houston, J. B., Lake, B. G., Lipscomb, J. C., Pelkonen, O. R., Tucker, G. T., and
15 Rostami-Hodjegan, A. (2007). Scaling factors for the extrapolation of in vivo metabolic
16 drug clearance from in vitro data: reaching a consensus on values of human microsomal
17 protein and hepatocellularity per gram of liver. *Curr Drug Metab* **8**, 33–45.
- 18 Barton, H. A., Creech, J. R., Godin, C. S., Randall, G. M., and Seckel, C. S. (1995).
19 Chloroethylene mixtures: pharmacokinetic modeling and in vitro metabolism of vinyl
20 chloride, trichloroethylene, and trans-1,2-dichloroethylene in rat. *Toxicol Appl*
21 *Pharmacol* **130**, 237–247.
- 22 Bartonicek, V. (1962). Metabolism and excretion of trichloroethylene after inhalation by human
23 subjects. *Br J Indust Med.* **19**:134–141.
- 24 Bernauer, U., Birner, G., Dekant, W., and Henschler, D. (1996). Biotransformation of
25 trichloroethene: dose-dependent excretion of 2,2,2-trichloro-metabolites and mercapturic
26 acids in rats and humans after inhalation. *Arch Toxicol* **70**, 338–346.
- 27 Birner G, Vamvakas S, Dekant W, Henschler D. (1993). Nephrotoxic and genotoxic N-acetyl-S-
28 dichlorovinyl-L-cysteine is a urinary metabolite after occupational 1,1,2-trichloroethene
29 exposure in humans: implications for the risk of trichloroethene exposure. *Environ*
30 *Health Perspect.* **99**:281–4.
- 31 Bloemen, L. J., Monster, A. C., Kezic, S., Commandeur, J. N., Veulemans, H., Vermeulen, N. P.,
32 and Wilmer, J. W. (2001). Study on the cytochrome P-450- and glutathione-dependent
33 biotransformation of trichloroethylene in humans. *Int Arch Occup Environ Health* **74**,
34 102–108.
- 35 Bois FY. (2000a). Statistical analysis of Fisher et al. PBPK model of trichloroethylene kinetics.
36 *Environ Health Perspect.* **108 Suppl 2**:275–82.

- 1 Bois FY. (2000b). Statistical analysis of Clewell et al. PBPK model of trichloroethylene kinetics.
2 *Environ Health Perspect.* **108 Suppl 2**:307–16.
- 3 Bronley-DeLancey, A., McMillan, D. C., McMillan, J. M., Jollow, D. J., Mohr, L. C., and Hoel,
4 D. G. (2006). Application of cryopreserved human hepatocytes in trichloroethylene risk
5 assessment: relative disposition of chloral hydrate to trichloroacetate and
6 trichloroethanol. *Environ Health Perspect* **114**, 1237–1242.
- 7 Brown RP, Delp MD, Lindstedt SL, Rhomberg LR, Beliles RP. (1997). Physiological parameter
8 values for physiologically based pharmacokinetic models. *Toxicol Ind Health.*
9 **13**:407–84.
- 10 Chiu, WA; Bois, RY. (2006) Revisiting the population toxicokinetics of tetrachloroethylene.
11 *Arch Toxicol* 80(6):382–385.
- 12 Chiu, W. A., Micallef, S., Monster, A. C., and Bois, F. Y. (2007). Toxicokinetics of inhaled
13 trichloroethylene and tetrachloroethylene in humans at 1 ppm: empirical results and
14 comparisons with previous studies. *Toxicol Sci* **95**, 23–36.
- 15 Clewell HJ 3rd, Gentry PR, Covington TR, Gearhart JM. (2000). Development of a
16 physiologically based pharmacokinetic model of trichloroethylene and its metabolites for
17 use in risk assessment. *Environ Health Perspect.* **108 Suppl 2**:283–305.
- 18 Dallas, C. E., Gallo, J. M., Ramanathan, R., Muralidhara, S., and Bruckner, J. V. (1991).
19 Physiological pharmacokinetic modeling of inhaled trichloroethylene in rats. *Toxicol*
20 *Appl Pharmacol* **110**, 303–314.
- 21 Elfarra, A. A., Krause, R. J., Last, A. R., Lash, L. H., and Parker, J. C. (1998). Species- and sex-
22 related differences in metabolism of trichloroethylene to yield chloral and
23 trichloroethanol in mouse, rat, and human liver microsomes. *Drug Metab Dispos*
24 **26**, 779–785.
- 25 Ertle T, Henschler D, Müller G, Spassowski M. (1972). Metabolism of trichloroethylene in man.
26 I. The significance of trichloroethanol in long-term exposure conditions. *Arch Toxicol.*
27 **29**:171–88.
- 28 Fernandez, J. G., Droz, P. O., Humbert, B. E., and Caperos, J. R. (1977). Trichloroethylene
29 exposure. Simulation of uptake, excretion, and metabolism using a mathematical model.
30 *Br J Ind Med* **34**, 43–55.
- 31 Fiserova-Bergerova, V., Tichy, M., and Di Carlo, F. J. (1984). Effects of biosolubility on
32 pulmonary uptake and disposition of gases and vapors of lipophilic chemicals. *Drug*
33 *Metab Rev* **15**, 1033–1070.
- 34 Fisher JW. (2000). Physiologically based pharmacokinetic models for trichloroethylene and its
35 oxidative metabolites. *Environ Health Perspect.* **108 Suppl 2**:265–73.
- 36 Fisher JW, Allen BC. (1993). Evaluating the risk of liver cancer in humans exposed to
37 trichloroethylene using physiological models. *Risk Anal.* **13**(1):87–95.

- 1 Fisher, J. W., Whittaker, T. A., Taylor, D. H., Clewell, H. J., 3rd, and Andersen, M. E. (1989).
2 Physiologically based pharmacokinetic modeling of the pregnant rat: a multiroute
3 exposure model for trichloroethylene and its metabolite, trichloroacetic acid. *Toxicol*
4 *Appl Pharmacol* **99**, 395–414.
- 5 Fisher JW, Gargas ML, Allen BC, Andersen ME. (1991). Physiologically based pharmacokinetic
6 modeling with trichloroethylene and its metabolite, trichloroacetic acid, in the rat and
7 mouse. *Toxicol Appl Pharmacol.* **109**:183–95.
- 8 Fisher, J. W., Mahle, D., and Abbas, R. (1998). A human physiologically based pharmacokinetic
9 model for trichloroethylene and its metabolites, trichloroacetic acid and free
10 trichloroethanol. *Toxicol Appl Pharmacol* **152**, 339–359.
- 11 Gargas, M. L., Burgess, R. J., Voisard, D. E., Cason, G. H., and Andersen, M. E. (1989).
12 Partition coefficients of low-molecular-weight volatile chemicals in various liquids and
13 tissues. *Toxicol Appl Pharmacol* **98**, 87–99.
- 14 Gelfand, A.E., Smith, A.F.M. (1990). Sampling-based approaches to calculating marginal
15 densities. *J Am Stat Assoc.* 85:398–409.
- 16 Gelman A, Bois F, Jiang J. (1996). Physiological pharmacokinetic analysis using population
17 modeling and informative prior distributions. *J Am Stat Assoc.* **91**:1400–1412.
- 18 Gelman A, Carlin JB, Stern HS, Rubin DB. (2004). Bayesian Data Analysis. New York:
19 Chapman & Hall/CRC.
- 20 Gilks, W.R., Richardson, S., Spiegelhalter, D.J., eds. (1996) Markov Chain Monte Carlo in
21 Practice. New York: Chapman & Hall/CRC Press.
- 22 Green, T., and Prout, M. S. (1985). Species differences in response to trichloroethylene. II.
23 Biotransformation in rats and mice. *Toxicol Appl Pharmacol* **79**, 401–411.
- 24 Green, T., Mainwaring, G. W., and Foster, J. R. (1997). Trichloroethylene-induced mouse lung
25 tumors: studies of the mode of action and comparisons between species. *Fundam Appl*
26 *Toxicol* **37**, 125–130.
- 27 Greenberg, M. S., Burton, G. A., and Fisher, J. W. (1999). Physiologically based
28 pharmacokinetic modeling of inhaled trichloroethylene and its oxidative metabolites in
29 B6C3F1 mice. *Toxicol Appl Pharmacol* **154**, 264–278.
- 30 Hack CE, Chiu WA, Jay Zhao Q, Clewell HJ.(2006). Bayesian population analysis of a
31 harmonized physiologically based pharmacokinetic model of trichloroethylene and its
32 metabolites. *Regul Toxicol Pharmacol.* **46**:63–83.
- 33 Hejtmancik MR, Trela BA, Kurtz PJ, Persing RL, Ryan MJ, Yarrington JT, Chhabra RS. (2002).
34 Comparative gavage subchronic toxicity studies of o-chloroaniline and m-chloroaniline
35 in F344 rats and B6C3F1 mice. *Toxicol Sci.* 69:234–43.
- 36 Hissink, E. M., Bogaards, J. J. P., Freidg, A. P., Commandeur, J. N. M., Vermeulen, N. P. E.,
37 and van Bladeren, P. J. (2002). The use of in vitro metabolic parameters and

- 1 physiologically based pharmacokinetic (PBPK) modeling to explore the risk assessment
2 of trichloroethylene. *Environmental Toxicology and Pharmacology* **11**, 259–271.
- 3 Jakobson, I., Holmberg, B., and Ekner, A. (1986). Venous blood levels of inhaled
4 trichloroethylene in female rats and changes induced by interacting agents. *Acta*
5 *Pharmacol Toxicol (Copenh)* **59**, 135–143.
- 6 Kaneko, T., Wang, P. Y., and Sato, A. (1994). Enzymes induced by ethanol differently affect the
7 pharmacokinetics of trichloroethylene and 1,1,1-trichloroethane. *Occup Environ Med* **51**,
8 113–119.
- 9 Keys, D. A., Bruckner, J. V., Muralidhara, S., and Fisher, J. W. (2003). Tissue dosimetry
10 expansion and cross-validation of rat and mouse physiologically based pharmacokinetic
11 models for trichloroethylene. *Toxicol Sci* **76**, 35–50.
- 12 Kimmerle, G., Eben, A. (1973a). Metabolism, excretion and toxicology of trichloroethylene after
13 inhalation. I. Experimental exposure on rats. *Arch Toxicol* **30**:115–126.
- 14 Kimmerle, G., Eben, A. (1973b). Metabolism, excretion and toxicology of trichloroethylene
15 after inhalation. II. Experimental human exposure. *Arch Toxicol* **30**:127–138.
- 16 Koizumi, A. (1989). Potential of physiologically based pharmacokinetics to amalgamate kinetic
17 data of trichloroethylene and tetrachloroethylene obtained in rats and man. *Br J Ind*
18 *Med* **46**, 239–249.
- 19 Laparé S, Tardif R, Brodeur J.(1995). Effect of various exposure scenarios on the biological
20 monitoring of organicsolvents in alveolar air. II. 1,1,1-Trichloroethane and
21 trichloroethylene. *Int Arch Occup Environ Health.* **67**:375–94.
- 22 Larson, J. L., and Bull, R. J. (1992a). Metabolism and lipoperoxidative activity of
23 trichloroacetate and dichloroacetate in rats and mice. *Toxicol Appl Pharmacol*
24 **115**, 268–277.
- 25 Larson, J. L., and Bull, R. J. (1992b). Species differences in the metabolism of trichloroethylene
26 to the carcinogenic metabolites trichloroacetate and dichloroacetate. *Toxicol Appl*
27 *Pharmacol* **115**, 278–285.
- 28 Lash, L. H., Tokarz, J. J., and Pegouske, D. M. (1995). Susceptibility of primary cultures of
29 proximal tubular and distal tubular cells from rat kidney to chemically induced toxicity.
30 *Toxicology* **103**, 85–103.
- 31 Lash, L. H., Visarius, T. M., Sall, J. M., Qian, W., and Tokarz, J. J. (1998). Cellular and
32 subcellular heterogeneity of glutathione metabolism and transport in rat kidney cells.
33 *Toxicology* **130**, 1–15.
- 34 Lash LH, Lipscomb JC, Putt DC, Parker JC. (1999a). Glutathione conjugation of
35 trichloroethylene in human liver and kidney: kinetics and individual variation. *Drug*
36 *Metab Dispos.* **27**:351–359.

- 1 Lash LH, Putt DA, Brashear WT, Abbas R, Parker JC, Fisher JW. (1999b). Identification of S-
2 (1,2-dichlorovinyl)glutathione in the blood of human volunteers exposed to
3 trichloroethylene. *J Toxicol Environ Health A*. **56**:1–21.
- 4 Lash LH, Putt DA, Parker JC. (2006). Metabolism and tissue distribution of orally administered
5 trichloroethylene in male and female rats: identification of glutathione- and cytochrome
6 P-450-derived metabolites in liver, kidney, blood, and urine. *J Toxicol Environ Health A*.
7 **69**:1285–309.
- 8 Lee, K. M., Bruckner, J. V., Muralidhara, S., and Gallo, J. M. (1996). Characterization of
9 presystemic elimination of trichloroethylene and its nonlinear kinetics in rats. *Toxicol*
10 *Appl Pharmacol* **139**, 262–271.
- 11 Lee, K. M., Muralidhara, S., Schnellmann, R. G., and Bruckner, J. V. (2000). Contribution of
12 direct solvent injury to the dose-dependent kinetics of trichloroethylene: portal vein
13 administration to rats. *Toxicol Appl Pharmacol* **164**, 46–54.
- 14 Lin JH. (1995). Species similarities and differences in pharmacokinetics. *Drug Metab Dispos*.
15 **23**:1008–21.
- 16 Lipscomb, J. C., Garrett, C. M., and Snawder, J. E. (1997). Cytochrome P450-dependent
17 metabolism of trichloroethylene: interindividual differences in humans. *Toxicol Appl*
18 *Pharmacol* **142**, 311–318.
- 19 Lipscomb, J. C., Garrett, C. M., and Snawder, J. E. (1998a). Use of Kinetic and Mechanistic
20 Data in Species Extrapolation of Bioactivation: Cytochrome-P450 Dependent
21 Trichloroethylene Metabolism at Occupationally Relevant Concentrations. *J Occup*
22 *Health* **40**, 110–117.
- 23 Lipscomb, J. C., Fisher, J. W., Confer, P. D., and Byczkowski, J. Z. (1998b). In vitro to in vivo
24 extrapolation for trichloroethylene metabolism in humans. *Toxicol Appl Pharmacol*
25 **152**, 376–387.
- 26 Lumpkin, M. H., Bruckner, J. V., Campbell, J. L., Dallas, C. E., White, C. A., and Fisher, J. W.
27 (2003). Plasma binding of trichloroacetic acid in mice, rats, and humans under cancer
28 bioassay and environmental exposure conditions. *Drug Metab Dispos* **31**, 1203–1207.
- 29 Merdink, J. L., Gonzalez-Leon, A., Bull, R. J., and Schultz, I. R. (1998). The extent of
30 dichloroacetate formation from trichloroethylene, chloral hydrate, trichloroacetate, and
31 trichloroethanol in B6C3F1 mice. *Toxicol Sci* **45**, 33–41.
- 32 Merdink, J. L., Stenner, R. D., Stevens, D. K., Parker, J. C., and Bull, R. J. (1999). Effect of
33 enterohepatic circulation on the pharmacokinetics of chloral hydrate and its metabolites
34 in F344 rats. *J Toxicol Environ Health A* **57**, 357–368.
- 35 Monster, A. C., Boersma, G., and Duba, W. C. (1976). Pharmacokinetics of trichloroethylene in
36 volunteers, influence of workload and exposure concentration. *Int Arch Occup Environ*
37 *Health* **38**, 87–102.
- 38 Monster, A. C., Boersma, G., and Duba, W. C. (1979). Kinetics of trichloroethylene in repeated
39 exposure of volunteers. *Int Arch Occup Environ Health* **42**, 283–292.

- 1 Müller G, Spassowski M, Henschler D. (1972). Trichloroethylene exposure and trichloroethylene
2 metabolites in urine and blood. *Arch. Toxicol.* **29**:335–340.
- 3 Muller, G., Spassovski, M., and Henschler, D. (1974). Metabolism of trichloroethylene in man.
4 II. Pharmacokinetics of metabolites. *Arch Toxicol* **32**, 283–295.
- 5 Muller, G., Spassowski, M., and Henschler, D. (1975). Metabolism of trichloroethylene in man.
6 III. Interaction of trichloroethylene and ethanol. *Arch Toxicol* **33**, 173–189.
- 7 Okino MS, Chiu WA, Evans MV, Power FW, Lipscomb JC, Tornero-Velez R, Dary CC,
8 Blancato JN, Chen C . 2005. Suitability of Using In Vitro and Computationally Estimated
9 Parameters in Simplified Pharmacokinetic Models. *Drug Metab Rev* 2005; 37(suppl.
10 2):162.
- 11 Paycok, Z.V., Powell, J.F. (1945). The excretion of sodium trichloroacetate. *J Pharmacol Exper*
12 *Therapeut.* **85**: 289–293.
- 13 Plummer M, Best N, Cowles K, Vines K. (2008). *coda: Output analysis and diagnostics for*
14 *MCMC*. R package version 0.13-3.
- 15 Price PS, Conolly RB, Chaisson CF, Gross EA, Young JS, Mathis ET, Tedder DR. (2003).
16 Modeling interindividual variation in physiological factors used in PBPK models of
17 humans. *Crit Rev Toxicol.* **33**:469–503.
- 18 Prout, M. S., Provan, W. M., and Green, T. (1985). Species differences in response to
19 trichloroethylene. I. Pharmacokinetics in rats and mice. *Toxicol Appl Pharmacol* **79**,
20 389–400.
- 21 Rodriguez, CE; Mahle, DA; Gearhart, JM; et al. (2007) Predicting age-appropriate
22 pharmacokinetics of six volatile organic compounds in the rat utilizing physiologically
23 based pharmacokinetic modeling. *Toxicol Sci* 98(1) :43-56.
- 24 Sarangapani R, Gentry PR, Covington TR, Teeguarden JG, Clewell HJ 3rd. (2003). Evaluation
25 of the potential impact of age- and gender-specific lung morphology and ventilation rate
26 on the dosimetry of vapors. *Inhal Toxicol.* **15**:987–1016.
- 27 Sato, A., Nakajima, T., Fujiwara, Y., and Murayama, N. (1977). A pharmacokinetic model to
28 study the excretion of trichloroethylene and its metabolites after an inhalation exposure.
29 *Br J Ind Med* **34**, 56–63.
- 30 Sato, A., and Nakajima, T. (1979). Partition coefficients of some aromatic hydrocarbons and
31 ketones in water, blood and oil. *Br J Ind Med* **36**, 231–234.
- 32 Schultz, I. R., Merdink, J. L., Gonzalez-Leon, A., and Bull, R. J. (1999). Comparative
33 toxicokinetics of chlorinated and brominated haloacetates in F344 rats. *Toxicol Appl*
34 *Pharmacol* **158**, 103–114.
- 35 Simmons, J. E., Boyes, W. K., Bushnell, P. J., Raymer, J. H., Limsakun, T., McDonald, A., Sey,
36 Y. M., and Evans, M. V. (2002). A physiologically based pharmacokinetic model for
37 trichloroethylene in the male long-Evans rat. *Toxicol Sci* **69**, 3–15.

- 1 Stenner, R. D., Merdink, J. L., Stevens, D. K., Springer, D. L., and Bull, R. J. (1997).
2 Enterohepatic recirculation of trichloroethanol glucuronide as a significant source of
3 trichloroacetic acid. Metabolites of trichloroethylene. *Drug Metab Dispos* **25**, 529–535.
- 4 Stewart, R. D., Dodd, H. C., Gay, H. H., and Erley, D. S. (1970). Experimental human exposure
5 to trichloroethylene. *Arch Environ Health* **20**, 64–71.
- 6 Templin, M. V., Parker, J. C., and Bull, R. J. (1993). Relative formation of dichloroacetate and
7 trichloroacetate from trichloroethylene in male B6C3F1 mice. *Toxicol Appl Pharmacol*
8 **123**, 1–8.
- 9 Templin, M. V., Stevens, D. K., Stenner, R. D., Bonate, P. L., Tuman, D., and Bull, R. J. (1995).
10 Factors affecting species differences in the kinetics of metabolites of trichloroethylene. *J*
11 *Toxicol Environ Health* **44**, 435–447.
- 12 Trevisan A, Giraldo M, Borella M, Maso S. (2001). Historical control data on urinary and renal
13 tissue biomarkers in naive male Wistar rats. *J Appl Toxicol*. 21(5):409-13.
- 14 Triebig, G., Essing, H.-G. , Schaller, K.-H., Valentin, H. (1976). Biochemical and psychological
15 examinations of test subjects exposed to trichloroethylene. *Zbl. Bakt. Hyg., I. Abt. Orig.*
16 **B 163**: 383–416.
- 17 Yu, K. O., Barton, H. A., Mahle, D. A., and Frazier, J. M. (2000). In vivo kinetics of
18 trichloroacetate in male Fischer 344 rats. *Toxicol Sci* **54**, 302–311.
- 19